JHR 97: 1301–1383 (2024)
doi: 10.3897/jhr.97.133255
https://jhr.pensoft.net

RESEARCH ARTICLE

JOURNAL OF Hymenoptera RESEARCH
A peer-reviewed open-access journal
The International Society of Hymenopterists

Integrative taxonomic revision of the Nearctic *Perilampus hyalinus* species complex (Hymenoptera, Chalcidoidea, Perilampidae) resolves 100 years of confusion about the host associations of *P. hyalinus* Say

Jeong Jae Yoo[1,2], D. Christopher Darling[1,2]

1 *Department of Natural History, Royal Ontario Museum, 100 Queen's Park, Toronto, Ontario, M5S 2C6, Canada* **2** *Department of Ecology and Evolutionary Biology, University of Toronto, Ontario, M5S 3B2, Canada*

Corresponding author: Jeong Jae Yoo (jjbiodiversity@gmail.com)

Academic editor: Ankita Gupta | Received 28 July 2024 | Accepted 17 October 2024 | Published 5 December 2024

https://zoobank.org/99F8596D-B97C-4E63-9C20-4BF550CC8E6D

Citation: Yoo JJ, Darling DC (2024) Integrative taxonomic revision of the Nearctic *Perilampus hyalinus* species complex (Hymenoptera, Chalcidoidea, Perilampidae) resolves 100 years of confusion about the host associations of *P. hyalinus* Say. Journal of Hymenoptera Research 97: 1301–1383. https://doi.org/10.3897/jhr.97.133255

Abstract

The enigmatic Nearctic parasitoid *Perilampus hyalinus* Say (Hymenoptera: Chalcidoidea: Perilampidae) has long been suspected as a species complex with a wide range of host associations and differing modes of parasitism. In this study we clarify the status of this species by combining morphological evidence, two genes (COI and ITS2) and host information and recognize ten species in the *P. hyalinus* species complex in the Nearctic region. Eight new species are described: *Perilampus arcus* Yoo & Darling, **sp. nov.**, *P. crassus* Yoo & Darling, **sp. nov.**, *P. neodiprioni* Yoo & Darling, **sp. nov.**, *P. monocteni* Yoo & Darling, **sp. nov.**, *P. pilosus* Yoo & Darling, **sp. nov.**, *P. seneca* Yoo & Darling, **sp. nov.**, *P. sonora* Yoo & Darling, **sp. nov.**, and *P. ute* Yoo & Darling, **sp. nov.** A reared specimen with a COI sequence is designated as the Neotype of *P. hyalinus* Say establishing this species as either a hyperparasitoid that parasitizes dipteran parasitoids of Orthoptera or a parasitoid of dipteran kleptoparasites of Crabronidae and Sphecidae that provision their nests with Orthoptera. *Perilampus sirsiris* (Argaman) and four of the new species are hyperparasitoids, parasitizing hymenopteran and dipteran parasitoids of Lepidoptera. *Perilampus neodiprioni* and *P. monocteni* can develop as both primary parasitoids of Diprionidae (Hymenoptera) and as hyperparasitoids, parasitizing dipteran and hymenopteran parasitoids of diprionid sawflies. *Perilampus neodiprioni* is strictly associated with *Neodiprion* sawflies, and *P. monocteni* is associated with *Monoctenus* sawflies.

Keywords

COI, ITS2, key, morphology, new species, parasitoid, species delimitation, systematics

Introduction

The *Perilampus hyalinus* species group contains the most conspicuous species of *Perilampus* in the Western Hemisphere. Specimens are large (3–5 mm) and brightly iridescent in color and are frequently collected on flowers. It is one of the 6 species groups recognized by Smulyan (1936) in the last comprehensive study of the genus and three species were recognized, two of which were new: *Perilampus carolinensis* and *P. regalis*. All remaining specimens were referred to the already enigmatic *P. hyalinus* Say.

Perilampus hyalinus Say has been shrouded in confusion for at least 100 years, since biological studies of these parasitoids indicated divergent host associations and modes of parasitism (Smith 1912; Kelly 1914; Smith 1958) and suggested that there were morphological differences in the first-instar larvae or planidia associated with various hosts (Ford 1922; Tripp 1962). The search for morphological differences of the adults that were correlated with these biological differences is still best summarized by Burks (1979:771), "This may be a species complex, rather than a single species; careful rearings have produced specimens, at present indistinguishable, that are either primary or secondary parasites".

Resolving the status of *P. hyalinus* could have important implications for the biological control of insect pests important to agriculture and forestry. Careful rearing studies have revealed *P. hyalinus* (*s.l*) as primary parasitoids attacking *Neodiprion* sawflies (Hymenoptera: Diprionidae), which are serious forest pests particularly in boreal forests (Alfaro and Fuentealba 2016; Johns et al. 2016). But this nominal species is also a common hyperparasitoid, parasitizing dipteran (Sarcophagidae and Tachinidae) and hymenopteran (Ichneumonoidea) primary parasitoids of Lepidoptera and Orthoptera (Smith 1912; Kelly 1914; Clausen 1940; Smith 1958), thereby possibly interfering with population regulation of insect herbivores by the primary parasitoids.

To clarify the status of the *P. hyalinus* species group, Yoo (2023) has incorporated molecular data from two genes (COI and ITS2) along with a critical analysis of morphological characters to identify 25 "candidate" species in which morphology and genes were in agreement, and 5 "candidate" species with unique combinations of morphological character states consistent across multiple specimens. A phylogenetic analysis of the molecular data indicated that the *P. hyalinus* species group is comprised of two strongly supported monophyletic species complexes, both of which contain species in the Nearctic and Neotropical regions (Fig. 1, modified from Yoo 2022): the *P. carolinensis species* complex (including *P. carolinensis* Smulyan, *P. regalis* Smulyan and 5 undescribed species, Yoo and Darling, in preparation) and the *P. hyalinus* species complex (including *P. hyalinus*). Phylogenetic analyses of the combined COI and ITS2 data suggest that the 9 Nearctic species of the *P. hyalinus* species complex belong to three separate clades of the *P. hyalinus* species group (Fig. 1).

In this paper we revise the *P. hyalinus* species complex and recognize 10 Nearctic species using morphology, molecular data (COI and ITS2), and host information. We also designate a Neotype for *Perilampus hyalinus* Say. Most of Thomas Say's type

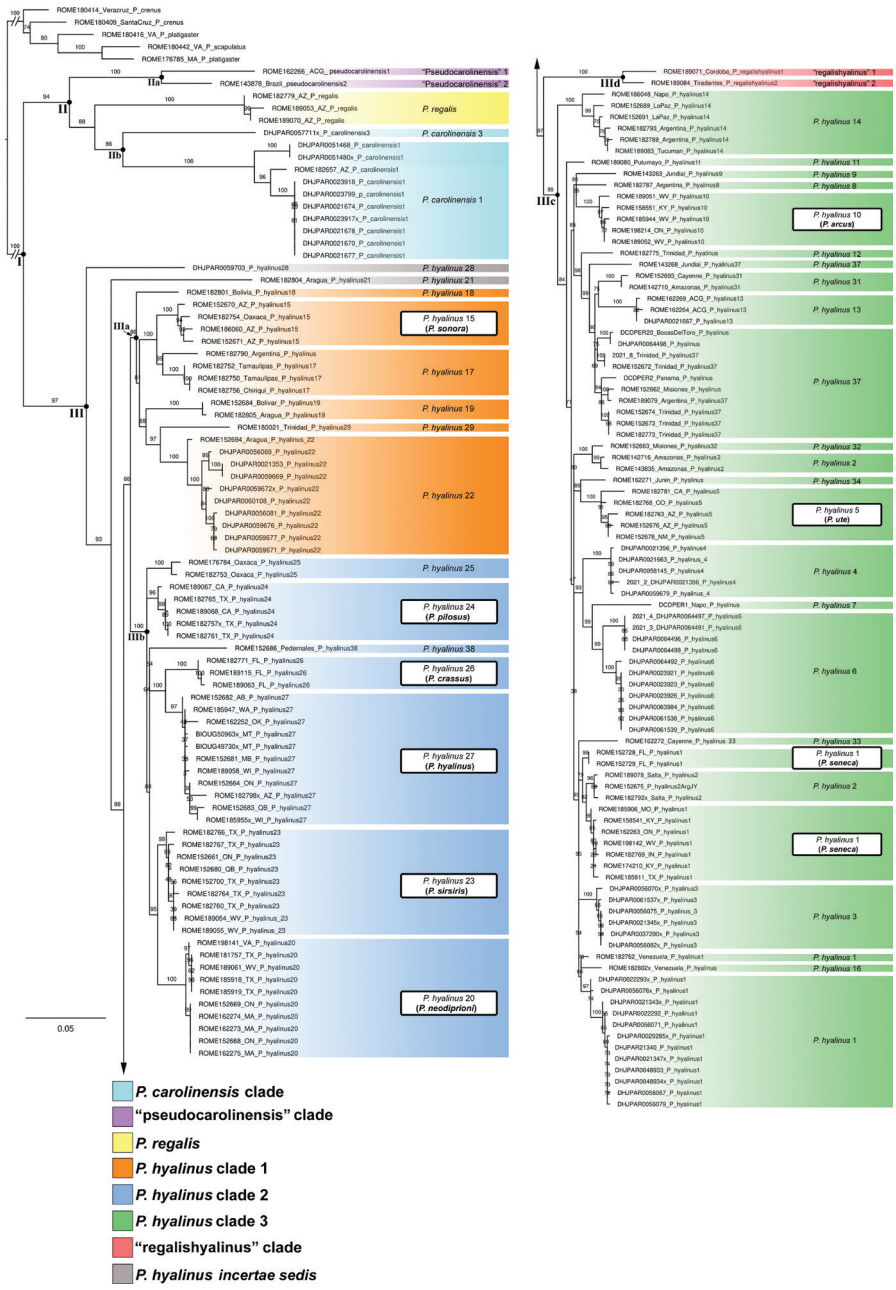

Figure 1. Maximum likelihood tree of *Perilampus hyalinus* species group retrieved from the combined analysis of COI and ITS2 (modified from Yoo 2023). Bootstrap support values are shown on the left side of the nodes. The roman numerals and black dots adjacent to the nodes indicate the major morphological clades recovered as monophyletic (I = *P. hyalinus* species group; II = *P. carolinensis* species complex; IIa = "pseudocarolinensis" clade; IIb = *P. carolinensis* clade; III = *P. hyalinus* species complex; IIIa = *P. hyalinus* clade 1; IIIb = *P. hyalinus* clade 2; IIIc = *P. hyalinus* clade 3; IIId = "regalishyalinus" clade. The morphospecies designation for the sequences is marked by vertical bars, colored according to their placements within their respective morphological subgroups. The names of the species described herein are indicated in white boxes.

material is regarded as lost and the surviving Say specimens are in the Museum of Comparative Zoology (MCZ), Harvard University (Mawdsley 1993). There are no specimens of Chalcidoidea described or identified by Say in the MCZ and a Neotype needs to be designated to fix the name *Perilampus hyalinus* objectively. The new species described and recognized herein present "exceptional need" (as defined by Article 75.3 of the International Code of Zoological Nomenclature [fourth edition] 1999) justifying the designation of a Neotype. We also discuss reasons for the diverse host associations in the *P. hyalinus* species complex and suggest areas for future research on the Nearctic species.

Methods

Morphology

Specimens were examined with a Leica MZ7.5 stereo zoom microscope and were illuminated with a Leica 20-watt halogen light source, filtered through a strip of translucent Mylar® film. Images of specimens were taken with a Keyence digital microscope VHX-7000 series, and edited with Adobe® Illustrator CC ver. 21.0.2 (Adobe Systems Inc., California, USA). The material examined and descriptions for each species were generated by a series of R coding commands and an Excel spreadsheet; the R-codes are freely available on GitHub (https://github.com/esdarling/r-taxonomy). The Excel spreadsheet for the species descriptions was output from Lucid Builder 3.3 (University of Queensland, Australia). Morphological terms mostly follow Darling (1983), Gibson (1997), and Darling and Yoo (2021) with the following modifications and additional terms. Frontal carina is a raised knife-edged ridge extending from the vertex (Fig. 2B: fc) ventrad along the margin of the parascrobal area (Fig. 2A: psa) to near the lower eye margin (Fig. 2A: fc). The pronotum is "carinulate" if it has a raised carina running along the upper posterior margin visible from dorsal view (Fig. 2H: ca). This state was discovered and termed as "bicarinulate" by Argaman (1990), but we prefer the term "carinulate" because only one distinct carina can be observed. The setae on the face are considered sparse if the distance between two adjacent setal pores is usually about equal to or longer than the length of the setae (Fig. 4I), or dense, if the distance between two adjacent setal pores is usually shorter than the length of the setae (Fig. 14I). Pits on male scape are depressions or indentations that have pores (Fig. 3F). Pores on the male scape are well documented for various groups of Chalcidoidea such as Torymidae (Goodpasture 1975), Perilampidae (Darling 1983), Eulophidae (Dahms 1984), and Aphelinidae (Shirley et al. 2019). Also referred to as release-and-spread structures (RRS), these pores are connected to glandular cells within the scape and suggest the release and spread of pheromone for mate-recognition during courtship (Isidoro et al. 1996). Courtship in Chalcidoidea often involves elaborate movements of male antennae (e.g. Girault and Sanders 1910; Barass 1960). The male scape of Perilampidae has conspicuous pits that contain pores (Darling 1983) and are likely

RRS. The scape morphology of males, e.g. the distributions and shape of pores and pits, are useful for species discrimination in Perilampidae and other Chalcidoidea (e.g. Darling 1983; Shirley et al. 2019; Darling and Yoo 2021). Interestingly, many female specimens of the *P. hyalinus* species group and other species of Perilampidae also have pits, albeit distinctively fewer in numbers and often inconspicuous or entirely absent (Fig. 3D, E cf. Fig. 3F), and do not show consistent interspecific variability. In addition, the pits on the female scape are restricted to mesad on the anterior surface, covering no more than 0.2 × scape length. It is unclear if the pits on the female scape contain pores. The pits on scape are considered sparse if separated by distance usually longer than diameter of pits (Fig. 7F, G), dense if separated by distance usually equal to or shorter than the diameter of pits (Fig. 17G, H). The pitted area of the male scape in the *P. hyalinus* species group is never swollen anteriad, in contrast to several species in the other groups with a swollen pitted area. The axillar shelf is a horizontal cliff-like edge on the axilla extending from the anterior to posterior margin of the axilla in lateral view (Fig. 2F: axsh). Males usually have more bulbous eyes and larger ocelli than females which results in shorter lateral ocellar line, ocular ocellar line, and postocellar line in males.

All measurements were taken with the Keyence Communication software, either directly from the specimens or from digital images, in which case care was taken to avoid problems associated with parallax. The measurements of each species were taken from four to five specimens per sex. Holotype and paratypes were measured for each new species. The primary type for the previously described Nearctic *P. hyalinus* complex species could not be borrowed for measurement (e.g. *P. sirsiris*). For this species, the measurements were taken from conspecific specimens that were sequenced and/or with collection localities close to that of the types. Most of the following abbreviations for measurements follow Darling (1983) and Gibson (1997): AL, anellus length; AxH, axillula height at midpoint; AxL, axillula length; CH, clypeus height; CW, clypeus width; EH, eye height; EL, eye length; FC, frontal carina width across maximum diameter of median ocellus in dorsal view; FCLO, shortest distance between frontal carina and lateral ocellus; Fu#L, funicular segment length; Fu#W, funicular segment width; HH, head height; HL, head length; HW, head width in dorsal view; PSA, parascrobal area width at maximum eye width; LPP, lateral panel of pronotum width; LOD, lateral ocellus diameter; LOL, lateral ocellar line, the shortest distance between the median and a lateral ocellus; ML, mesosoma length in lateral view; MW, mesosoma width in dorsal view; MOD, median ocellus diameter; MSL, malar space length; MSC, length of mesoscutum in lateral view; OOL, ocular ocellar line, the shortest distance between the eye and a lateral ocellus; PL, pedicel length; PN, pronotum length in dorsal view; POL, postocellar line, the shortest distance between the lateral ocelli ; PPT, prepectus width; PW, pronotum width in dorsal view; PSW, width of parascrobal area at maximum eye length; SC, length of mesoscutellum in lateral view; SCH, supraclypeal area height; SCW, supraclypeal area width; SW, scrobe width at maximum width of head in anterior view; WL, wing length; WW, wing width. In addition to specified ratios (e.g. POL/OOL), POL, OOL, and LOL were compared with LOD as ratios (LOD: POL: OOL: LOL).

Material examined

Specimens were examined from the following collections: American Museum of Natural History, New York City, NY, United States (AMNH); California State Collection of Arthropods, Sacramento, CA, United States (CSCA); California Academy of Sciences, San Francisco, CA, United States (CAS); Canadian National Collection of Insects, Arachnids, and Nematodes, Ottawa, ON, Canada (CNC); Centre for Biodiversity Genomics, University of Guelph, Guelph, ON, Canada (CBG); Cornell University Insect Collection, Ithaca, NY, United States (CUIC); University of Guelph Insect Collection, Guelph, ON, Canada (DEBU); Entomological Museum at Utah State University, Logan, UT, United States (EMUS); Field Museum of Natural History, Chicago, IL, United States (FMNH); Florida State Collection of Arthropods, Gainesville, FL, United States (FSCA); Great Lakes Forestry Centre, Sault Ste. Marie, ON, Canada (GLFC); Illinois Natural History Survey, Champaign, IL, United States (INHS); Ministry of Agriculture, Fisheries and Food in Québec, Québec City, QC, Canada (MAPAQ); Museum of Comparative Zoology, Harvard University, Cambridge, MA, United States (MCZC); Natural History Museum, Berlin, Germany (MNHB); National Museum of Natural History, Paris, France (MNHN); Hungarian National Museum, Budapest, Hungary (HNHM); North Carolina State University Insect Collection, Raleigh, NC, United States (NCSU); Natural History Museum, London, United Kingdom (NHMUK); the Royal Ontario Museum, Toronto, ON, Canada (ROM); Snow Entomological Museum Collection, Lawrence, KS, United States (SEMC); Texas A&M University, College Station, TX, United States (TAMU); University of Arkansas, Fayetteville, AR, United States (UAAM); University of Arizona Insect Collection, Tucson, AZ, United States (UAIC); University of California, Davis, CA, United Staes (UCDC); University of Central Florida, Orlando, FL, United States (UCFC); University of Colorado Museum, Boulder, CO, United States (UCMC); Entomology Research Museum, University of California, Riverside, CA, United States (UCRC); W.R. Enns Entomology Museum, University of Missouri, Columbia, MO, United States (UMRM); Smithsonian National Museum of Natural History, Washington, DC, United States (USNM); Insect Collection, University of Texas, Austin, TX, United States (UTIC); Wisconsin Insect Research Collection, University of Wisconsin-Madison, WI, United States (WIRC); J.B. Wallis/R.E. Roughley Museum of Entomology, University of Manitoba, Winnipeg, MB, Canada (WRME). The primary types of the previously described species of the *P. hyalinus* species group were studied by examining available specimens or images sent by the repositories the repositories (Suppl. material 6). A summary of the non-type specimens examined is provided for each species in the Suppl. materials. The specimens of particular interest that are mentioned in Variation and/or Remarks sections or that were unsequenced and collected from outside the Nearctic region are listed as Additional Material Examined. The label data of holotypes are reported as verbatim.

DNA sequencing

Hind legs and/or middle legs were removed from the specimens of each morphospecies for DNA extraction. The molecular work was done either Canadian Centre for DNA Barcoding (CCDB) at the University of Guelph or in the Laboratory of Molecular Systematics (LMS) at Royal Ontario Museum. At LMS, DNA was extracted using a Qiagen DNeasy Blood and Tissue Kit following the manufacturer's instructions and DNA was eluted with 50 µl of AE buffer. Each 25 µl PCR reaction consisted of 1 µl of template DNA, 18.89 µl ddH2O, 0.56 µl dNTPs [10 mM], 0.05 µl Platinum Taq (Invitrogen), 1 µl [0.01 mM] each of the universal COI primers LCO1490 and HCO2198 (Folmer et al. 1994) and 2.5 µl 10 × PCR buffer (Invitrogen). PCR thermo-cycling conditions were an initial hot start of 94 °C for 1 min, 5 cycles of denaturation at 94 °C for 30 s, annealing at 42 °C for 40 s and extension at 72 °C for 1 min, then 35 cycles of denaturation at 94 °C for 30 s, annealing at 46 °C for 40 s and extension at 72 °C for 1 min, with a final extension at 72 °C for 5 min. Three microliters of PCR products were combined with 3 µl loading dye and visualised using 1% agarose gel. Only amplicons with single, intense bands were sequenced. Before sequencing the remaining 23 µl of PCR product was treated with 0.5 ul of ExoSAP-IT (Applied Biosystems) and 1.5 µl ddH2O and placed in a thermocycler under the following conditions: 37 °C for 15 min, 80 °C for 15 min, and then a 4 °C hold. Each sequencing reaction consisted of 2 µl of PCR product along with 0.5 µl BIG DYE 3.1 reagent (Applied Biosystems), 0.5 µl LCO1490/HCO2198 primer, 5 µl ddH20 and 2 µl 5 × sequencing buffer (Invitrogen) and were then run on an ABI 3730 capillary sequencer (Applied Biosystems). At CCDB, DNA was extracted using the automated CCDB glass fiber membrane method for 96-well plates (Ivanova et al. 2006). PCR amplification and sequencing reactions followed standard CCDB protocols (Hajibabaei et al. 2005). Identical primers were used in both institutions for PCR amplification: primers LepF1 (5'- ATTCAACCAAT CATAAAGATATTGG-3') and LepR1 (5'TAAACTTCTGGATGTCCAAAAAATCA-3') were used for COI; and ITS2F (5'TGTGAACTGCAGG ACACATG-3') and ITS2R2 (5'-TCTCGCCTGCTCTGAGGT-3') were used for ITS2. At CCDB, various mixes of primers were also used for additional amplifications for the taxa with poor quality DNA. The majority of the assembled sequences were uploaded to and downloaded from the Barcode of Life Data Systems (Ratnasingham and Hebert 2007). Prior to alignment, trace files of COI sequences were inspected with Chromas ver. 2.6.6 (Technelysium Pty Ltd., Helensvale, Australia) and edited where necessary for quality control.

Molecular analyses

The *Perilampus platigaster* species group is regarded as the sister group to the *P. hyalinus* species group based on two putative morphological synapomorphies, frontal carina and finger-like axillula (Darling 1996), and was used as the outgroup. COI sequences were aligned with MUSCLE algorithm (Edgar 2004) implemented in

MEGA ver. 10.1.6 (Kumar et al. 2018) with default settings. ITS2 sequences were aligned with MAFFT v.5 online server (Katoh 2013) with default settings except for the alignment strategy was changed to L-INS-i, and scoring matrix for the sequences was changed to 1PAM/K=2. COI and ITS2 datasets were concatenated with MEGA ver. 10.1.6, using only the specimens that were successfully sequenced for both genes. COI and ITS2 sequences were trimmed with MEGA ver. 10.1.6 to a maximum length of 600 bp and 450 bp, respectively. Sequences shorter than 50% of the maximum alignment length were excluded from the analyses. jModelTest (Darriba et al. 2012) implemented in IQ-TREE ver.2.1.3 (Nguyen et al. 2015) was used to select the most suitable nucleotide substitution models for the phylogenetic analyses, restricted to only those supported by MrBayes, for the analyses under Bayesian Information Criterion: GTR +I+G4 for COI; and HKY+G4 for ITS2. Maximum likelihood (ML) and Bayesian phylogenetic inference (BI) analyses were conducted for both single and concatenated datasets, using IQ-TREE ver.2.1.3 and MrBayes ver. 3.2.7 (Huelsenbeck et al. 2001; Ronquist et al. 2012), respectively. Each ML analysis was conducted in IQ-TREE ver.2.1.3, with 1000 initial parsimony trees, 20 best trees retained during search, and 1000 ultrafast bootstrap iterations for branch support (Hoang et al. 2018). The convergence was evaluated by inspecting the trace plots with Tracer ver. 1.7.1 (Rambaut et al. 2018) to verify if all estimated sample sizes (ESS) were > 200. The first 25% of the samples were discarded as burn-in, and the remaining trees were used to construct the 50% majority rule consensus tree. All trees were visualized with Figtree ver. 1.4.4 (Rambaut 2018) and further edited with Adobe® Illustrator CC ver. 21.0.2.

The pairwise uncorrected p-distances within and between preliminary species inferred from morphology were calculated in PAUP* 4.0a169 (Swofford 2003) using minimal evolution and constraining negative branch lengths to be non-negative, ignoring gaps for affected sites, with equal rates for variable sites, and estimating variation for all substitutions. For each morphospecies, the minimum interspecific distances to the nearest neighbor and the maximum intraspecific distances were obtained.

Three molecular species delimitation methods were employed for each locus to estimate the number of molecular operational taxonomic units (MOTUs): Automatic Barcoding Gap Discovery (ABGD) (Puillandre et al. 2011), Barcode Index Number (BIN) system (Ratnasingham and Hebert 2013), and Poisson Tree Processes (PTP) (Zhang et al. 2013). The finalization of preliminary species was based on comparison across the partitioning of morphospecies and MOTUs, further supported with available host information. ABGD delimits MOTUs by recursively partitioning the data using the barcode gap between pairwise interspecific and intraspecific distances (Puillandre et al. 2011). In ABGD, the position of the barcode gap is inferred based on a range of genetic intraspecific divergences (P) and relative gap width (X) defined a priori. In this study, ABGD method was performed on the online web application (https://bioinfo.mnhn.fr/abi/public/abgd/abgdweb.html) with pairwise uncorrected p-distances calculated with PAUP. Default P values from 0.001 to 0.1 were used for both the COI and ITS2 datasets. The number of steps was set to 30, and the X

value of 0.5 was analyzed. ABGD resulted in highly variable number of MOTUs across the *P* values, likely due to the lack of clear barcoding gaps (Yoo 2023). The partitioning schemes from Yoo (2023) that were best corroborated by morphology and other delimitation methods were presented as the most biologically plausible (Puillandre et al. 2011). The initial and recursive partitions at P = 0.0057–0.0067 was selected for COI. The recursive partition at P = 0.0036–0.0067 was selected for ITS2. The BIN system is another distance-based species delimitation method. Barcode of Life Data Systems (Ratnasingham and Hebert 2007) automatically assigned BINs to each sequence with Refined Single Linkage Analysis (RESL) which delimits molecular operational taxonomic unit based on a 2.2% threshold of sequence divergence, then refined by Markov clustering (Ratnasingham and Hebert 2013). Since BOLD currently assigns BINs only for COI, this method could not be applied for the ITS2 sequences. PTP is a tree-based species delimitation method which models speciation rates using the number of substitutions obtained from branch lengths of phylogenetic tree (Zhang et al. 2013). Under the assumption that there are a significantly higher number of substitutions between species than within species, the method identifies the transition points between speciation and coalescent processes (Zhang et al. 2013). The PTP analyses were performed using the online web application (https://species.h-its.org) using the above ML trees obtained from IQ-TREE ver.2.1.3 as inputs. 500,000 MCMC generations, thinning value of 100, a burn-in of 10%, and outgroups were removed to improve the species delimitation. MCMC chains did not converge despite using the available maximum number of generations (500,000), thus only the results of maximum likelihood solutions are reported. With ITS2, the inclusion of the complete *P. hyalinus* species group data set resulted in grouping of the majority of the species in the *P. hyalinus* species complex into two molecular taxonomic units (MOTUs) while the exclusion of most divergent species such as those in the *P. carolinensis* species complex partitioned MOTUs closer to morphology and COI (Yoo 2023). This is likely due to the greater degree of uneven branch length distributions between *P. carolinensis* species complex and the most members in the *P. hyalinus* species complex in ITS2. Because PTP assumes constant speciation and coalescent rates across phylogeny (Zhang et al. 2013), the algorithm may have classified longer branches outside the *P. hyalinus* species complex as speciation processes, while classifying the mostly shorter branches within the species complex as coalescence processes (Yoo 2023). Therefore, the results from two separate PTP analyses with ITS2 were merged to obtain the total MOTU partitioning scheme.

Species distributions

The species distribution maps were made with the online GIS tool SimpleMappr (Shorthouse 2010), and further edited with Adobe® Illustrator CC ver. 21.0.2 (Adobe Systems Inc., California, USA). The complete data for each specimen, including species, type status, locality information with coordinates and sequencing information is

archived on the TMS Collections Management System (ROM) and will be added to the Global Biodiversity Information Facility (www.GBIF.org) after publication and the validation of the new species.

Host associations

The host association of individual specimens was obtained from the associated labels, available host remains, and/or publications. Where necessary, the host names were updated to reflect the current nomenclature. In many instances, the dipteran or ichneumonid primary parasitoid hosts pupated inside the cocoons or pupae of their herbivore hosts. This necessitated a careful examination of the inner contents of the cocoons and pupae to determine whether the *Perilampus* had developed as primary or hyperparasitoids. The sawfly cocoons and lepidopteran pupae from which *Perilampus* exited were either dissected (Fig. 26B cf. 26A) or their interiors were examined through the exit hole (Fig. 26A: eh) using halogen light sources. The presence of parasitoid cocoons (Fig. 26C, E: Ic) or puparia (Fig. 26D, F, H: Tp) indicated the development as hyperparasitoids, while their absence (Fig. 26B, G) indicated primary parasitoids.

Results

The molecular analysis provides strong support for both the *P. hyalinus* species group and the *P. hyalinus* species complex—both the ML and BI analyses yielded similar tree topologies (Fig. 1, Suppl. material 1: BS ≥ 96, PP = 1). In addition, the *P. hyalinus* species complex is further divided into three well supported major clades (Figs 1, Suppl. material 1: BS ≥ 86, PP ≥ 0.90) and eight of nine Nearctic morphospecies, including the parasitoids associated with *Neodiprion* sawflies, show well supported monophyly with the combined data (Figs 1, Suppl. material 1 BS ≥ 95, PP = 1) or at least one or both loci (Suppl. materials 2–4, COI BS ≥ 92, PP ≥ 0.76; ITS2 BS ≥ 90, PP ≥ 0.94). The eight species were also successfully delimited with at least one gene (Suppl. materials 2, 5). The molecular analysis pertaining to the entire Western Hemisphere and phylogenetic structure within the *P. hyalinus* species group are discussed in detail in Yoo (2023).

The BINs assigned for each specimen by BOLD are shown in the material examined. The current BINs (December 28, 2023) and the number of BINed specimens are indicated in the remarks section for each species. The pairwise uncorrected distances for each gene for the Nearctic species are summarized in Table 1. The minimum interspecific divergences with COI range from 1.2% to 4.6%, and maximum intraspecific divergences range from 0.7% to 2.3%. The minimum interspecific divergences with ITS2 range from 0.7% to 4.5%, and maximum intraspecific divergences range from 0 to 0.7%. The overlap of minimum interspecific and maximum intraspecific divergences suggests the absence of a global barcode gap (Wiemers and Fiedler 2007; Kvist 2016) in the Nearctic *P. hyalinus* species complex in both COI and ITS2.

Table 1. Pairwise uncorrected p-distances for two genes among Nearctic members of the *Perilampus hyalinus* species complex. Intraspecific distances are along the diagonal, ITS2/COI. Interspecific distances for COI are below diagonal, for ITS2 are above diagonal.

	P. arcus	*P. crassus*	*P. neodiprioni*	*P. hyalinus*	*P. pilosus*	*P. seneca*	*P. sirsiris*	*P. sonora*	*P. ute*
P. arcus	**0/0–1.2**	4.5	4.1	3.4–4.5	4.1–4.2	0.7	4.5–4.8	3.1	2.1–2.8
P. crassus	4.0–5.5	**0/0.2–0.5**	2.8	1.0	2.4	3.8	2.4–2.8	3.4–3.5	4.5–5.2
P. neodiprioni	4.0–5.3	2.7–3.7	**0/0–0.9**	1.7	2.4	3.4	1.7–2.1	2.8	4.5–4.9
P. hyalinus	4.2–6.2	1.6–4.0	3.0–4.7	**0/0–2.3**	1.4	2.8	1.4–1.7	2.4	3.4–4.2
P. pilosus	3.5–4.4	2.3–3.6	2.3–3.4	1.2–2.9	**0/0–1.0**	3.4	2.1–2.4	2.4	4.1–4.9
P. seneca	2.5–4.0	4.0–5.3	3.4–4.7	4.3–6.7	3.8–5.2	**0/0.2–0.7**	3.8–4.1	2.4	1.4–2.1
P. sirsiris	3.3–4.5	2.2–4.1	1.3–2.6	2.1–3.8	1.3–2.2	3.2–5.0	**0–0.3/0–1.3**	3.1–3.5	4.5–5.6
P. sonora	3.9–5.8	4.2–6.3	4.0–5.2	4.6–6.5	3.7–4.8	3.4–5.4	3.5–4.7	**0–0.3/1.0–1.3**	3.8–4.5
P. ute	3.1–4.4	3.7–5.5	3.2–4.2	4.1–6.5	4.1–6.5	2.2–3.0	2.9–4.7	4.0–5.2	**0–0.7/0.3–2.0**

Perilampus hyalinus species group

Figs 2A, B, D, F, H, 3

Family Perilampidae Fŏrster, 1856

Genus *Perilampus* Latreille, 1809

Taltonos Argaman, 1990 (subjective synonym, Darling, 1996).

P. hyalinus species group sensu Smulyan (1936) and Darling (1996)

Description. Female. Color: head and body entirely or at least partially brightly iridescent (Fig. 2A, H).

Head: in anterior view weakly transverse, slightly wider than high, HW/HH 1.2–1.3; slightly wider than pronotum, HW/PW 1.1–1.2. Frontal carina: distinct, extended from posterior margin of median ocellus (Fig. 2B) to near lower eye margin (Fig. 2A); in dorsal view narrow near median ocellus. Ocelli: median ocellus in line with lateral ocelli or only slightly advanced (Figs 2B, 12G). Eye: slightly shorter than head height, EH/HH 0.6–0.7. Vertex: rounded behind. Occiput: with vertical groove below vertex, with subparallel costulae; occipital carina absent. Malar space (Fig. 2A): with oblique striae obliterating malar sulcus (Fig. 2D). Clypeus (Fig. 3A): weakly transverse to strongly transverse, CW/CH 1.3–1.6; lateral sulci straight or weakly curved, strongly divergent; with small and indistinct tentorial pits; epistomal sulcus concave, deeper and more distinct than lateral sulci; ventral margin concave or nearly flat. Supraclypeal area (Fig. 3A): subquadrate; shorter and narrower than clypeus, SCH/CH 0.5–0.6. Scape (Figs 3C–E): length about 0.6 × EH; narrow throughout; pits absent or if present distad covering no more than 0.2 × scape length (Figs 3 D, E). Flagellum (Fig. 3I): anellus transverse, AL/PL about 0.3; Fu1 subquadrate, Fu1L/Fu1W 1.0–1.1; subequal to or slightly longer in length than pedicel, Fu1L/PL 1.0–1.3; Fu2 subquad-

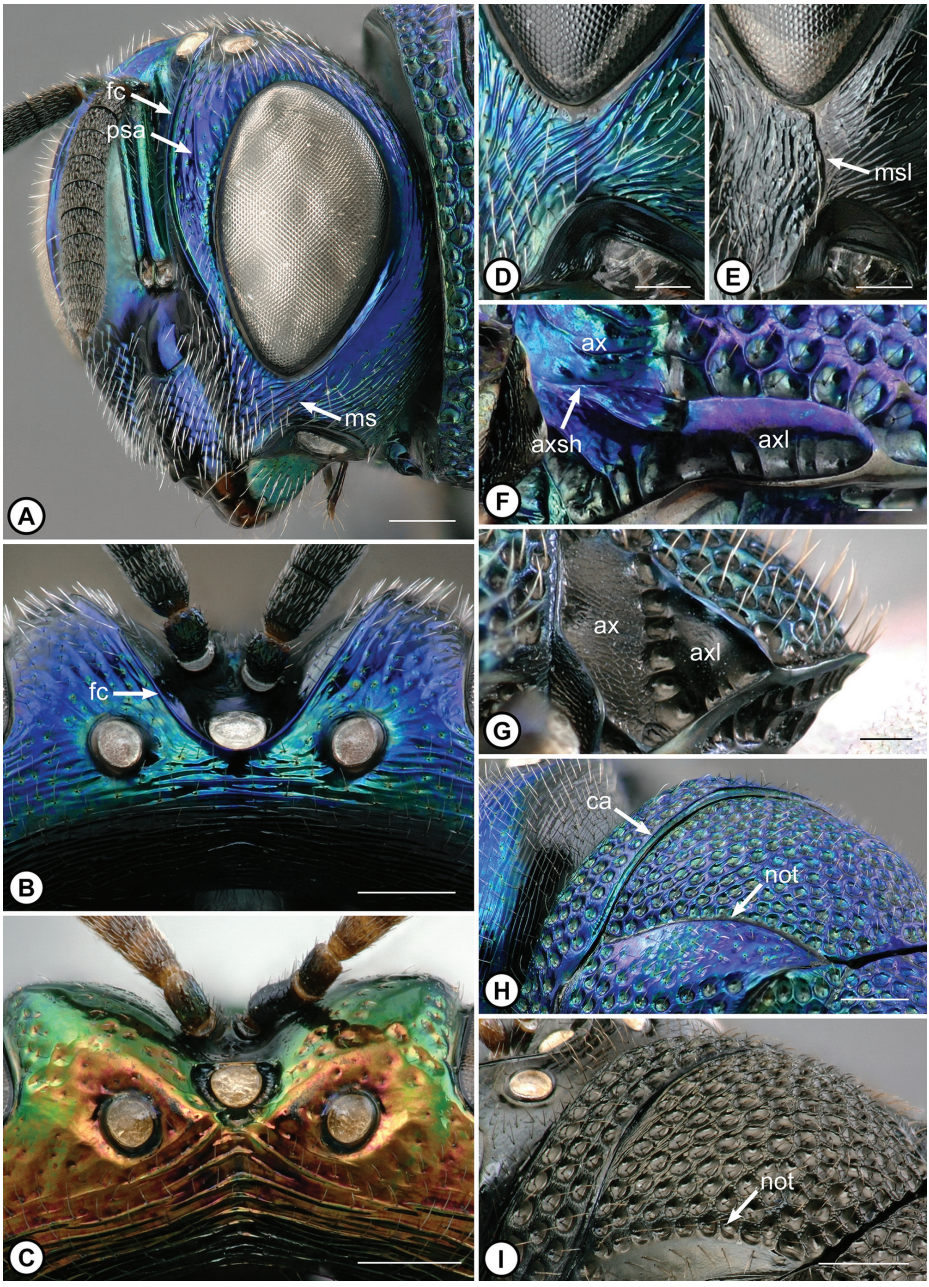

Figure 2. The morphological characters of *Perilampus hyalinus* species group (A B D H F) and other *Perilampus* species groups (C E G I) **A** head, anterior-oblique view, *P. seneca* **B** vertex, dorsal view, *P. neodiprioni* **C** vertex, dorsal view, *P. auratus* **D** malar space, *P. seneca* **E** malar space, *P. platigaster* **F** axilla and axillula, *P. hyalinus* **G** axilla and axillula, *Perilampus* sp. **H** pronotum and mesoscutum, posterior oblique view, *P. neodiprioni* **I** pronotum and mesoscutum, posterior oblique view, *P. platigaster*. Abbreviations: ax, axilla; axl, axillula; axsh, axillar shelf; ca, carina; fc, frontal carina; ms, malar space; msl, malar sulcus; not, notaulus; psa, parascrobal area. [**A** ROME182769; **B, H** ROME162273; **C** ROME162320; **D** ROME199563; **E** ROME141508; **F** ROME162229; **G** ROME182831; **I** DHJPAR0038540]. Scale bars: 250 μm (**A–C, H, I**); 100 μm (**D–G**).

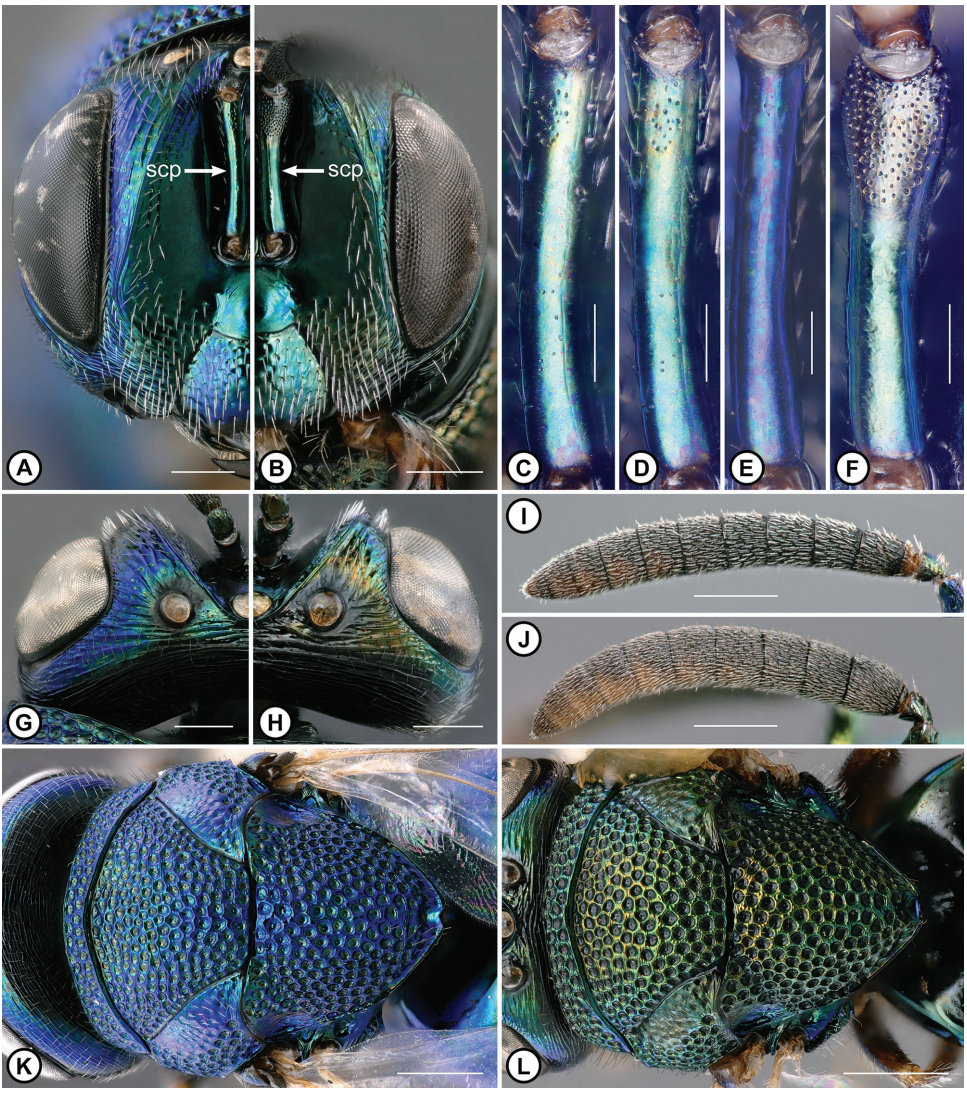

Figure 3. Sexual dimorphism in the *Perilampus hyalinus* species group **A** female head, anterior view, *P. seneca* **B** male head, anterior view, *P. seneca* **C** female scape anterior margin, *P. seneca* **D** female scape inner margin, *P. seneca* **E** female scape inner margin, *P. neodiprioni* **F** male scape anterior margin, *P. neodiprioni* **G** female head, dorsal view, *P. seneca* **H** male head, dorsal view, *P. seneca* **I** female flagellum, *P. seneca* **J** male flagellum, *P. seneca* **K** female habitus, dorsal view, *P. neodiprioni* **L** male habitus, dorsal view, *P. neodiprioni*. Abbreviation: scp, scape. [**A** ROME199563; **B** ROME183976; **C, D** ROME199531; **E** ROME198219; **F** ROME198147]. Scale bars: 250 μm (**A, B, G–J)**; 100 μm (**C–F**); 500 μm (**K, L**).

rate or transverse, Fu3–Fu7 transverse; clava 4-segmented, C1–3 as long dorsad as ventrad, with distinct terminal button (C4).

Mesosoma: slightly longer than wide, ML/MW 1.2–1.3. Pronotum: carinulate (Fig. 2H); short, PN/MSC about 0.2; shorter along midline, 0.5–0.7 length laterad;

anterior margin sharp, all rows of punctures on same plane. Lateral panel of pronotum: without flange (Fig. 4D) or with flange below level of mesothoracic spiracle in posterior oblique view (Fig. 16D: arrow); anterior margin sharp, all rows of punctures on same plane. Prepectus: wide and triangular; differentiated from pronotum with distinct suture; ventral strap short, without row of alveolae; central area of lateral panel smooth, with foveae along dorsal and posterior margins. Mesoscutum (Fig. 2H): midlobe without tubercle; notaulus distinct and continuous, uninterrupted by sculpture of mesoscutum. Mesoscutellum: without tubercle; slightly longer than mesoscutum, SC/MSC 1.2–1.3; strongly vaulted, frenum ventrad and not visible in the dorsal view. Axilla: with axillar shelf (Fig. 2F). Axillula: elongate and finger-like, AxL/AxH usually 2.0 or greater (Fig. 2F). Metanotum: short, length 0.4–0.5 × length of propodeum along midline. Propodeum: width about 3 × length along midline; submedian area smooth to weakly imbricate, with foveae or groove laterad median carina, delimited laterad and ventrad by complete plicae, dorsad by transverse band of foveae; callus with angulate process below spiracle, and alveolate-rugose, with alveolae sometimes obliterated below spiracle; nucha with transverse to arcuate rugae. Fore wing: elongate, WL/WW 2.3–2.4; hyaline, with yellow or brown venation; parastigma swollen with weak equilateral triangular process; postmarginal vein 0.7–0.8 × as long as marginal vein; stigmal vein 0.3–0.4 × as long as marginal vein; stigma with weak uncus.

Metasoma: petiole short and straplike, with weak transverse wrinkles; petiolar flange short with ventral margin of upper area with shallow emargination mesad; antecostal sulcus transverse, with weak vertical carinae laterad and smoothened mesad; Mt2 with trapezoidal demarcation and shallow median groove, imbricate and wrinkled anteriad, and smooth posterad without lateral protruberances along midline, posterior margin straight and sparsely setose; Mt3 smooth.

Male. As in female, except: Color: mesonotum sometimes nearly entirely black or with cupreous iridescence (Fig. 3L cf. Fig. 3K). Eye: in dorsal view often more bulbous (Fig. 3H cf. Fig. 3G). Ocellus: often larger (Fig. 3H cf. Fig. 3G). Ocellar ratios LOD: POL: OOL: LOL: often shorter. Frontal carina: distance from lateral ocellus usually shorter. Malar space: MSL/EH often shorter. Flagellum: slightly wider (Fig. 3J cf. Fig. 3I). Scape (Fig. 3F): in anterior view weakly expanded distad, 1.3–1.4 × width above radicle; with distinct pits on anterior surface (Fig. 3F cf. Fig. 3D, E); pitted surface not swollen in lateral view. Aedeagus: without a pair of lateral spines.

Diagnosis. The *P. hyalinus* species group is characterized by: brightly iridescent coloration (Fig. 2A, H), distinct frontal carina extended from posterior margin of median ocellus (Fig. 2B cf. Fig. 2C) to near lower eye margin (Fig. 2A), oblique costae obliterating malar sulcus (Fig. 2D cf. Fig. 2E), carinulate pronotum (Fig. 2H cf. Fig. 2I), distinct and uninterrupted notaulus (Fig. 2H), axilla with axillar shelf (Fig. 2F cf. Fig. 2G), and elongate and finger-like axillula (Fig. 2F cf. Fig. 2G). The *P. platigaster* species group has a similar structure of the frontal carina, axilla, and axillula, but is distinguished by having a malar sulcus (Fig. 2E cf. Fig. 2D) and the general body color black with or without weak iridescent reflections (Fig. 2I cf. Fig. 2H).

Distribution. The *P. hyalinus* species group occurs exclusively in the Western Hemisphere, from the southern Canada to Argentina.

Host association. The previously published host records indicate that species are mostly hyperparasitoids, parasitizing dipteran (Tachinidae and Sarcophagidae) and hymenopteran parasitoids (Ichneumonoidea) of Lepidoptera, Orthoptera, and rarely, Phasmatoidea and Coleoptera (e.g. Smith 1912; Smith 1958; Pitts et al. 2002; Janzen and Hallwachs 2009). Smith (1912) gave a detailed description of the biology of *P. hyalinus* Say as an indirect hyperparasitoid—the planidia actively searches and burrows into the host of the primary parasitoid (e.g. caterpillars), but can only feed and develop on the dipteran or hymenopteran parasitoids. There are relatively fewer cases of primary parasitoids in the *P. hyalinus* species group, and the best documented are the parasitoids of *Neodiprion* sawflies (Hymenoptera: Diprionidae) (Tripp 1962).

Remarks. This species group was hypothesized as a monophyletic group based on morphological characters (Darling 1996) and was well corroborated in our combined analysis of COI and ITS2 (Fig. 1). The oblique costae obliterating the malar sulcus (Fig. 2D) is the only shared and putatively derived character exclusive to this species group. Other character states (e.g. frontal carina) are widely distributed across Perilampidae in varying combinations, and a comprehensive phylogenetic analysis of this family is required to understand their evolution. Yoo (2023) recognized two clades in the *P. hyalinus* species group supported by COI+ITS2 and morphology: the *P. carolinensis* species complex, which has a parascrobal area abruptly narrowed in lateral view and the lateral panel of pronotum without a flange (Fig. 1 Clade II), and the *P. hyalinus* species complex which has a parascrobal area usually gradually narrowed in lateral view and the lateral panel of pronotum with or without a flange (Fig. 1 Clade III). The *P. hyalinus* species complex is further divided into three major clades which are congruent in genetic and morphological characters, for example the density of pits on the male scape, the shape of the lateral panel of the pronotum, and color of the mesonotum in females (Yoo 2023). The species in the *P. hyalinus* clade 3 (IIIc, Fig. 1), including *P. arcus*, *P. seneca*, and *P. ute*, are distinguished by a usually densely pitted male scape (Figs 17G, 17H, 19H, 19I, 21G, 21H) and the lateral panel of pronotum with a triangular flange (Figs 16D, 18D, 20D). The species in the *P. hyalinus* clade 1 (IIIa, Fig. 1), including *P. sonora*, can be recognized by the cupreous mesonotum in females (Fig. 22B), in addition to the usually sparse pits on the male scape (Fig. 23G, H) and the lateral panel of the pronotum that lacks a triangular flange (Fig. 22D). The *P. hyalinus* clade 2 species (IIIb, Fig. 1), including *P. crassus*, *P. neodiprioni*, *P. hyalinus*, *P. monocteni*, *P. pilosus*, and *P. sirsiris*, also has a sparsely pitted male scape (Figs 5G, H, 7F, G, 9G, H, 11G, H, 13G, H, 15F, G) and the lateral panel of pronotum without a triangular flange (Figs 4D, 6D, 8D, 10D, 12D, 14D). But the *P. hyalinus* clade 2 species do not have the strong cupreous mesonotum in females (e.g. Fig. 4B), except in *P. pilosus* (Fig. 15A).

Key to the Nearctic *P. hyalinus* species group

1 Parascrobal area in lateral view abruptly narrowed towards lower eye margin (A, B); outer orbit with long and wide smooth area (A, B); lower face sparsely setose (C, D)..... ***P. carolinensis* species complex, 2**

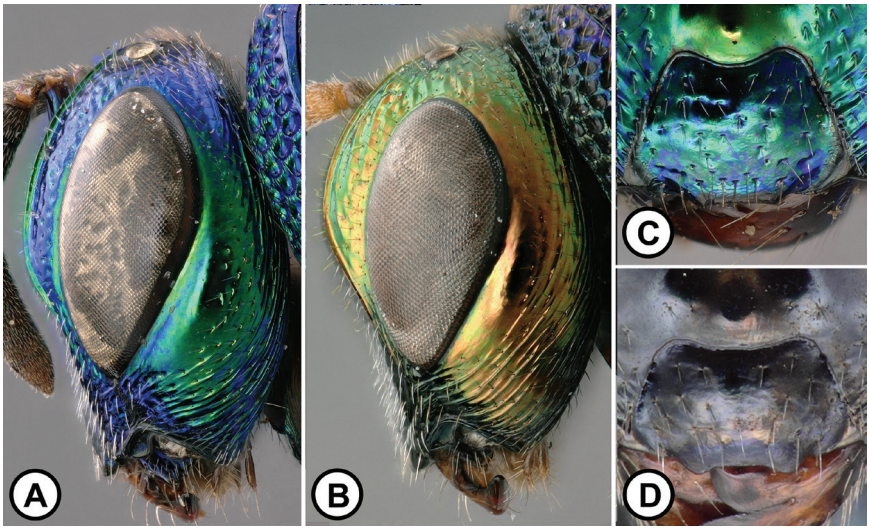

– Parascrobal area in lateral view gradually narrowed towards lower eye margin (a, b); outer orbit with short and narrow smooth area (a) or entirely striate (b), rarely with long and wide smooth area; lower face densely (c) or sparsely (d) setose..... ***P. hyalinus* species complex, 3**

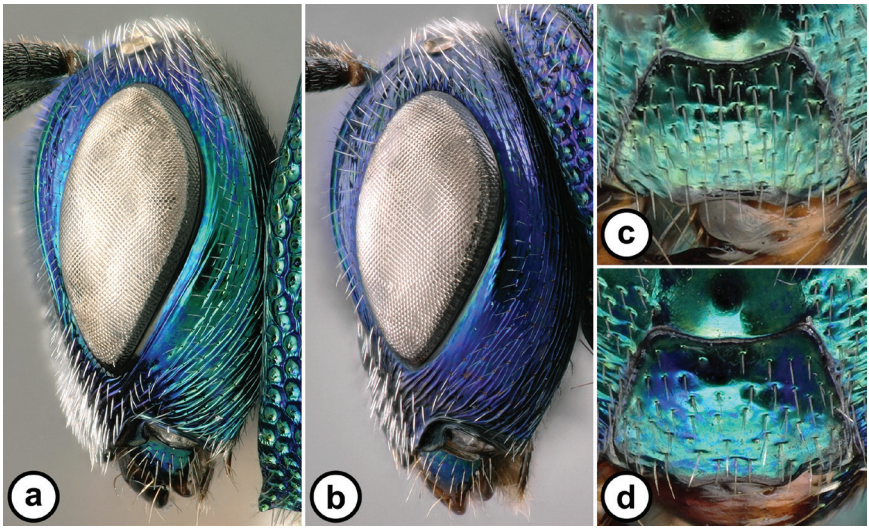

2(1) Head cupreous; parascrobal area in lateral view abruptly narrowed at or above midheight of the eye (A); median ocellus advanced to form a narrow triangle with lateral ocelli (B); female flagellum yellow .....***P. regalis*** **Smulyan**

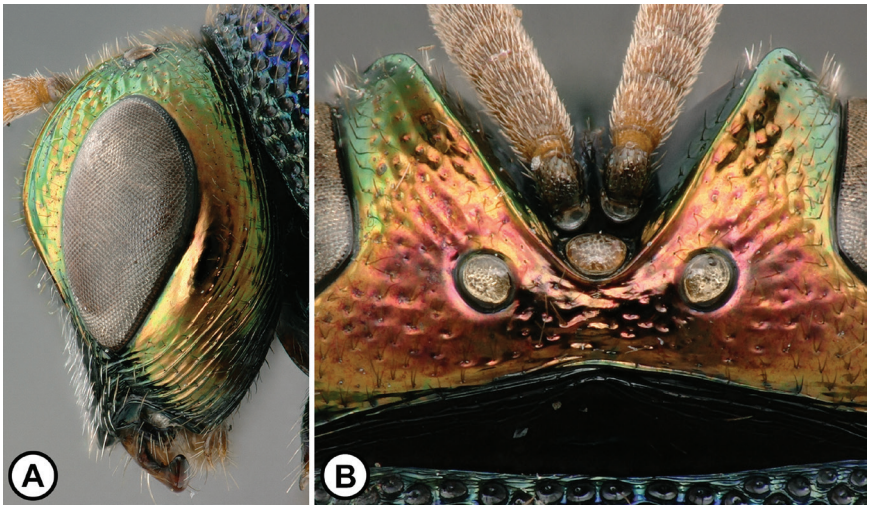

– Head greenish to violaceous; parascrobal area in lateral view abruptly narrowed below midheight of the eye (a); median ocellus in line with lateral ocelli (b); female flagellum black or brown.....***P. carolinensis*** **Smulyan**

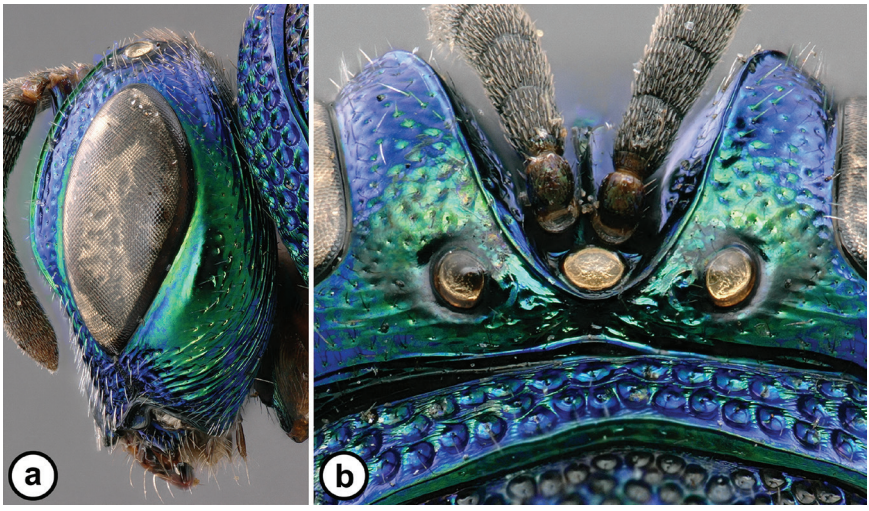

3(1) Median ocellus advanced to form a narrow triangle with lateral ocelli (C); lower face densely setose, with dense and widely distributed setae laterad torulus (A female, B male, circled); lateral panel of pronotum without flange (D, lateral view; E, oblique posterior view); male scape sparsely pitted (F). [Southwestern U.S and Northwestern Mexico]...***P. pilosus*** **Yoo & Darling, sp. nov.**

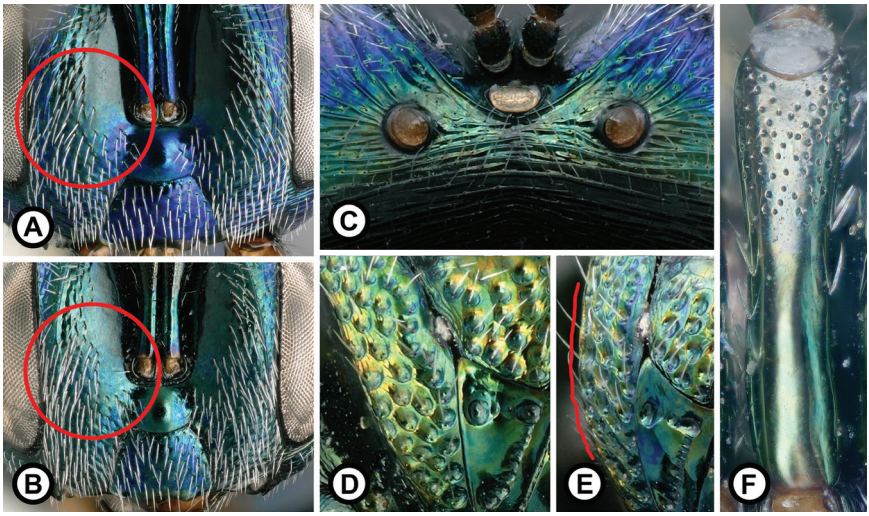

– Ocellar triangle variable (d, e); lower face sparsely (a female) or densely setose (b, c male), with sparse (a, circled) or dense and narrowly distributed setae laterad torulus (b, c, circled); lateral panel of pronotum without (f, posterior oblique view) or with flange (g, posterior oblique view); male scape variable..... **4**

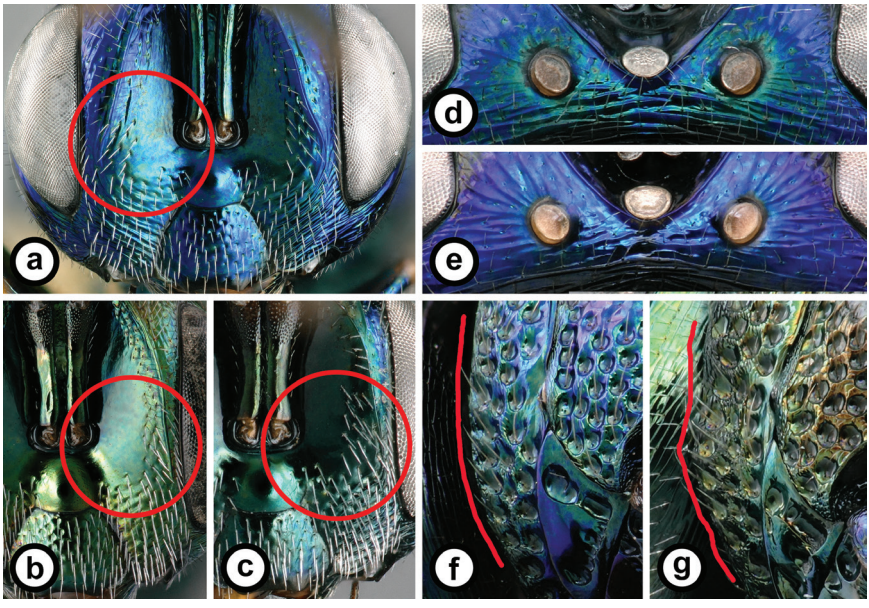

4(3) Parascutal carina (A, circled) angulate (B) or steeply curved (C), often with weak flange (arrows, B, C) **5**

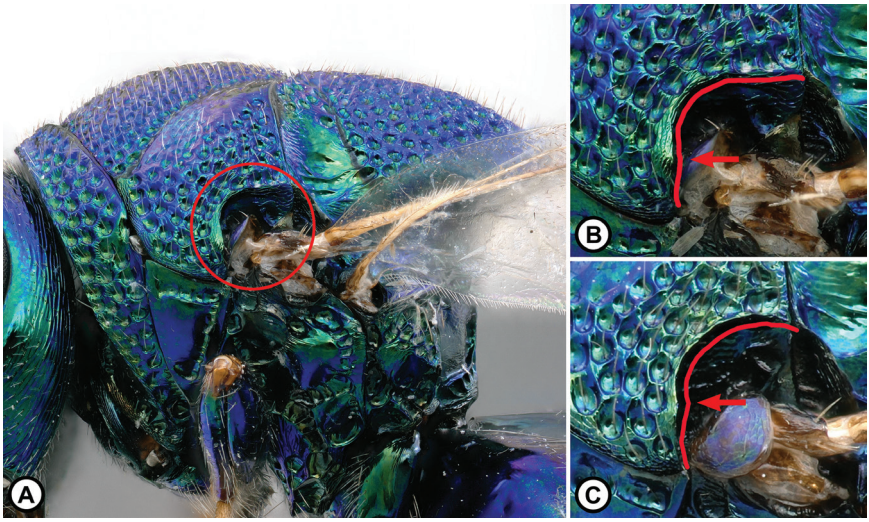

– Parascutal carina (a, circled) broadly curved, without flange (b, c) **6**

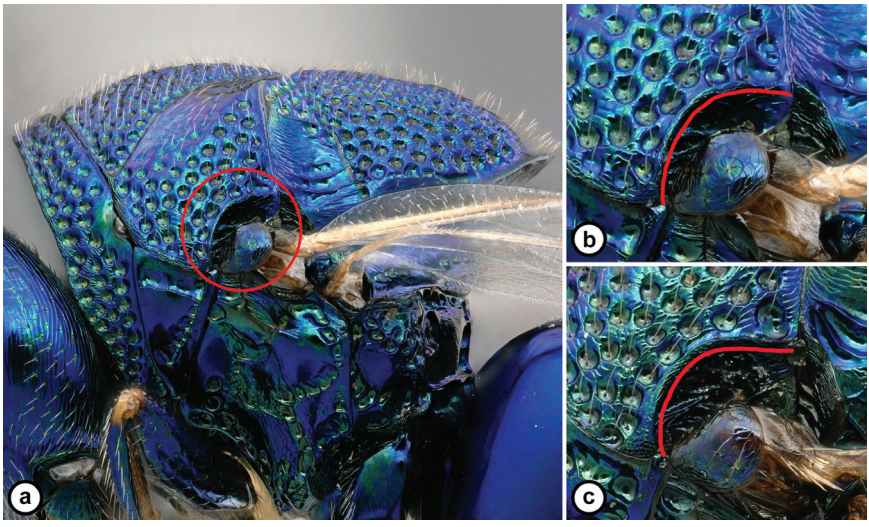

5(4) Lateral panel of pronotum without flange or with small rounded flange in posterior oblique view (A); parascutal carina usually angulate (B), rarely steeply curved (C); male scape sparsely pitted (D).....***P. sirsiris*** **(Argaman)**

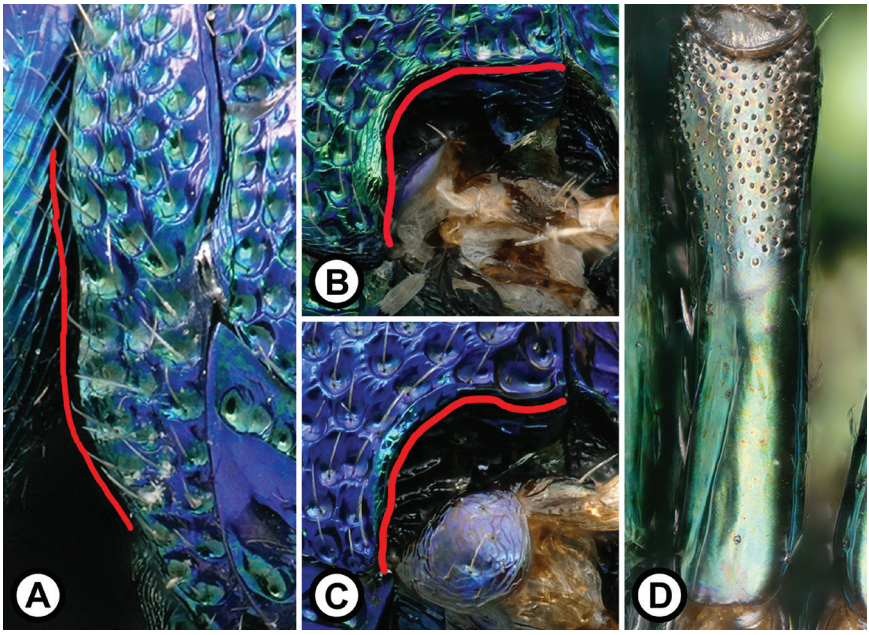

– Lateral panel of pronotum usually with small acuminate triangular flange in posterior oblique view (a); parascutal carina steeply curved (b, c); male scape densely pitted (d) .....***P. arcus*** **Yoo & Darling**

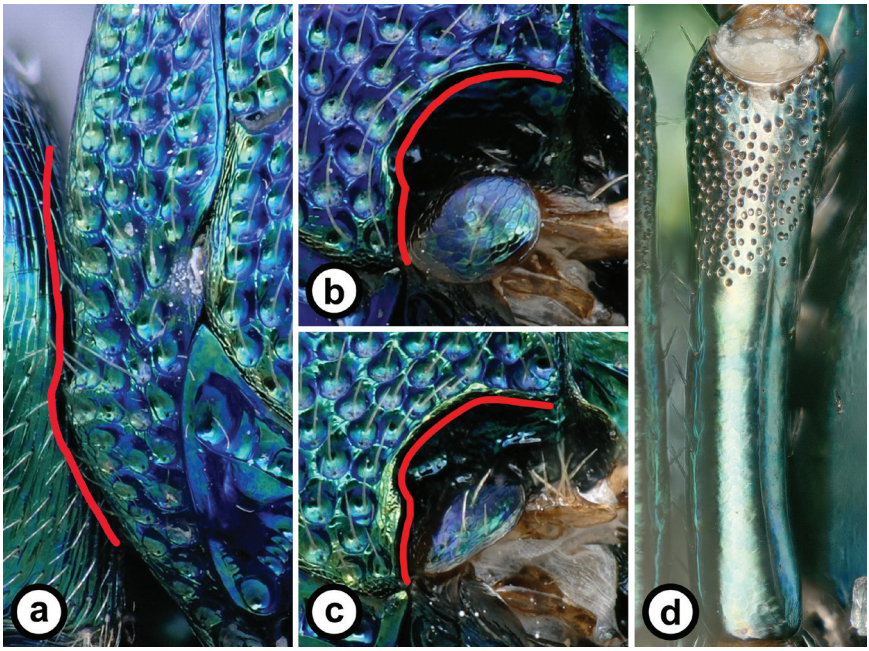

6(4) Mesonotum cupreous in both sexes (A female, B male); lateral panel of pronotum without flange in posterior oblique view (C); male scape with short pitted area, about 0.3 × scape length, and pits sparse (D, E). [Southwestern U.S to Southern Mexico] ..... ***P. sonora* Yoo & Darling, sp. nov.**

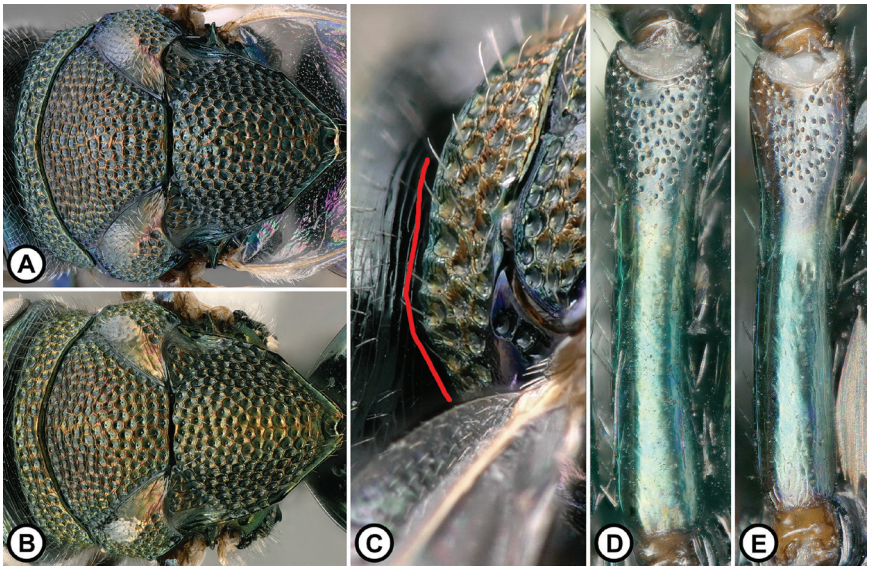

– Mesonotum entirely or mostly green to violaceous blue in both sexes (a), or cupreous in males (b); shape of lateral panel of pronotum variable (c, d); male scape variable (e, f); if male mesonotum strongly cupreous, then lateral panel of pronotum usually with triangular flange in oblique posterior view (d) and male scape with densely pitted area (e) 7

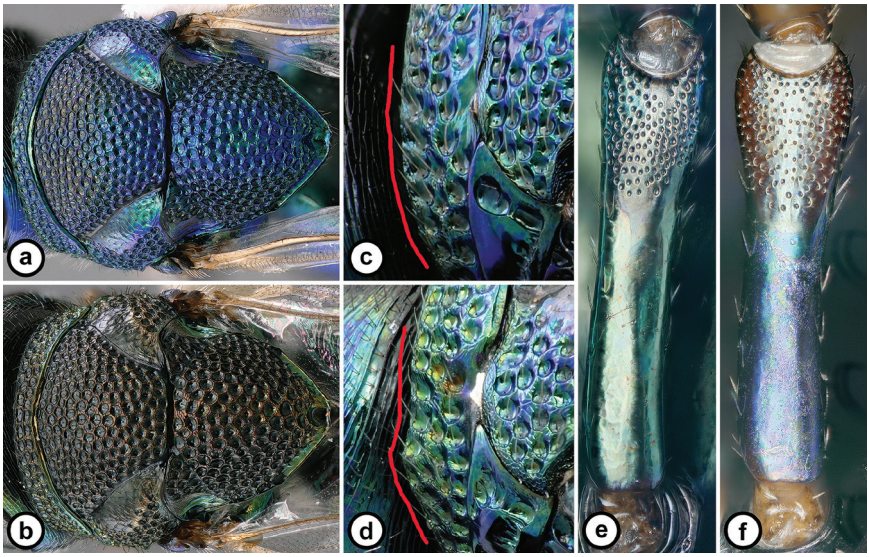

7(6) Mesoscutal lateral lobes smooth to weakly corarious along notaulus (A); lateral panel of pronotum often with triangular flange in posterior oblique view (B, C); median ocellus in line with lateral ocelli (D); axilla carinate ventrad (E); male scape densely pitted (F) **8**

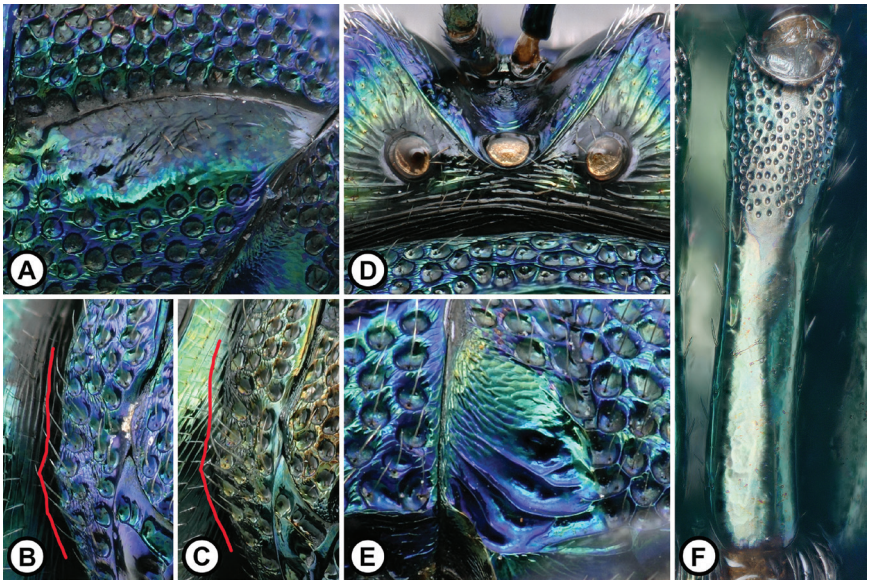

– Mesoscutal lateral lobes usually punctate along notaulus (a, b); lateral panel of pronotum without flange (c) or with small rounded flange (d); median ocellus in line with lateral ocelli or advanced and forming a narrow triangle (e); axilla areolate-rugose (f, g) or carinate ventrad; male scape sparsely pitted (h) **9**

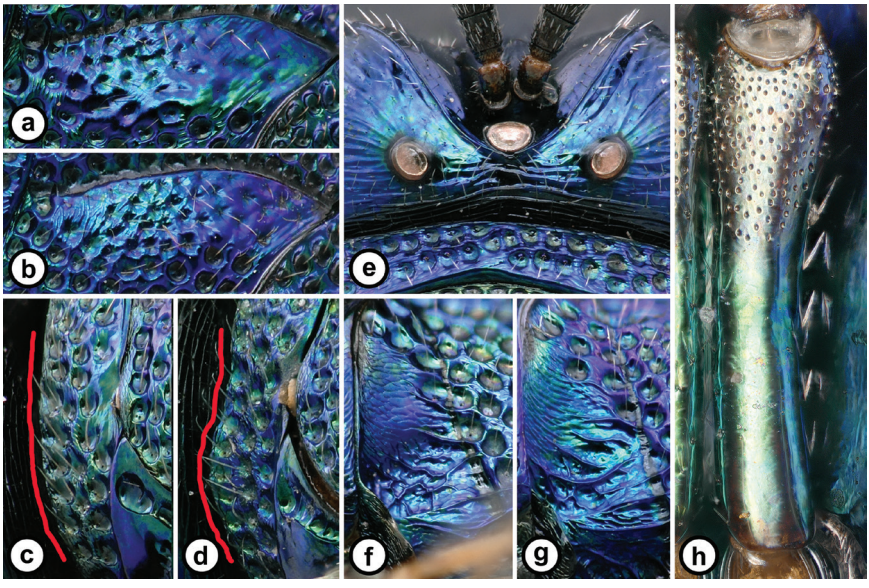

8(7) Lateral panel of pronotum usually with large triangular flange in posterior oblique view (A, female, B, male); female vertex without black coloration between frontal carina and ocellus (C); male mesonotum mostly black (D) [Southwestern U.S].....***P. ute*** **Yoo & Darling, sp. nov.**

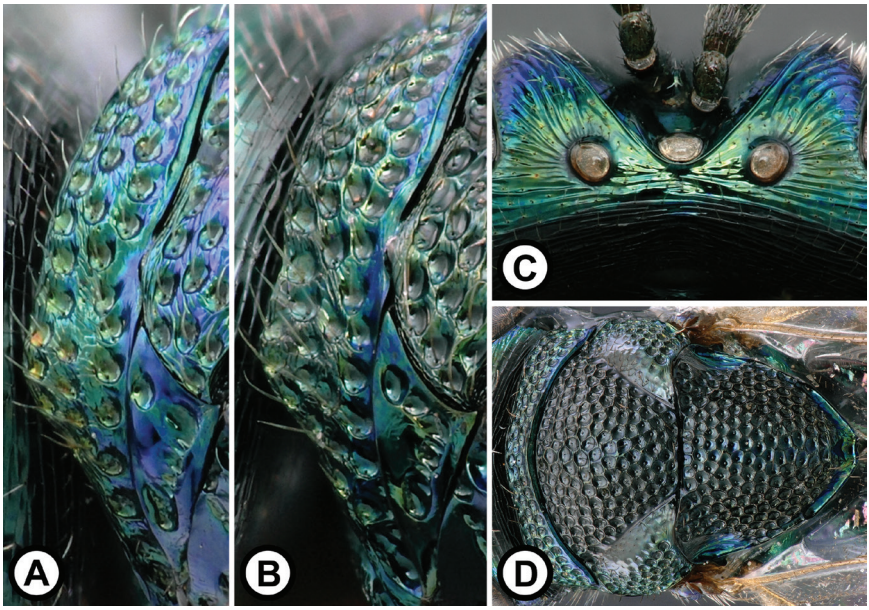

– Lateral panel of pronotum usually with small acuminate triangular flange (a, female, b, male); female vertex with black coloration between frontal carina and ocellus (arrow, c); male mesonotum with cupreous iridescence (d) ....***P. seneca*** **Yoo & Darling, sp. nov.**

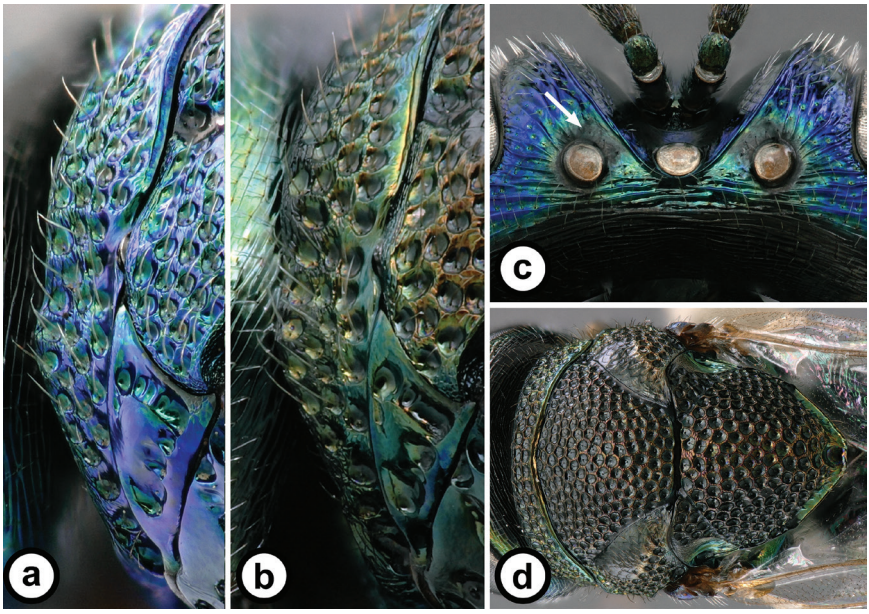

9(7) Ventral margin of clypeus nearly straight, weakly iridescent (A, B); mesoscutal lateral lobes sculpture along notaulus always strongly punctate (C, D) ....***P. crassus*** **Yoo & Darling, sp. nov.**

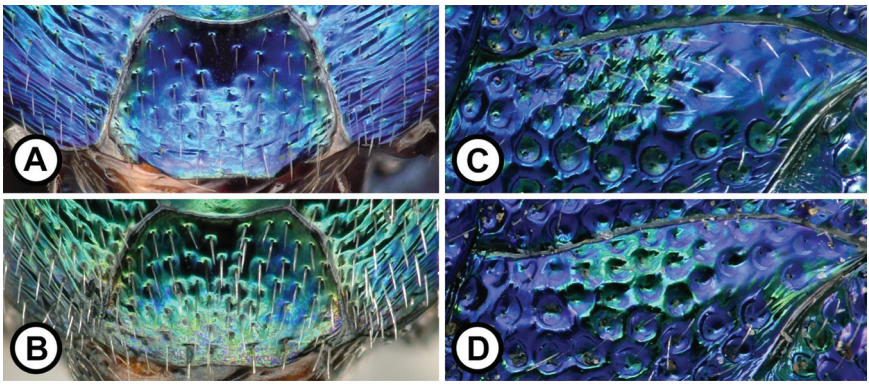

– Ventral margin of clypeus concave and black (a, b); sculpture of lateral lobe of mesoscutum along notaulus weaker, rarely smooth (c, d) **10**

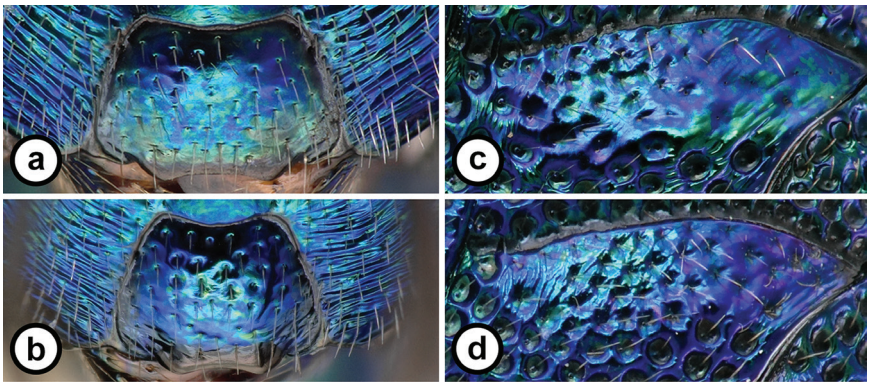

10(9) Clypeus with wide bare area without setae near dorsal margin, extending ventrad medially (A, B). [Parasitoids of *Monoctenus* spp. or hyperparasitoids, parasitizing their dipteran parasitoids] .... ***P. monocteni* Yoo & Darling, sp. nov.**

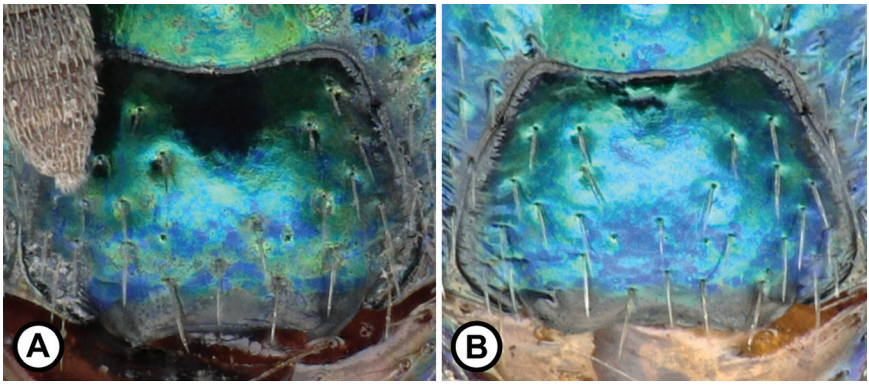

– Clypeus with setae evenly distributed (a) or with small bare area without setae medially (b) [Parasitoids associated with *Neodiprion* spp. or Orthoptera] **11**

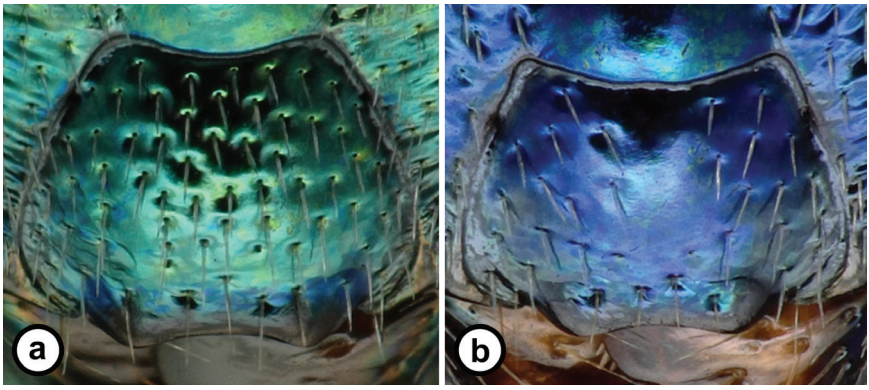

11(10) Axillula usually with piliferous punctures dorsad (arrows, A, B); mesofemoral depression variable, often imbricate-alveolate (C, D); inner margins at apex of mesoscutellum gradually diverging (E, F). [Parasitoids of *Neodiprion* spp. or hyperparasitoids, parasitizing their dipteran and hymenopteran parasitoids] ..... ***P. neodiprioni* Yoo & Darling, sp. nov.**

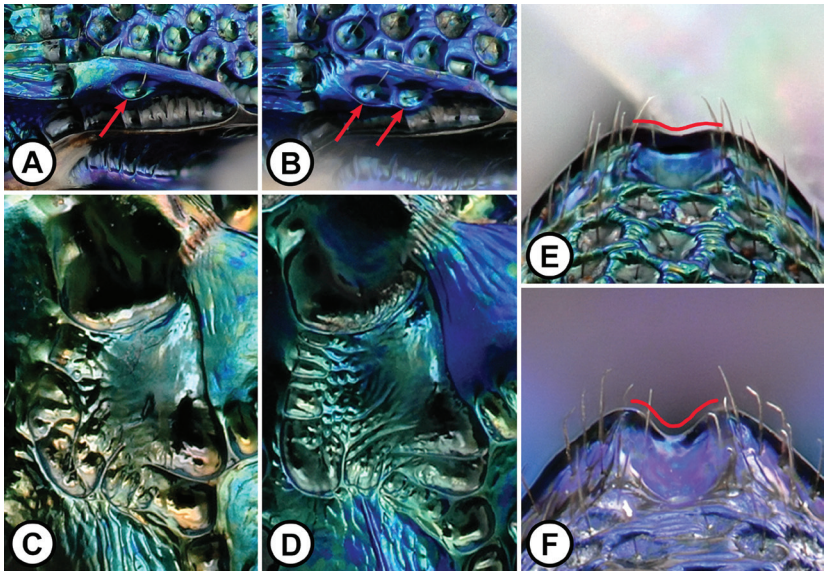

– Axillula smooth dorsad (a); mesofemoral depression variable, but never imbricate-alveolate (b, c); inner margins at apex of mesoscutellum gradually (d) or abruptly diverging (e). [Hyperparasitoids, parasitizing dipteran parasitoids of Acrididae, Gryllidae, or dipteran kleptoparasites of Crabronidae and Sphecidae that provision their nests with Orthoptera] ..... ***P. hyalinus* Say**

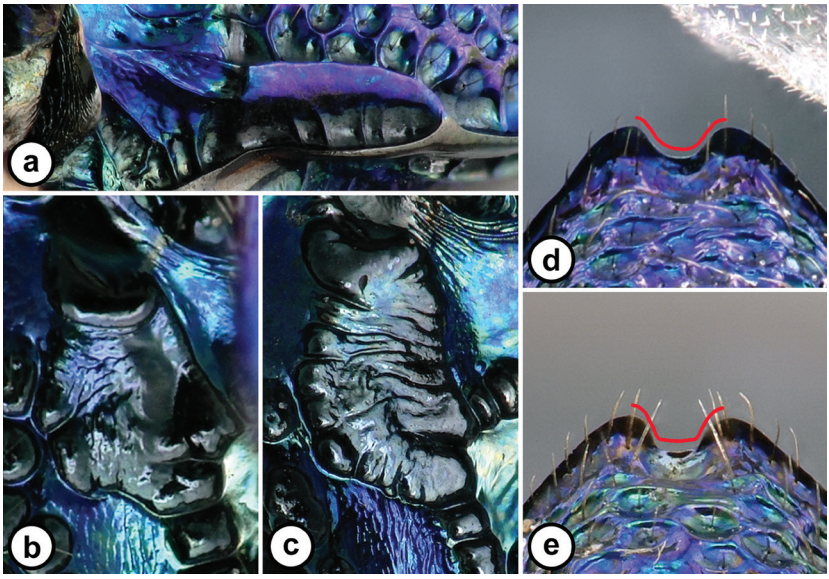

***Perilampus hyalinus* Say, rev. stat.**
Figs 4, 5, 24A, B

Perilampus hyalinus Say, 1829:79. (original description, sex not indicated). Type locality: USA, Pennsylvania. Type material: Type lost. Neotype. "USA:OH: Montgomery Co. New Carlisle 39.989583, -84.029056, Ex. *Ceracia dentate*, Ex. *Melanoplus femurrubrum* prob. 26.x.2014 M. D. Sheaffer". The neotype is point-mounted (Male ROME204130, USNM). BOLD:AEA0382. ROM Online Collection.
Perilampus entellus Walker, 1843:103 (original description). Type locality: Ohio, USA. Type Material. Lectotype, B.M. Type Hym. 5.2285, NHMUK014583126 (Images examined).
Perilampus aciculatus Provancher, 1889:199 (original description). Type locality: Ottawa, Canada. Type material. Lectotype, 1359, Université Laval, Québec City, Canada (Images examined). Note: Year of publication incorrect as 1887 in subsequent references to *P. aciculatus* (see Barron 1975:391).
Perilampus aciculatus, Lectotype, Gahan and Rohwer 1918:106.
Perilampus aciculatus Smuylan, 1936:380 (tentative synonym of *P. hyalinus* Say).
Perilampus aciculatus Peck, 1963:519 (subjective synonym of *P. hyalinus* Say).
Perilampus aciculatus Burks, 1963:1259 (subjective synonymy "probably correct").
Perilampus entellus, Lectotype, Burks 1975:150 (subjective synonym of *P. hyalinus* Say).
Taltonos hyalinus (Say). Argaman, 1990:205 (new combination).
Taltonos aciculatus (Provancher), Argaman, 1991:5 (new combination).
Taltonos entellus (Walker), Argaman, 1991:9 (new combination).
Perilampus hyalinus Say. Darling, 1996:113 (*Taltonos*, subjective synonym of *Perilampus*).
Perilampus aciculatus Darling, 1996:113 (*Taltonos*, subjective synonym of *Perilampus*).
Perilampus entellus Darling, 1996:113 (*Taltonos*, subjective synonym of *Perilampus*).
Perilampus aciculatus, **New synonymy** based on Neotype designation herein.
Perilampus entellus, **New synonymy** based on Neotype designation herein.

Material examined. Canada: 77 females, 47 males. USA: 67 females, 31 males. (Suppl. materials).

Additional material examined. Canada: 1 female. Ontario: 1 female. Durham R.M., Glen Major Forest: (1 female: ROME152664-ROME; BOLD:AEA0382; ITS2). Mexico: 2 females. Jalisco: 1 female. (1 female: ROME200751-HNHM). Sonora: 1 female. (1 female: ROME162260-USNM).

Description. Female (Fig. 4). Length: 2.9–4.4 mm. Color: head iridescent greenish blue or violet; mesosoma and metasoma iridescent greenish blue or violet; clypeus ventral margin black (Fig. 4I); antenna with scape and pedicel weakly iridescent greenish blue or violet, flagellum brown or black, lighter ventrad and distad.

Head (Fig. 4G–I): in dorsal view transverse, width slightly greater than twice length, HW/HL 2.1–2.2. Frontal carina: in anterior view straight to weakly sinuate below midlevel of eye; in dorsal view gradually narrowed V shape around median ocellus, FC/MOD 1.5–1.9; distance from lateral ocellus short to long, FCLO/LOD 0.6–1.0. Scrobal cavity (Fig. 4H): in anterior view wide, SW/HW about 0.5. Ocelli (Fig. 4G):

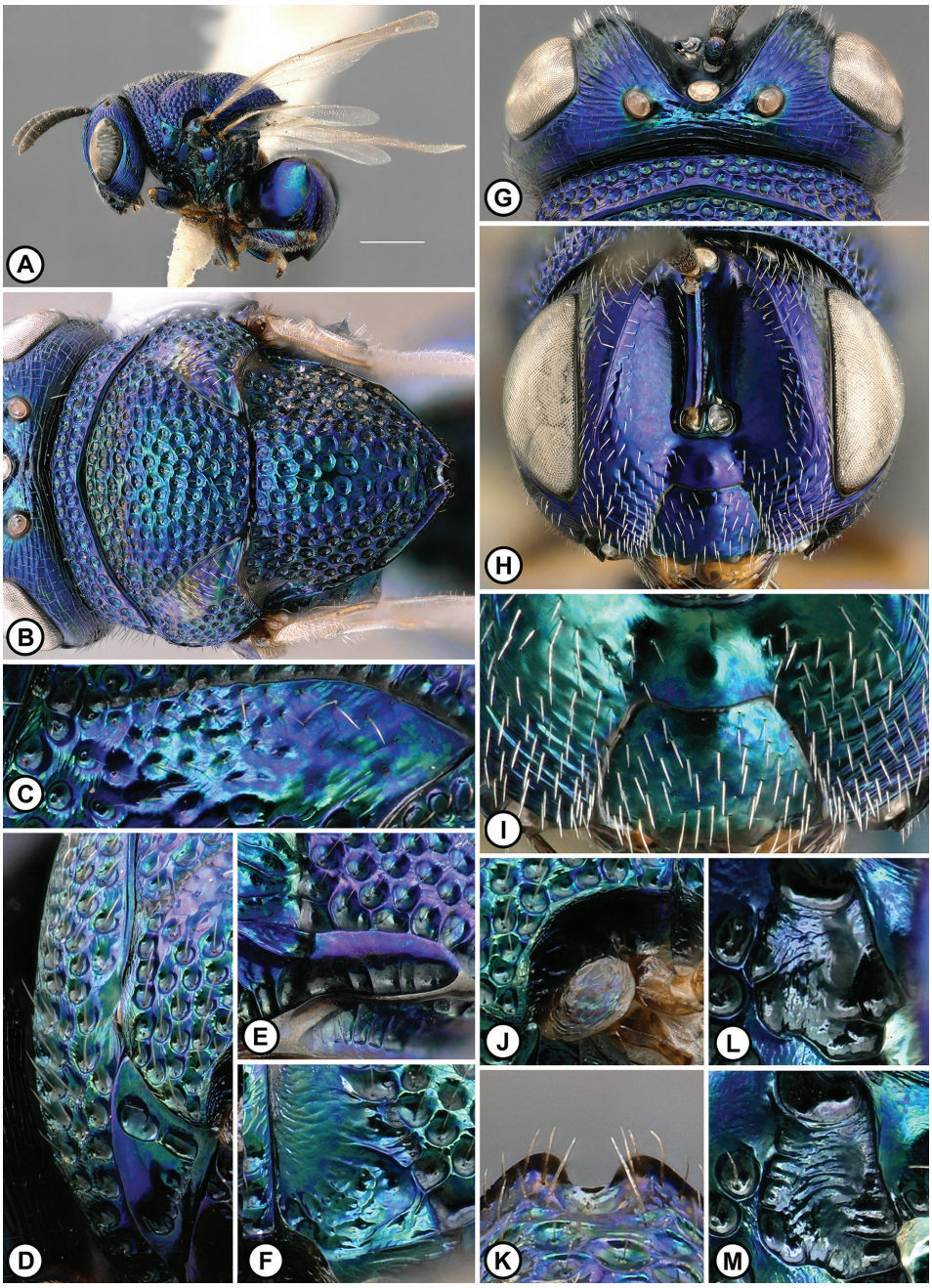

Figure 4. *Perilampus hyalinus* Female **A** habitus, lateral view **B** habitus dorsal view **C** lateral lobe of mesoscutum along notaulus **D** lateral panel of pronotum, posterior oblique view **E** axillula **F** axilla **G** head, dorsal view **H** head, anterior view **I** lower face **J** parascutal carina **K** mesoscutellum apex **L, M** mesofemoral depression. [**A** ROME185913; **B, K** ROME189058; **C, M** ROME185947; **D, F** ROME189056; **E, G** ROME162229; **H** ROME167636; **I** ROME189060; **L** ROME162246]. Scale bar: 1 mm (**A**).

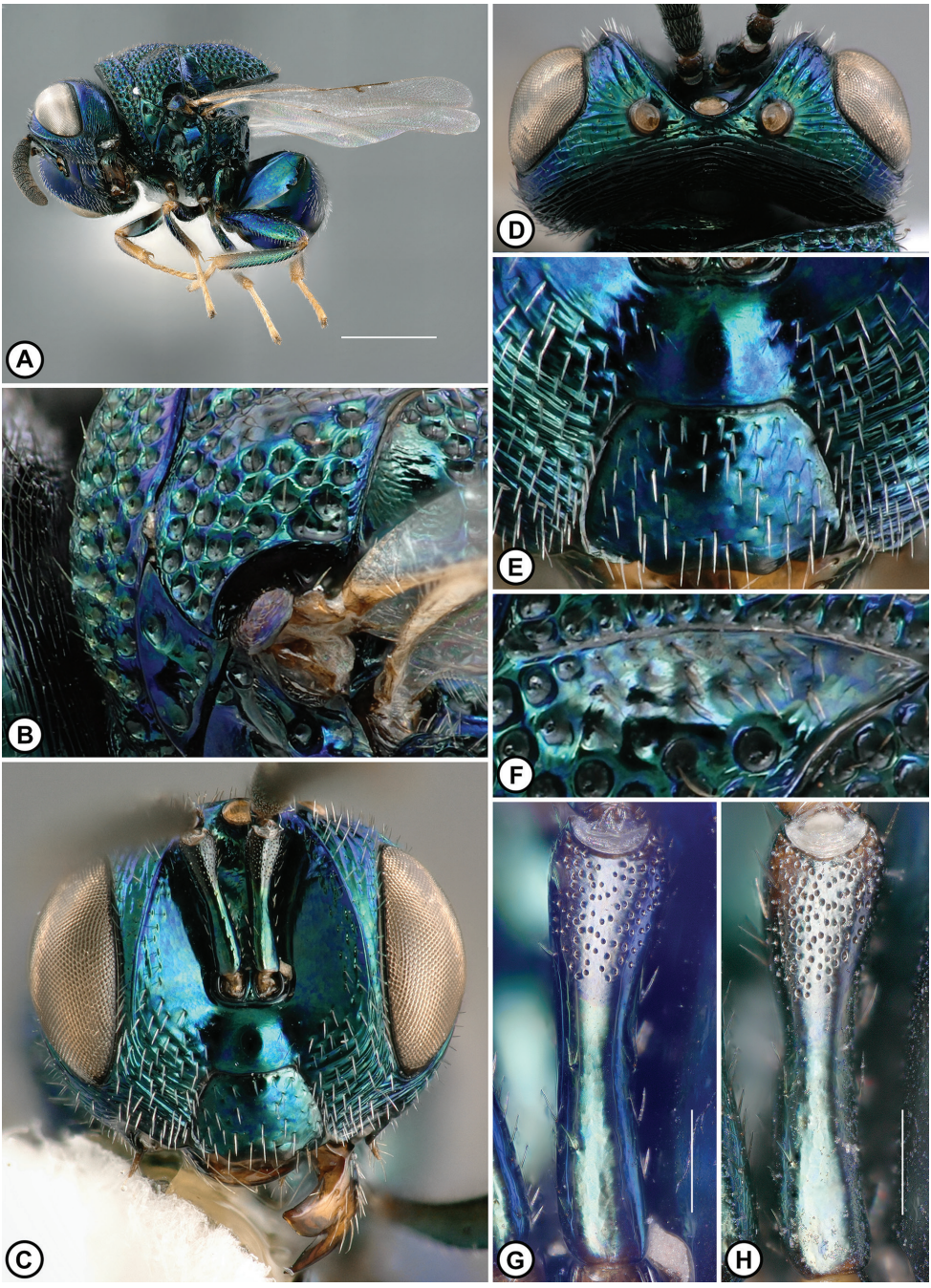

Figure 5. *Perilampus hyalinus* Male **A** habitus, lateral view **B** lateral panel of pronotum and parascutal carina, posterior oblique view **C** head, anterior view **D** head, dorsal view **E** lower face **F** lateral lobe of mesoscutum along notaulus **G, H** scape. [**A** Neotype, ROME204130; **B–D, F, G** ROME182798; **E** ROME167638; **H** ROME189059]. Scale bars: 1 mm (**A**); 100 μm (**G, H**).

a line between anterior margin of lateral ocelli nearly bisecting median ocellus. POL/OOL 1.7–1.9. Ocellar ratios LOD: POL: OOL: LOL 1, 3.3–3.5, 1.8–2.0, 1.2–1.4. Vertex: with strong to weak transverse striations, without large piliferous punctures. Parascrobal area: in lateral view gradually narrowed towards lower eye margin; width narrow, PSW/EL about 0.3; sculpture strongly to weakly striate, without large piliferous punctures. Gena: entirely or mostly striate along outer eye margin with narrow and short smooth area, striate behind. Malar space: MSL/EH 0.2–0.3. Lower face (Fig. 4H, I): with setae sparse laterad torulus, and usually sparse below. Clypeus (Fig. 4I): CW/CH 1.3–1.5; ventral margin concave; setae evenly distributed, or with small bare area without setae medially.

Mesosoma (Fig. 4B–F, J–M): Lateral panel of pronotum: slightly narrower than or about as wide as prepectus, LPP/PPT 0.7–0.9; without flange below level of mesothoracic spiracle in posterior oblique view (Fig. 4D). Mesofemoral depression: smooth, weakly imbricate (Fig. 4L), or rugulose (Fig. 4M). Mesoscutum: punctures angulate, with narrow or slightly wide and weakly coriarious interspaces (Fig. 4B); lateral lobe usually weakly punctate with coriarious or smooth interspaces along notaulus (Fig. 4C); parascutal carina broadly curved, acuminate (Fig. 4J). Mesoscutellum: apex with inner margin gradually or abruptly diverging (Fig. 4K); punctures angulate, with narrow or slightly wide and weakly coriarious interspaces. Axilla (Fig. 4F): in lateral view imbricate dorsad and rugose-areolate or carinate ventrad. Axillula (Fig. 4E): smooth dorsad. Fore wing: stigma small, 2.0–2.5 × as wide as postmarginal vein.

Male (Fig. 5). Length: usually smaller, 2.6–3.8 mm. As in female, except: Color: mesonotum sometimes with weak cupreous iridescence. Frontal carina (Fig. 5D): distance from lateral ocellus shorter, FCLO/LOD 0.5–0.6. Scape (Fig. 5G, H): pits sparse, covering 0.3–0.4 × scape length.

Diagnosis. *Perilampus hyalinus* is morphologically similar to *P. neodiprioni*, but the axillula is always smooth dorsad without piliferous punctures (Fig. 4E cf. Fig. 8E), the sculpture of the mesofemoral groove is usually smooth to weakly imbricate or rugulose (Fig. 4L, M cf. Fig. 8L, M), and the inner margins of the apex of the mesoscutellum are often abruptly diverged (Fig. 4K cf. Fig. 8K).

Distribution (Fig. 25A)**.** Throughout USA and southern Canada, and possibly western Mexico: Canada (Alberta, British Columbia, Manitoba, New Brunswick, Ontario, Quebec), USA (Arizona, Colorado, Illinois, Indiana, Kansas, Maryland, Montana, New York, North Dakoda, Oklahoma, Pennsylvania, Utah, Washington, Wisconsin), Mexico (Sonora, Jalisco).

Host associations. *Perilampus hyalinus* is a hyperparasitoid, attacking dipteran parasitoids of Orthoptera and dipteran kleptoparasites of Crabronidae and Sphecidae provisioning with Orthoptera and rarely parasitoids of dipteran parasitoids attacking Phasmida (ROME204120). Hosts: Tachinidae (Diptera). *Ceracia dentata* (Coquillett) from *Melanoplus femurrubrum* (De Geer) (Acrididae). Tachinidae from Phasmatidae. Sarcophagidae (Diptera). *Sarcophaga* sp. from *Melanoplus sanguinipes* (Fabricius). Sarcophagids from Tettigoniidae and Oecanthinae collected in the nests of *Isodontia mexicana* (Saussure) (Sphecidae) (Medler 1965). *Senotainia trilineata* (Wulp) and *S. vigilans*

Allen from nests of *Tachysphex terminatus* (Smith) and *T. validus* Cresson (Crabronidae) (Spofford and Kurczewski 1984). Possibly *Nemestrinidae* (Diptera) from *M. sanguinipes*. Unidentified Diptera from *Melanoplus differentialis* (Thomas). Unidentified parasitoid of *Orphullela* sp. (Acrididae).

Variation. A female from Ontario (ROME152664), Canada, has a smooth vertex. COI and ITS2 suggest that this specimen is a rare morphological variant of *P. hyalinus*.

Remarks. The identity of *P. hyalinus* has long been obscured by the presumed lost type specimen (Mawdsley 1993) and the morphological similarity of specimens exhibiting different parasitism strategies and host associations (Burks 1979). Say's (1829) original description contains neither host information nor sufficient details on morphology for determining with certainty which of the Nearctic species treated herein should be regarded as *P. hyalinus* Say. To clarify this situation a neotype is designated herein, a reared specimen collected near the original type locality (Pennsylvania) which establishes this species as a parasitoid of dipteran parasitoids and dipteran kleptoparasites associated with Orthoptera. This species is supported by molecular analyses in both genes (Fig. 1, Suppl. material 5) and there are 14 BINed specimens, including the neotype on BOLD (AEA0382) collected and reared from throughout the range of this species. *Perilampus hyalinus* Say is the most abundant species in collections in the eastern Nearctic region. This species is morphologically close to *P. neodiprioni*, and can usually be distinguished by the sculpture of its axillula dorsad and mesofemoral groove. However, these characters are not always reliable distinguishing these two species (see Remarks in *P. neodiprioni*). While these characters are not always reliable distinguishing these two species, they are clearly differentiated in both COI and ITS2 (Fig. 1)

Perilampus sirsiris (Argaman)

Figs 6, 7, 24C

Ichneumon cyaneus Brullé, 1846:21 (Plate V, #4). Type locality: USA, "Carolina". Type material: **Holotype.** "Carolina". (Female Paris EY35408, MNHN) (images examined).
Perilampus cyaneus Dalla Torre, 1898:355 (new combination ?).
Perilampus hyalinus Viereck, 1910:647 (subjective synonym *P. cyaneus* ?, cited by Peck 1963).
Taltonos sirsiris Argaman, 1990:15. Replacement name, *Perilampus cyaneus* Brullé (nec Fabricius 1798).
Perilampus sirsiris Darling, 1996:113 (*Taltonos*, subjective synonym of *Perilampus*).
Perilampus eucyaneus Özdikmen, 2011. Unnecessary replacement name.

Material examined. Canada: 4 females, 8 males. USA: 17 females, 11 males. (Suppl. materials).

Description. Female (Fig. 6). Length: 2.5–4.5 mm. Color: head iridescent greenish blue or violet, usually without black coloration between lateral ocellus and frontal

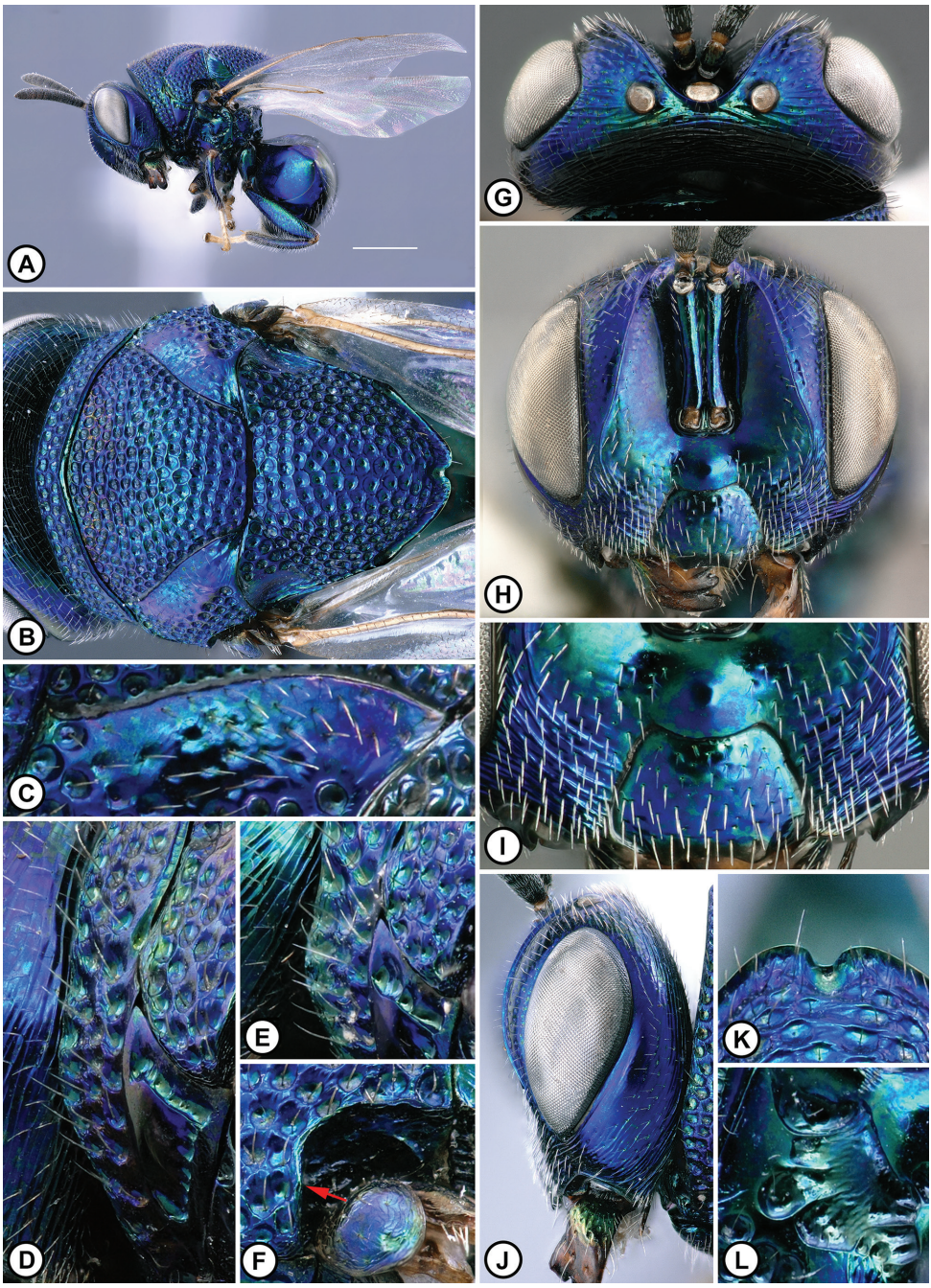

Figure 6. *Perilampus sirsiris* Female **A** habitus, lateral view **B** habitus, dorsal view **C** lateral lobe of mesoscutum along notaulus **D, E** lateral panel of pronotum, posterior oblique view **F** parascutal carina **G** head, dorsal view **H** head, anterior view **I** lower face **J** head, lateral view **K** mesoscutellum apex **L** mesofemoral depression. [**A, B, D, F, H, J, K** ROME182764; **E, G, L** ROME189054; **I** ROME182766]. Scale bar: 1 mm (**A**).

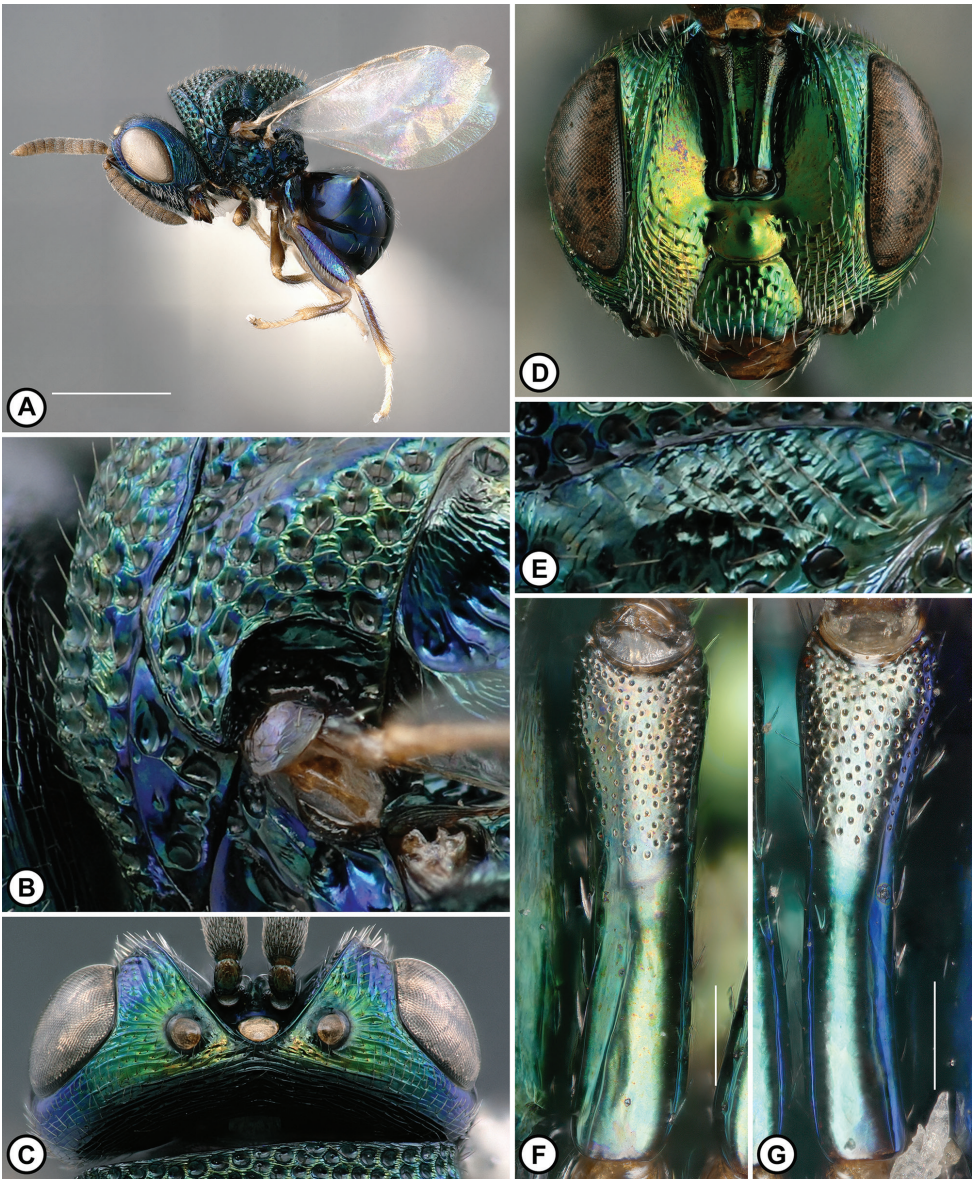

Figure 7. *Perilampus sirsiris* Male **A** habitus, lateral view **B** lateral panel of pronotum, parascutal carina, and axilla, posterior oblique view **C** head, dorsal view **D** head, anterior view **E** lateral lobe of mesoscutum along notaulus **F, G** scape. [**A** ROME162278; **B** ROME204099; **C** ROME199527; **D** ROME162281; **F** ROME152680; **E** ROME162281; **G** ROME185910]. Scale bars: 1 mm (**A**); 100 μm (**F, G**).

carina; mesosoma, and metasoma iridescent greenish blue or violet; clypeus ventral margin black (Fig. 6I); antenna with scape and pedicel weakly iridescent greenish blue or violet, flagellum brown or black, lighter ventrad and distad.

Head (Fig. 6G–J): in dorsal view transverse, width slightly greater than twice length, HW/HL 2.1–2.2. Frontal carina: in anterior view straight to weakly sinuate below midlevel of eye; in dorsal view gradually narrowed V shape around median ocellus, FC/MOD 1.5–1.9; distance from lateral ocellus short, FCLO/LOD 0.6–0.7. Scrobal cavity (Fig. 6H): in anterior view wide, SW/HW about 0.5. Ocelli (Fig. 6G): a line between anterior margin of lateral ocelli reaching anterior margin of median ocellus. POL/OOL 1.7–2.0. Ocellar ratios LOD: POL: OOL: LOL 1, 3.1–3.3, 1.6–1.9, 1.0–1.1. Vertex: with strong to weak transverse striations, without large piliferous punctures. Parascrobal area: in lateral view gradually narrowed towards lower eye margin; width narrow, PSW/EL about 0.3; sculpture strongly to weakly striate, or rarely smooth, without large piliferous punctures. Gena (Fig. 6J): entirely or mostly striate along outer eye margin with narrow and short smooth area, striate behind. Malar space: MSL/EH 0.2–0.3. Lower face (Fig. 6H, I): with setae sparse laterad torulus, and usually sparse below. Clypeus (Fig. 6I): CW/CH 1.3–1.4; ventral margin concave; setae evenly distributed, or with small bare area without setae medially.

Mesosoma (Fig. 6B – F, K, L): Lateral panel of pronotum: slightly narrower than prepectus, LPP/PPT 0.7–0.8; without flange or with small rounded flange below level of mesothoracic spiracle in posterior oblique view (Fig. 6D, E). Mesofemoral depression: usually smooth, weakly imbricate, or rugulose (Fig. 6L). Mesoscutum: punctures angulate, with narrow or slightly wide and weakly coriarious interspaces (Fig. 6B); lateral lobe weakly punctate with coriarious or smooth interspaces (Fig. 6C), or smooth, along notaulus; parascutal carina usually angulate, rarely steeply curved, often weakly flanged (Fig. 6F, arrow). Mesoscutellum: apex with inner margins gradually or abruptly diverging (Fig. 6K); punctures angulate, with narrow or slightly wide and weakly coriarious interspaces. Axilla: in lateral view imbricate dorsad and carinate or rugose-areolate ventrad. Axillula: smooth dorsad. Fore wing: stigma small, 2.0–2.5 × as wide as postmarginal vein.

Male (Fig. 7). Length: usually smaller, 1.7–3.8 mm. As in female, except: Color: mesonotum sometimes with weak cupreous iridescence. Frontal carina (Fig. 7C): distance from lateral ocellus shorter, FCLO/LOD 0.3–0.4. Scape (Fig. 7F. G): pits sparse, covering about 0.4 × scape length.

Diagnosis. *Perilampus sirsiris* and *P. arcus* are the only Nearctic species with steeply curved or angulate parascutal carina often with a flange (Fig, 6F, 7B, 20E, 21B cf. Figs 8J, 9B). *Perilampus sirsiris* differs from *P. arcus* in usually having an angulate parascutal carina (Fig. 6F cf. Fig. 20F), a flat lateral panel of pronotum or with a small rounded flange in posterior oblique view (Fig. 6D, E cf. Fig. 20D), and the male scape with sparsely pitted surface distad (Fig. 7F, G cf. Fig. 21G, H).

Distribution (Fig. 25C). Throughout USA and southern Canada: Canada (Ontario, Quebec, British Columbia), USA (Arkansas, Florida, Kansas, Maryland, Missouri, Montana, Oregon, Texas, West Virginia).

Host association. *Perilampus sirsiris* is a hyperparasitoid, a parasitoid of dipteran and hymenopteran parasitoids of Lepidoptera, rarely of hymenopteran parasitoids of

argid sawflies. Hosts: Tachinidae (Diptera) from *Hyphantria cunea* (Drury) (Erebidae) and *Malacosoma disstria* Hübner (Lasiocampidae). Sarcophagidae (Diptera) from *Neophasia menapia* (C. & R. Felder) (Pieridae). Braconidae (Hymenoptera). *Cotesia hyphantriae* (Riley) from *Hyphantria cunea* (Drury). Ichneumonidae (Hymenoptera) from *Arge* sp. (Hymenoptera).

Variation. There is a rare variant from Manitoulin Island, Ontario, a male (ROME152661) which has a wide bare area without setae on the clypeus similar to *P. monocteni*, but confirmed as *P. sirsiris* by the steeply curved parascutal carina and COI and ITS2.

Remarks. The descriptions of *P. sirsiris* provided in Brullé (1846) and Argaman (1990) are insufficient for species discrimination, but the holotype of this species is intact (MNHN). The images of the holotype sent by the MNHN (Fig. 24C) provided sufficient morphological details for associating the holotype with one of the common Nearctic species based on the key and redescription provided herein. Argaman's descriptions of color and pronotal flange ("Head and sides of thorax golden-green to bluish", "with a triangularly acute lobe opposite to upper top of prepectus") do not match the holotype of *P. cyaneus*. Due to the dubious nature of the type specimen listed in his annotated checklist, where he states that the holotype is in his private collection (Argaman 1991), Argaman clearly did not examine Brullé's type. It is likely that the "Types" in Argaman's checklist represent the specimens he regards as conspecifics, rather than the actual extant types (Darling 1996). We examined two additional NHMH specimens from Jalisco, Mexico misidentified as *P. sirsiris* by Argaman (1991), identified herein as a female *P. hyalinus* (ROME200751) and male *P. ute* (ROME200740). The only other literature record of *P. sirsiris* is Graenicher (1909), which mentions the preference of *P. hyalinus* and *P. sirsiris* for flowers of *Erigeron canadensis* Linnaeus. However, given the poor description of *P. sirsiris* by Brullé and the absence of an indication that Graenicher had examined the type, it is unclear if the observed species was indeed *P. sirsiris*.

The steeply curved or angulate parascutal carina often with a flange (Figs 6F, 7B) is one of the key diagnostic features of *P. sirsiris*. *Perilampus arcus* (Figs 20E, 21B) also has a similarly modified parascutal carina, but the phylogenetic placement of the two species (Fig. 1) suggests convergent evolution within the *P. hyalinus* species complex. This state is also widely distributed in other species of Perilampidae, including some species of the *P. platigaster* species group, and is almost certainly derived independently. Both genes and species delimitation methods support *P. sirsiris* (Fig. 1, Suppl. material 5) and there are 10 BINed specimens on BOLD (AEM7685) from throughout the range of this species (Quebec to Texas) and one specimen (ROME185904, Missouri) with a COI sequence reared from *Hyphantia cunea.*

Perilampus sirsiris parasitizes dipteran and hymenopteran parasitoids of Lepidoptera, which feed on the leaves of deciduous trees. Interestingly, the hosts of *P. sirsiris* also include sarcophagid parasitoids of the pine butterfly, *N. menapia* (Pieridae)—this is the only species associated with pines other than *P. neodiprioni*, the hypothesized sister species of *P. sirsiris* (Fig. 1) (see Remarks for *P. neodiprioni* below).

***Perilampus neodiprioni* Yoo & Darling, sp. nov.**
https://zoobank.org/E1D68A20-14BD-4FAE-864E-99E9FE508E38
Figs 8, 9

Type locality. Canada, Ontario, Haliburton County.

Type material. ***Holotype.*** "CANADA: ONT. Haliburton Hwy 16, 3.8 m. E. Minden Ex: *Neodiprion lecontei* in red pine plantation. VIII.28.93. DC Darling", "Lab Reared 1994 S. Perlman M.Sc. thesis", "BOLD COI-5P Sequence, 325bp". The holotype is card-mounted (Female ROME183975, ROM). ROM Online Collection.

Paratypes. Canada: 3 males. Ontario: 3 males. Nipissing Dist., Algonquin P.P., Cameron Road: (3 males: ROME152669-CNC; BOLD:AEE8879; ITS2; ROME152668-ROME; BOLD:AEE8879; ITS2; ROME183971-ROME; BOLD:AEE8879). USA: 1 female, 2 males. Massachusetts: 1 female, 2 males. Franklin Co., Montague, Montague Plains WMA: (1 female: ROME162273-USNM; BOLD:AEE8879; ITS2. 2 males: ROME162275-ROME; BOLD:AEE8879; ITS2; ROME162274-USNM; BOLD:AEE8879; ITS2).

Material examined. Canada: 79 females, 97 males. USA: 36 females, 33 males. (Suppl. materials).

Additional material examined. Belize: 9 females, 4 males. Stann Creek District: 9 females, 4 males. 4 1/2 mis., Stann Creek Valley: (4 females: ROME185928-USNM; ROME185929-USNM; ROME199572-USNM; ROME199573-USNM. 1 male: ROME185926-USNM); 5 1/2 mi Stann Creek Valley: (1 male: ROME201411-FSCA); Stann Creek Valley: (5 females: ROME185927-USNM; ROME199574-USNM; ROME199575-USNM; ROME199576-USNM; ROME199578-USNM. 2 males: ROME199571-USNM; ROME199577-USNM).

Etymology. The specific epithet is a noun in the genitive case meaning "of *Neodiprion*", in reference to the species' predilection for pine sawflies and their primary parasitoids.

Description. Female (Fig. 8). Length: 3.5–5.0 mm. Color: head iridescent greenish blue or violet, usually without black coloration between lateral ocellus and frontal carina; mesosoma, and metasoma iridescent greenish blue or violet; clypeus ventral margin black (Fig. 8I); antenna with scape and pedicel weakly iridescent greenish blue or violet, flagellum brown or black, lighter ventrad and distad.

Head (Fig. 8G–I): in dorsal view transverse, width slightly greater than twice length, HW/HL 2.1–2.2. Frontal carina: in anterior view straight to weakly sinuate below midlevel of eye; in dorsal view gradually narrowed V shape around median ocellus, FC/MOD 1.5–1.9; distance from lateral ocellus short, FCLO/LOD 0.6–0.7. Scrobal cavity: in anterior view wide, SW/HW about 0.5. Ocelli (Fig. 8G): a line between anterior margin of lateral ocelli reaching anterior margin of median ocellus or nearly bisecting median ocellus. POL/OOL 1.8–2.0. Ocellar ratios LOD: POL: OOL: LOL 1, 3.0–3.3, 1.6–1.8, 1.1–1.4. Vertex: with strong to weak transverse striations, without large piliferous punctures. Parascrobal area: in lateral view gradually narrowed towards lower eye margin; width narrow, PSW/EL about 0.3; sculpture strongly to weakly striate, rarely smooth, without large piliferous punctures. Gena: entirely or mostly stri-

ate along outer eye margin with narrow and short smooth area, striate behind. Malar space: MSL/EH 0.2–0.3. Lower face (Fig. 8H, I): with setae sparse laterad torulus, and usually sparse below. Clypeus (Fig. 8I): CW/CH 1.3–1.4; ventral margin concave; setae evenly distributed, or with small bare area without setae medially.

Mesosoma (Fig. 8B–F, J–M): Lateral panel of pronotum: slightly narrower than or about as wide as prepectus, LPP/PPT 0.7–0.9; without flange or with small rounded flange below level of mesothoracic spiracle in posterior oblique view (Fig. 8D). Mesofemoral depression: imbricate-alveolate (Fig. 8L, M), or weakly imbricate, rugulose, or smooth. Mesoscutum: punctures angulate, with narrow or slightly wide and weakly coriarious interspaces (Fig. 8B); lateral lobe usually weakly punctate with coriarious interspaces along notaulus (Fig. 8C); parascutal carina broadly curved, acuminate (Fig. 8J). Mesoscutellum: apex with inner margins gradually diverging (Fig. 8K), rarely rounded; punctures angulate, with narrow or slightly wide and weakly coriarious interspaces. Axilla: in lateral view imbricate dorsad and rugose-areolate (Fig. 8F) or carinate ventrad. Axillula (Fig. 8E): usually with one or more piliferous punctures dorsad. Fore wing: stigma small, 2.0–2.5 × as wide as postmarginal vein.

Male (Fig. 9). Length: usually smaller, 2.7–3.8 mm. As in female, except: Color: mesonotum sometimes with weak cupreous iridescence. Frontal carina (Fig. 9D): distance from lateral ocellus shorter, FCLO/LOD 0.5–0.6. Scape (Fig. 9G, H): pits sparse, covering 0.3–0.4 × scape length.

Diagnosis. *Perilampus neodiprioni* can usually be distinguished by an axillula with one or more piliferous punctures dorsad (Fig. 8E cf. Fig. 4E). The specimens with a smooth axillula are most similar to *P. hyalinus*, but can often be differentiated by the imbricate-alveolate sculpture of the mesofemoral depression (Fig. 8L, M cf. Fig. 4L, M); and the gradually diverging inner margins of the apex of the mesoscutellum (Fig. 8K cf. Fig. 4K).

Distribution (Fig. 25B). South-eastern Canada and central and eastern USA: Canada (Ontario, Quebec), USA (Arkansas, Florida, Illinois, Massachusetts, Michigan, New York, North Carolina, Texas, Virginia, West Virginia, Wisconsin). Possibly Belize (Stan Creek District).

Host association. *Perilampus neodiprioni* can develop as a primary parasitoid attacking *Neodiprion* sawflies (Fig. 26B), or as a hyperparasitoid that parasitizes dipteran (Fig. 26D) and hymenopteran parasitoids of *Neodiprion* sawflies (Fig. 26C, E). Hosts: Diprionidae (Hymenoptera). *Neodiprion pratti banksianae* Rohwer. *Neodiprion excitans* Rohwer. *Neodiprion lecontei* (Fitch). *Neodiprion merkeli* Ross. *Neodiprion pinetum* (Norton). *Neodiprion rugifrons* Middleton. *Neodiprion swainei* Middleton *Neodiprion virginianus* Rohwer. Tachinidae (Diptera). *Vibrissina spinigera* (Townsend) from *N. swainei* (Tripp 1962). Tachinids from *N. lecontei* and *N. virginianus* Ichneumonidae (Hymenoptera). *Olesicampe lophyri* (Riley) and *Endasys subclavatus* (Say) from *N. swainei* (Tripp 1962). Ichneumonids from *N. lecontei*.

Remarks. Both COI and ITS2 support *P. neodiprioni* as a distinct species (Fig. 1, Suppl. material 5). There are 10 BINed specimens on BOLD (AEE8879) collected from the eastern and central Nearctic region north of Mexico, most of which are reared from

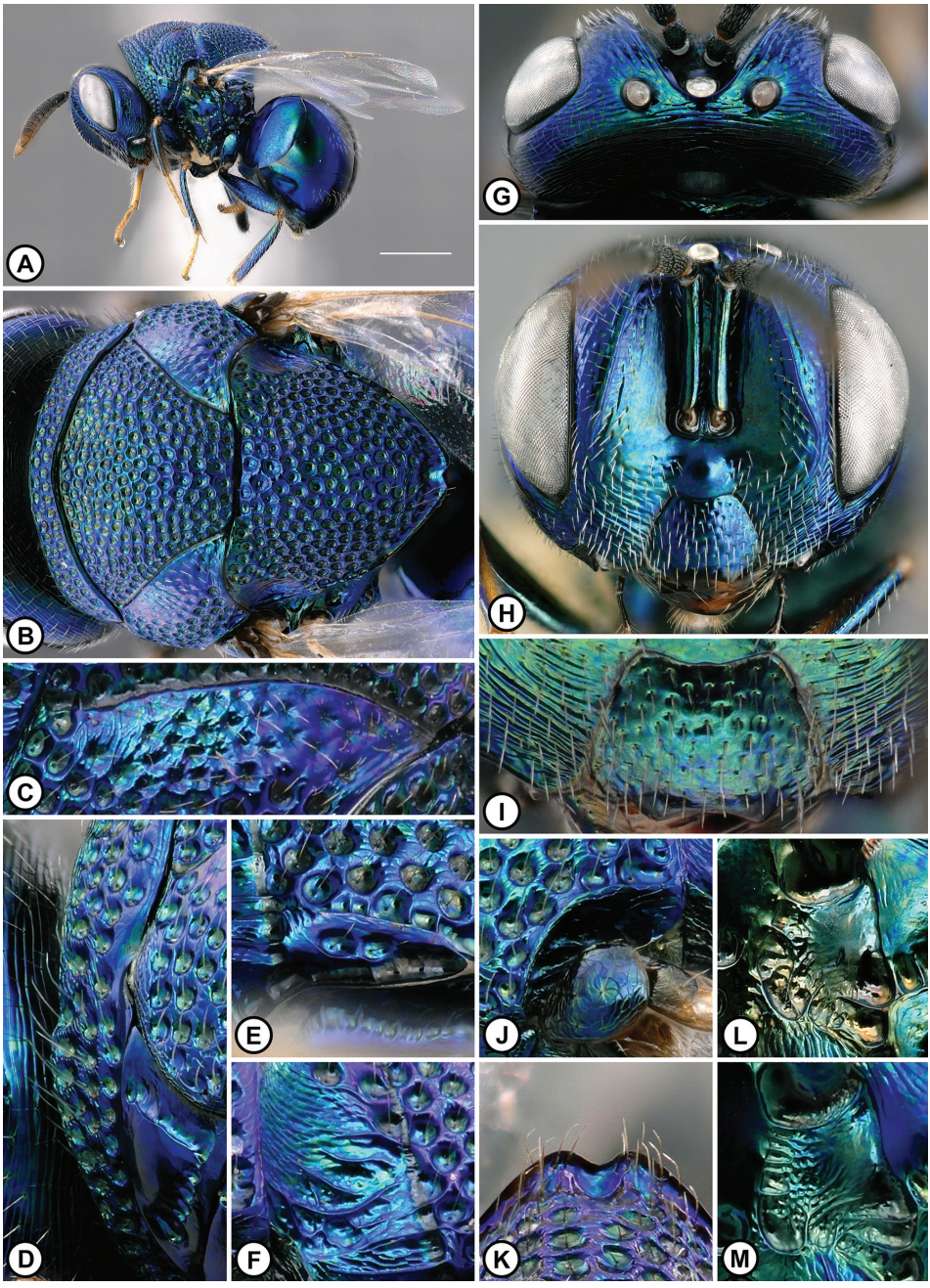

Figure 8. *Perilampus neodiprioni* Female **A** habitus, lateral view **B** habitus, dorsal view **C** lateral lobe of mesoscutum along notaulus **D** lateral panel of pronotum, posterior oblique view **E** axillula **F** axilla **G** head, dorsal view **H** head, anterior view **I** clypeus **J** parascutal carina **K** mesoscutellum apex **L, M** mesofemoral depression. [**A–E, G, H, J, L** Paratype, ROME162273; **F, M** Paratype, ROME198146; **I** ROME181757; **K** ROME189061]. Scale bar: 1 mm (**A**).

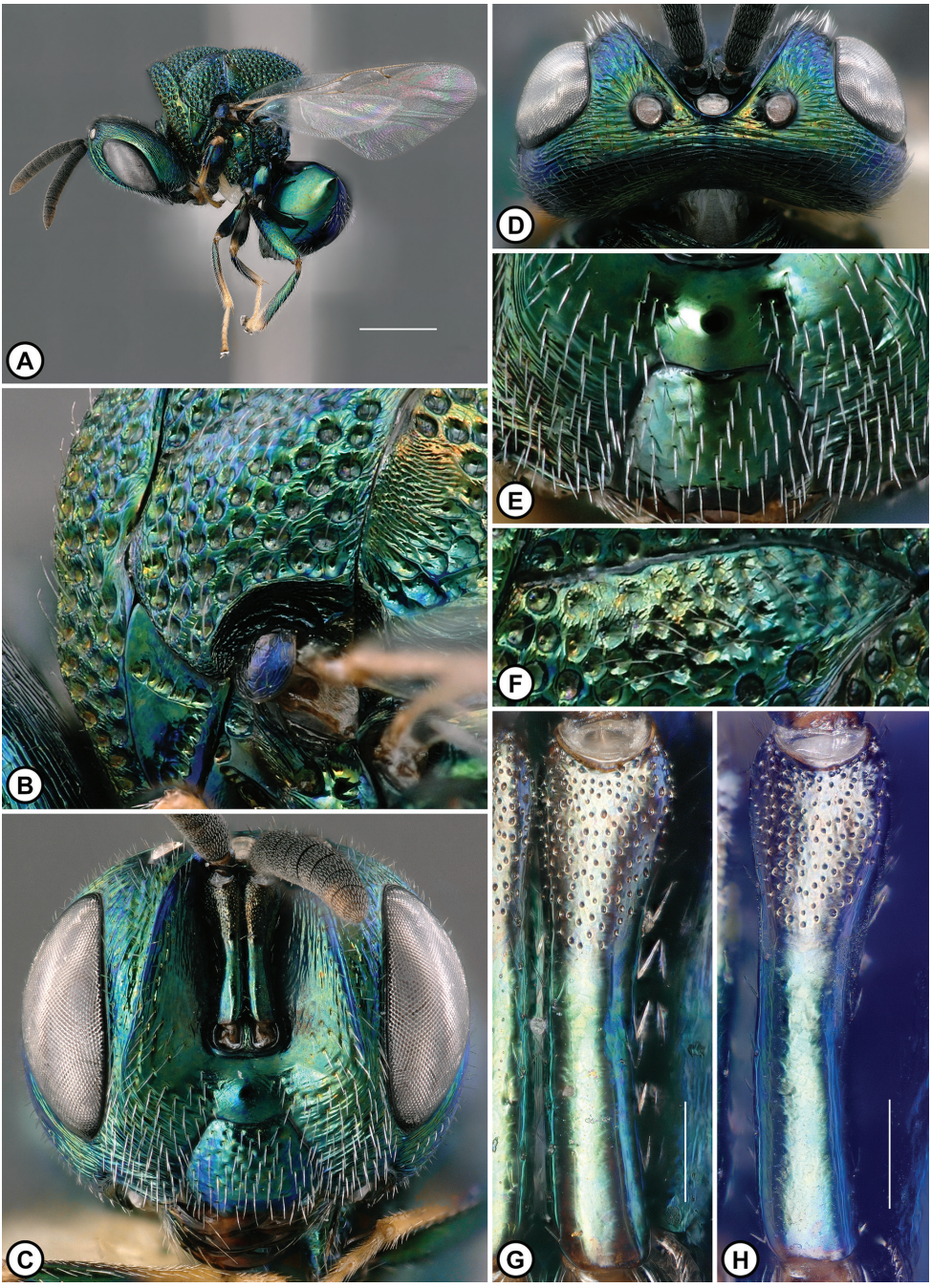

Figure 9. *Perilampus neodiprioni* Male **A** habitus, lateral view **B** lateral panel of pronotum, parascutal carina, and axilla **C** head, anterior view **D** head, dorsal view **E** lower face **F** lateral lobe of mesoscutum along notaulus **G, H** scape. [**A–D, F** Paratype, ROME162274; **E** ROME185922; **G** ROME152634; **H** ROME97556]. Scale bars: 1 mm (**A**); 100 μm (**G, H**).

Diprionidae that feed on pine trees. There are no completely reliable morphological characters to distinguish *P. neodiprioni* from *P. hyalinus* Say, the hyperparasitoids associated with Orthopteroidea. Imbricate-alveolate sculpture on the mesofemoral groove are found only in *P. neodiprioni*, but weakly imbricate, rugose, or smooth sculpture of mesofemoral groove are found in both species. Likewise, mesoscutellar teeth at the apex with steeply diverging inner margins are found only in *P. hyalinus*, but gradually diverging inner margins are found in both species. The presence of one or more piliferous punctures on axillula dorsad is a unique state found only in *P. neodiprioni* in the *P. hyalinus* species group. But its diagnostic value is somewhat limited because the axillula is punctate in 72% and smooth in 28% of the total studied specimens (n = 188). And the proportion of specimens with punctate axillula seems to show geographical variation: 84% of 136 specimens in the northeastern USA and southeastern Canada, fewer than half in the central USA (9 of 20) and Florida (7 of 25), and all the specimens from Belize (17) are punctate.

Genetic analysis suggests there are at least two distinct COI clades of *P. neodiprioni* in the Nearctic region: Ontario and Massachusetts; and Virginia, West Virginia, and Texas (Suppl. material 2). However, these COI clades are delimited as a single species by the distance-based methods (Suppl. material 5). The geographical distribution of each clade coincides with the post-glacial re-colonization pathways of *N. lecontei* populations from the Atlantic coast and Texas refugia (Bagley et al. 2016). This pattern is likely an indication of the fragmentation and genetic differentiation of *P. neodiprioni* populations during glaciation, and eventual post-glacial range expansion of parasitoids following their recolonizing sawfly hosts prior to secondary contact. ITS2 showed no genetic differentiation between the populations and both distance- and tree-based methods merged both populations as a single species (Suppl. materials 2, 5). This probably represents active interbreeding between the *P. neodiprioni* populations, which would result in full recombination of nuclear DNA, whereas the variation of non-recombinant COI accumulated during isolation was retained after secondary contact (Després 2019). Sequencing of Floridan specimens could reveal if there is a third distinct population of *P. neodiprioni* originated from the proposed southern glacial refugia near North and South Carolina that expanded their distribution with the sawfly hosts toward Florida (Bagley et al. 2016). The Belize specimens failed to sequence, and their potential genetic differentiation is yet to be explored. Specimens from Ontario and Massachusetts, which form one of the two COI clades, were selected as the type series.

Perilampus neodiprioni is the only species in the *P. hyalinus* species complex that exhibits an exclusive association with pine sawflies, more commonly as a primary parasitoid but also as a hyperparasitoid. An exception is a single *P. neodiprioni* specimen reared from *Diprion similis* (Hartig) in Ontario (ROME207314), but it lacks associated host remains and the collector had noted the uncertainty in their identification in the collection form. While it isn't surprising that *P. neodiprioni* can develop on *D. similis*, this sawfly species is non-native in the Nearctic region and not relevant to the evolutionary history of *P. neodiprioni*.

A large number of *P. neodiprioni* specimens were reared from *Neodiprion lecontei* cocoons in the 1940s at the Dominion Parasite Laboratory (DPL) in Belleville, Ontar-

io and subsequently transferred to the CNC. The 230 reared *P. neodiprioni* specimens are predominantly primary parasitoids (215) and only 15 are hyperparasitoids, 14 parasitoids of Ichneumonidae and one parasitoid of Tachinidae. The reared specimens from the other localities are also comprised of mostly primary parasitoids. Of the total 62 reared *P. neodiprioni* specimens associated with pine sawfly cocoons, 49 are primary parasitoids of *Neodiprion* spp., 13 are hyperparasitoids, of which 11 are parasitoids of Ichneumonidae and two are parasitoids of Tachinidae. There are however, two reared series that are only or mostly hyperparasitoids: Masschusetts (ROME162273–162275, 3 of 3) and Arkansas (ROME152640–152643, 185915, 185916, and 185956, 6 of 7). Tripp (1962) and Wilkinson et al. (1966) also documented *Perilampus* developing as both primary and hyperparasitoids associated with pine sawflies. It is unclear if *P. neodiprioni* can develop as hyperparastioids of the other primary parasitoids of pine sawflies with equal success. For example, Tripp (1962) and Hinks (1971) reported rare to no cases of *Perilampus* developing as hyperparasitoid on Diptera, but Wilkinson et al. (1966) reported predominance of hyperparasitoids on Diptera. Reared specimens examined in this study show that it is rarer for *P. neodiprioni* to develop on dipteran parasitoids than on hymenopteran parasitoids in both the DPL collection (0.4% vs 6%) and from other localities (3.2% vs 17.7%).

Neodiprion species are often serious pests in boreal forests (Alfaro and Fuentealba 2016; Johns et al. 2016) which suggests that *P. neodiprioni* could be an effective biological control agent, but this is complicated because this species can develop both as a primary parasitoid and as a hyperparasitoid. Evaluation of the biocontrol potential of *P. neodiprioni* will depend on the relative prevalence of other hymenopteran and dipteran primary parasitoids and their effectiveness as biological control agents —*P. neodiprioni* as a hyperparasitoid could interfere with the population dynamics of these strictly primary parasitoids (Schooler et al. 2011).

The shift in ecology from hyperparasitoid associated with Lepidoptera to primary or hyperparasitoid associated with pine sawflies is suggested by the sister species relationship between *P. neodiprioni* and *P. sirsiris* (Suppl. material 1), and their associations with pine trees. *Perilampus sirsiris* is the only known hyperparasitoid in the *P. hyalinus* species complex that is associated with gymnosperms as well as angiosperms. It is possible that the common ancestor of *P. neodiprioni* and *P. sirsiris* was a hyperparasitoid species which expanded the oviposition sites to include pines, where planidia would have encountered both Lepidoptera caterpillars and *Neodiprion* larvae. Pine sawfly larvae were likely suitable hosts for planidia that inadvertently burrowed into this novel host, driving the evolution of parasitoid capable of developing as a primary parasitoid of *Neodiprion* sawflies.

***Perilampus monocteni* Yoo & Darling, sp. nov.**
https://zoobank.org/296E0AB0-1E13-42EE-AE4E-27444553C977
Figs 10, 11

Type locality. Canada, Ontario, Peterborough County, Aspley.

Type material. ***Holotype*.** "CANADA, Ontario, Aspley No. S64-3469-01, 22.III. 1965 Ex. *Monoctenus juniperinus* On e.w. cedar, Lot 65.418". The *Monoctenus* associated with the holotype was later re-identified as *M. fulvus* (Kevin Barber, personnel communication). The holotype is point-mounted (Female ROME201079, CNC). ROM Online Collection.

***Paratypes*.** Canada: 7 females, 2 males. Ontario: 7 females, 2 males. City of Ottawa., Bells Corners: (5 females: ROME207334-CNC; ROME207332-GLFC; ROME207333-GLFC; ROME207331-ROME; ROME207335-USNM. 2 males: ROME207329-CNC; ROME207328-ROME). Haliburton Co., Haliburton: (1 female: ROME207336-CNC). Peterborough Co., Apsley: (1 female: ROME201078-CNC).

Additional material examined. Canada: 1 female, 1 male. Ontario: 1 female, 1 male. City of Ottawa., Bells Corners: (1 male: ROME207330-CNC). Renfrew Co., Beachburg: (1 female: ROME201101-CNC).

Etymology. The specific epithet is a noun in the genitive case meaning "of *Monoctenus*", in reference to the species' host preference for *Monoctenus* sawflies and their parasitoids.

Description. Female (Fig. 10). Length: 2.1–3.8 mm. Color: head iridescent greenish blue or violet; mesosoma and metasoma iridescent greenish blue or violet; clypeus ventral margin black (Fig. 10I, J); antenna with scape and pedicel weakly iridescent greenish blue or violet, flagellum brown or black, lighter ventrad and distad.

Head (Fig. 10G–J): in dorsal view transverse, width slightly greater than twice length, HW/HL 2.1–2.2. Frontal carina: in anterior view straight to weakly sinuate below midlevel of eye; in dorsal view gradually narrowed V shape around median ocellus, FC/MOD 1.5–1.6; distance from lateral ocellus short, FCLO/LOD 0.6–0.7. Scrobal cavity: in anterior view wide, SW/HW about 0.5. Ocelli (Fig. 10G): a line between anterior margin of lateral ocelli reaching anterior margin of median ocellus. POL/OOL 1.8–2.0. Ocellar ratios LOD: POL: OOL: LOL: 1, 2.9–3.4, 1.8–2.0, 1.0–1.2. Vertex: with strong to weak transverse striations, without large piliferous punctures. Parascrobal area: in lateral view gradually narrowed towards lower eye margin; width narrow, PSW/EL about 0.3; sculpture strongly to weakly striate, without large piliferous punctures. Gena: entirely or mostly striate along outer eye margin with narrow and short smooth area, striate behind. Malar space: MSL/EH about 0.2. Lower face (Fig. 10H, I, J): with setae sparse laterad torulus, and sparse below. Clypeus (Fig. 10I, J): CW/CH 1.4–1.5; ventral margin concave; with wide bare area without setae near dorsal margin, extended ventrad medially.

Mesosoma (Fig. 10B–F, K, L): Lateral panel of pronotum: about as wide as prepectus, LPP/PPT 0.8–0.9; without flange or with small rounded flange below level of mesothoracic spiracle in posterior oblique view (Fig. 10D). Mesofemoral depression: smooth (Fig. 10L), weakly imbricate, or rugulose. Mesoscutum: punctures angulate, with narrow or slightly wide and weakly coriarious interspaces (Fig. 10B); lateral lobe usually weakly punctate with coriarious or smooth interspaces along notaulus (Fig. 10C); parascutal carina broadly curved, acuminate (Fig. 10E). Mesoscutellum: apex

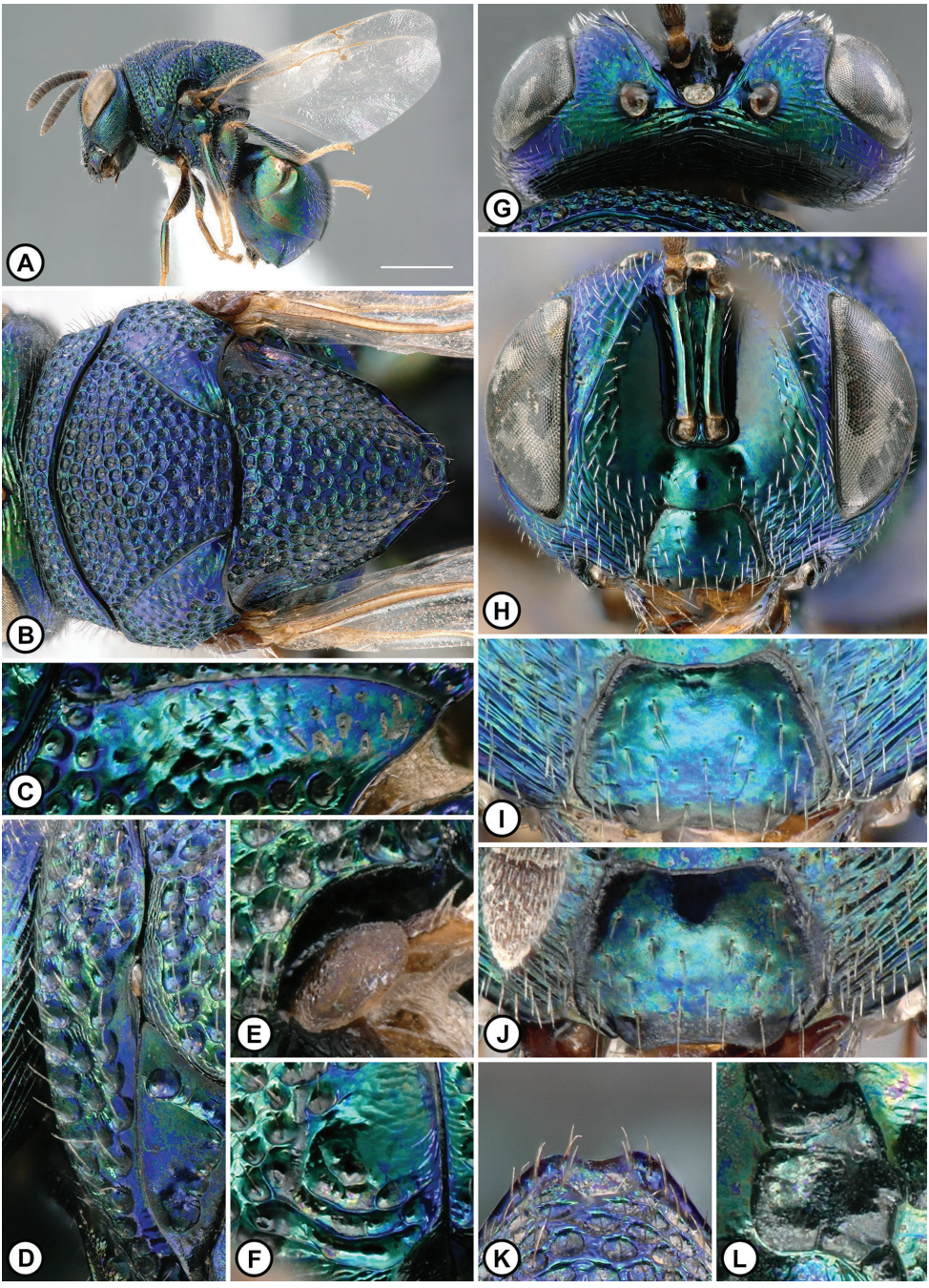

Figure 10. *Perilampus monocteni* Female **A** habitus, lateral view **B** habitus, dorsal view **C** lateral lobe of mesosucutm along notaulus **D** lateral panel of pronotum, posterior oblique view **E** parascutal carina **F** axilla **G** head, dorsal view **H** head, anterior view **I, J c**lypeus **K** mesoscutellum apex **L** mesofemoral depression. [**A, B, D, K** Paratype, ROME201078; **C** Paratype, ROME207336; **E, J, L** Holotype, ROME201079; **F** Paratype, ROME207331; **G–I** Paratype, ROME207334]. Scale bar: 1 mm (**A**).

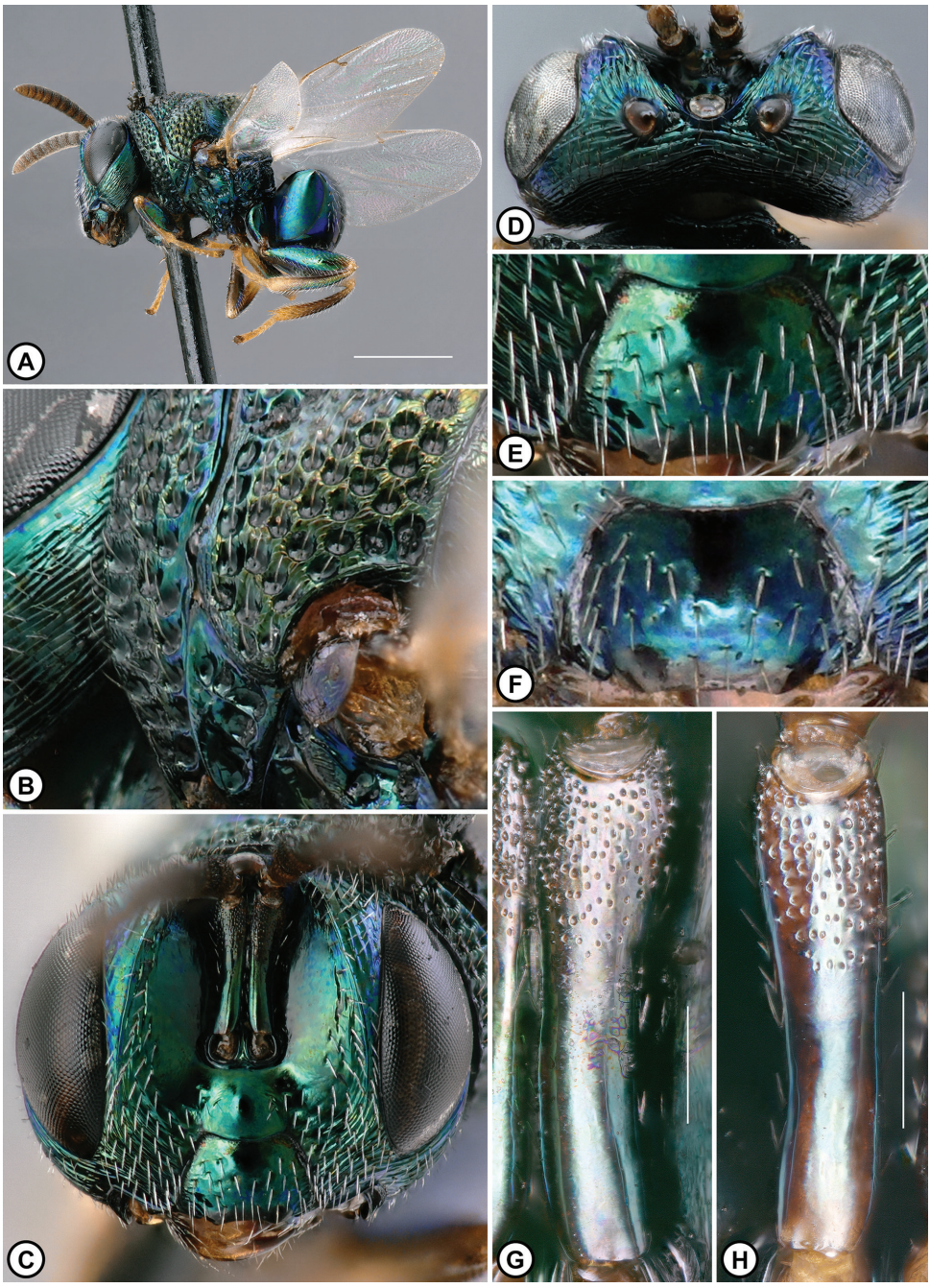

Figure 11. *Perilampus monocteni* Male **A** habitus, lateral view **B** lateral panel of pronotum, parascutal carina **C** head, anterior view **D** head, dorsal view **E, F** clypeus **G, H** scape. [**A–C, E, G** Paratype, ROME207328 **D, F, H** Paratype, ROME207329]. Scale bars: 1 mm (**A**); 100 μm (**G, H**).

with inner margins gradually diverging (Fig. 10K); punctures angulate, with narrow or slightly wide and weakly coriarious interspaces. Axilla: in lateral view imbricate dorsad, and rugose-areolate (Fig. 10F) or carinate ventrad. Axillula: smooth dorsad. Fore wing: stigma small, 2.0–2.5 × as wide as postmarginal vein.

Male (Fig. 11). Length: usually smaller, 2.7–2.9 mm. As in female, except: Color: mesonotum sometimes with weak cupreous iridescence. Frontal carina (Fig. 11D): distance from lateral ocellus shorter, FCLO /LOD 0.3–0.4. Scape (Fig. 11G, H): pits sparse, covering about 0.4 × scape length.

Diagnosis. *Perilampus monocteni* can be distinguished by a clypeus with a wide and bare area without setae near the dorsal margin, which is extended ventrad medially (Figs 10I, J, 11E, F cf. Figs 4I, 5E).

Distribution (Fig. 25B). Eastern Canada (Ontario).

Host association. *Perilampus monocteni* can develop as a primary parasitoid of cedar sawflies (Fig. 26G), or as a hyperparasitoid, a parasitoid of dipteran parasitoids of cedar sawflies (Fig. 26H). Hosts: Diprionidae (Hymenoptera). *Monoctenus fulvus* (Norton), *M. suffusus* (Cresson). Tachinidae (Diptera). Tachinids from *M. suffusus.*

Variation. A female and male reared from *Monoctenus* spp. have slight variations in the clypeal setae. One has two setae on the mostly bare area of the clypeus dorsad (ROME201101), and the other lacks a distinctive bare area on clypeus dorsad (ROME207330). The host records and absence of diagnostic characters specific to the other species suggest that these two specimens are *P. monocteni*.

Remarks. The available specimens of *P. monocteni* are unsuitable for the sequencing method used in this study. Despite the lack of genetic data, the species hypothesis of *P. monocteni* is supported by the distinctive setal distribution pattern on the clypeus and a unique host association. *Perilampus monocteni* is a paraisitoid strictly associated with Diprionidae similar to *P. neodiprioni.* However, *P. monocteni* parasitizes cedar sawflies and their parasitoids, unlike *P. neodiprioni* which parasitizes pine sawflies and their parasitoids. Of the total six specimens associated with *Monoctenus* cocoons, three were primary parasitoids of cedar sawflies (ROME207330, 207332, and 207336) and three were hyperparasitoids that parasitized dipteran parasitoids of cedar sawflies. (ROME207328, 207333, and 207335). The known distribution is restricted to eastern Ontario but this may be due to the solitary larval feeding behaviour of *Monoctenus* spp. (Rose et al. 2010)—in comparison, many *Neodiprion* spp. are characterized by gregarious larval feeding behaviour (Haack and Mattson 1993) and more conspicuous and more often collected. The combination of sparse pits on a male scape, the lack of a triangular flange on the lateral panel of pronotum, and the female mesoscutum without strong cupreous iridescence suggest that *P. monocteni* is clearly a member of the *P. hyalinus* complex clade 2 but its precise phylogenetic placement needs to be determined with genetic data. But if the parasitism associated with conifer-feeding sawflies was derived only once in the *P. hyalinus* species complex, *P. monocteni* is probably the sister species of *P. neodiprioni*, which is also a member of clade 2.

***Perilampus crassus* Yoo & Darling, sp. nov.**
https://zoobank.org/54557ED2-7D2D-424A-9D8F-519098A2470D
Figs 12, 13

Type locality. USA, Florida, Gainesville.

Type material. ***Holotype.*** "USA: FL: Alachua Co.: nr. Gainesville airport, 45 m 29°42'0"N, 82°15'40"W 2.Oct.2016 A. Baker, A. Knyshov, J. Zhang swp AB16.028". The holotype is point-mounted (Female ROME182771, UCRC). BOLD:AEE9250/ITS2. ROM Online Collection.

Paratypes. USA: 1 female, 2 males. Florida: 1 female, 2 males. Putnam Co., Ordway-Swisher Biol. Station, Rd. C6: (1 female: ROME189115-MCZC; BOLD:AEE9250; ITS2. 2 males: ROME189062-MCZC; ITS2; ROME189063-MCZC; BOLD:AEE9250; ITS2).

Material examined. USA: 9 females, 4 males. (Suppl. materials).

Additional material examined. Cuba: 1 female. (1 female: ROME189093–USNM).

Etymology. The specific epithet is the Latin adjective *crassus* (coarse), in reference to the punctate sculpture on the lateral lobes of the mesoscutum along notaulus.

Description. Female (Fig. 12). Length: 3.0–4.8 mm. Color: head iridescent greenish blue or violet; mesosoma and metasoma iridescent greenish blue or violet; clypeus ventral margin entirely iridescent (Fig. 12I); antenna with scape and pedicel weakly iridescent greenish blue or violet, flagellum brown or black, lighter ventrad and distad.

Head (Fig. 12G–J): in dorsal view transverse, width slightly greater than twice length, HW/HL 2.1–2.2. Frontal carina: in anterior view straight to weakly sinuate below midlevel of eye; in dorsal view gradually narrowed V shape around median ocellus, FC/MOD 1.5–1.7; distance from lateral ocellus short, FCLO/LOD 0.6–0.7. Scrobal cavity: in anterior view wide, SW/HW about 0.5. Ocelli (Fig. 12G): a line between anterior margin of lateral ocelli reaching anterior margin of median ocellus or nearly bisecting median ocellus. POL/OOL 1.7–2.1. Ocellar ratios LOD: POL: OOL: LOL 1, 3.1–3.4, 1.5–1.9, 1.1–1.3. Vertex: with strong to weak transverse striations, without large piliferous punctures. Parascrobal area: in lateral view gradually narrowed towards lower eye margin; width narrow, PSW/EL about 0.3; sculpture strongly to weakly striate, without large piliferous punctures. Gena (Fig. 12J): entirely striate along outer eye margin, striate posterad. Malar space: MSL/EH 0.2–0.3. Lower face (Fig. 12H, I): with setae sparse laterad torulus, and usually sparse below. Clypeus: CW/CH about 1.4; ventral margin nearly straight; setae evenly distributed, or with small bare area without setae medially.

Mesosoma (Fig. 12B–F, K, L): Lateral panel of pronotum: about as wide as prepectus, LPP/PPT about 0.9; without flange below level of mesothoracic spiracle in posterior oblique view (Fig. 12D). Mesofemoral depression: smooth, rugulose, weakly imbricate, or imbricate-alveolate (Fig. 12L). Mesoscutum: punctures angulate, with narrow or slightly wide and weakly coriarious interspaces (Fig. 12B); lateral lobe strongly punctate with coriarious or smooth interspaces along notaulus (Fig. 12C); parascutal

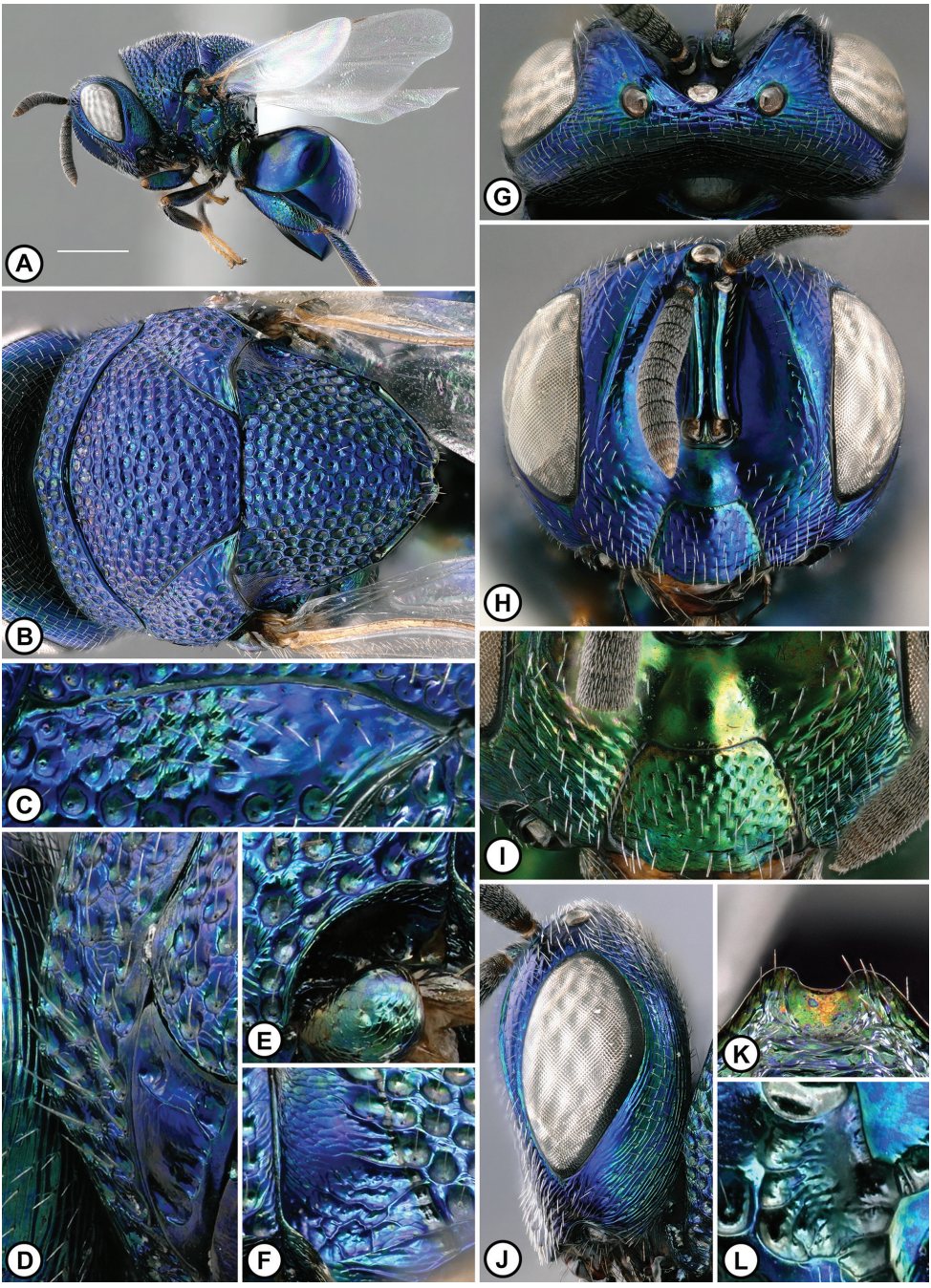

Figure 12. *Perilampus crassus* Female **A** habitus, lateral view **B** habitus, dorsal view **C** lateral lobe of mesoscutum along notaulus **D** lateral panel of pronotum, posterior oblique view **E** parascutal carina **F** axilla **G** head, dorsal view **H** head, anterior view **I** lower face **J** head, lateral view **K** mesoscutellum apex **L** mesofemoral depression. [**A–H, J, L** Holotype, ROME182771 **I** ROME189085 **K** ROME189115]. Scale bar: 1 mm (**A**).

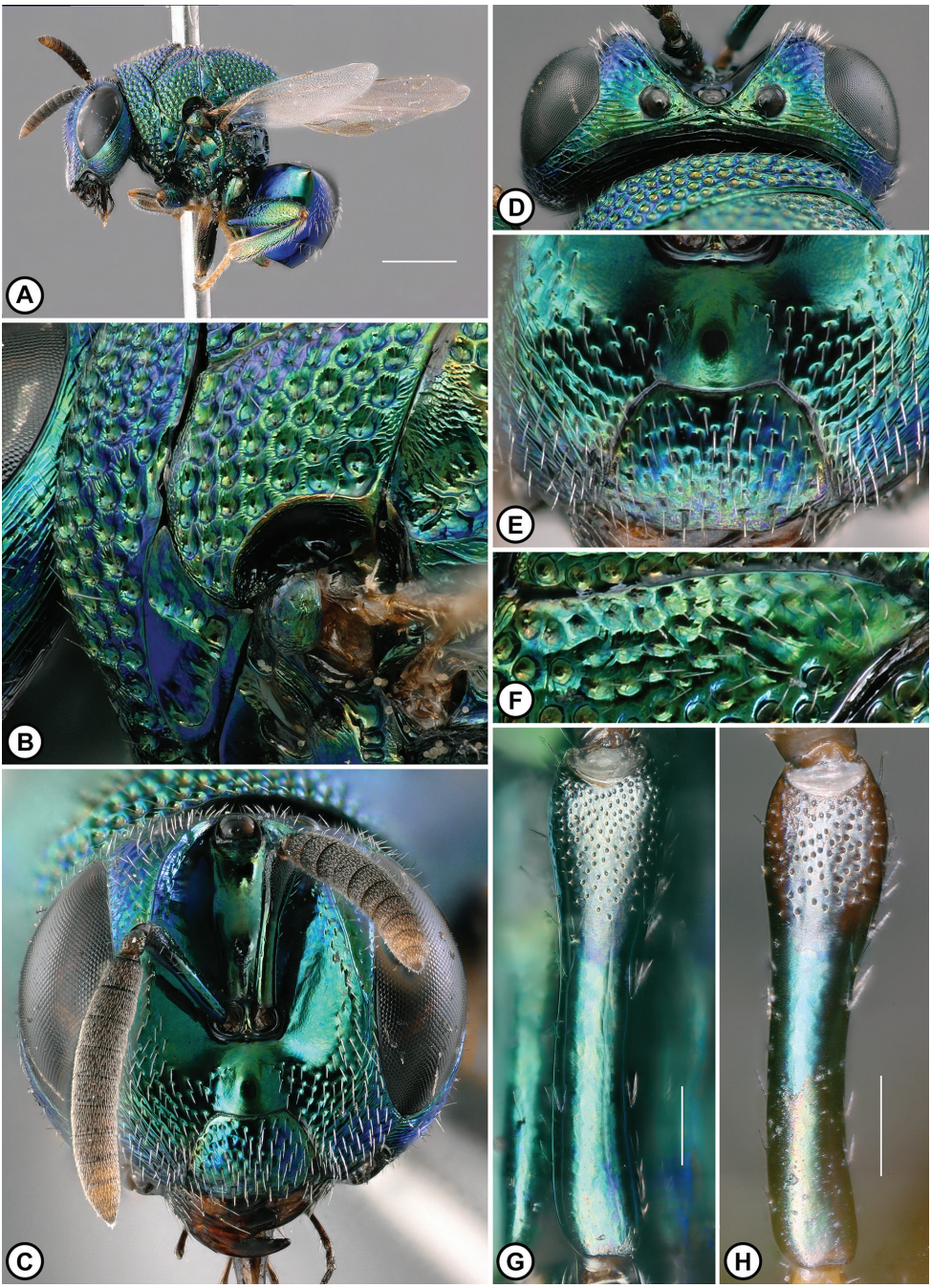

Figure 13. *Perilampus crassus* Male **A** habitus, lateral view **B** lateral panel of pronotum, parascutal carina, and axilla, posterior oblique view **C** head, anterior view **D** head, dorsal view **E** lower face **F** lateral lobe of mesoscutum along notaulus **G, H** scape. [**A, B, G** Paratype, ROME189063; **C, E, F** Paratype, ROME189062; **H** ROME189117]. Scale bars: 1 mm (**A**); 100 μm (**G, H**).

carina broadly curved, acuminate (Fig. 12E). Mesoscutellum: apex with inner margins gradually or abruptly diverging (Fig. 12K); punctures angulate, with narrow or slightly wide and weakly coriarious interspaces. Axilla: in lateral view imbricate dorsad and rugose-areolate (Fig. 12F) or carinate ventrad. Axillula: smooth dorsad. Fore wing: stigma small, 2.0–2.5 × as wide as postmarginal vein.

Male (Fig, 13). Length: usually smaller, 3.0–3.8 mm. As in female, except: Frontal carina (Fig. 13D): distance from lateral ocellus as wide or shorter, FCLO/LOD 0.5–0.6. Scape (Fig. 13G, H): pits sparse, covering about 0.3 × scape length.

Diagnosis. *Perilampus crassus* can be distinguished by a weakly iridescent and nearly straight ventral margin of clypeus (Figs 12I, 13E cf. Figs 8I, 18I). Also, the lateral lobe of mesoscutum is more strongly punctate along the notaulus than in the other species with punctate sculpture (Figs 12C, 13F cf. Figs 4C, 5F, 8C, 9F).

Distribution (Fig. 25A). Central and southern USA: USA (Arkansas, Florida, Kansas, New Mexico, Texas). Possibly Cuba.

Host association. Hosts unknown.

Remarks. This species is supported by both genes (Fig. 1, Suppl. material 5), and there are three BINed specimens on BOLD (AEE9250) from Florida. Only specimens from Florida were successfully sequenced and the degree of intraspecific genetic variability in this species is unclear. A single specimen collected from avocado fruit imported from Cuba (ROME189093) suggests that the distribution of *P. crassus* extends to the Greater Antilles.

Perilampus pilosus Yoo & Darling, sp. nov.

https://zoobank.org/1C7022C2-2C90-4627-BF19-CF0C558ACC3D
Figs 14, 15

Type locality. USA, Texas, 3.5 mi SE La Sauceda.

Type material. *Holotype*. "USA, Texas, Presidio Co. Big Bend Ranch SNA McGuirks Tanks on desert willows 12.V.1990, R Wharton". The holotype is point-mounted (Female ROME182765, TAMU). BOLD:AEF0151/ITS2. ROM Online Collection.

***Paratypes*.** USA: 3 females, 3 males. Arizona: 2 females. Graham Co., Pinaleno Mountains, Ash Creek near Cluff Ranch Wildlife Area, 14 km SW Pima, 32°47.69'N, 109°51.42'W: (1 female: ROME152679-CNC; ITS2). Pinaleno Mountains, Gilespie Wash, 10 km W Jct. 191 on hwy 266, 32°33'91"N, 109°45'59"W: (1 female: ROME182819-USNM; BOLD:AEF0151). California: 1 female, 1 male. San Bernardino Co., Joshua Tree N.P., 29 Palms, JTNP, Oasis of Mara, 34°07'42"N, 116°02'19"W: (1 female: ROME189067-UCRC; COI; ITS2. 1 male: ROME189068-UCRC; BOLD:AEF0151; ITS2). Texas: 2 males. Presidio Co., Big Bend Ranch SNA, McGuirks Tanks: (1 male: ROME182761-TAMU; BOLD:AEF0151; ITS2). Big Bend Ranch SNA, McGuirks Tanks, 29°28'34"N, 103°49'12"W: (1 male: ROME182757-TAMU; BOLD:AEF0151; ITS2).

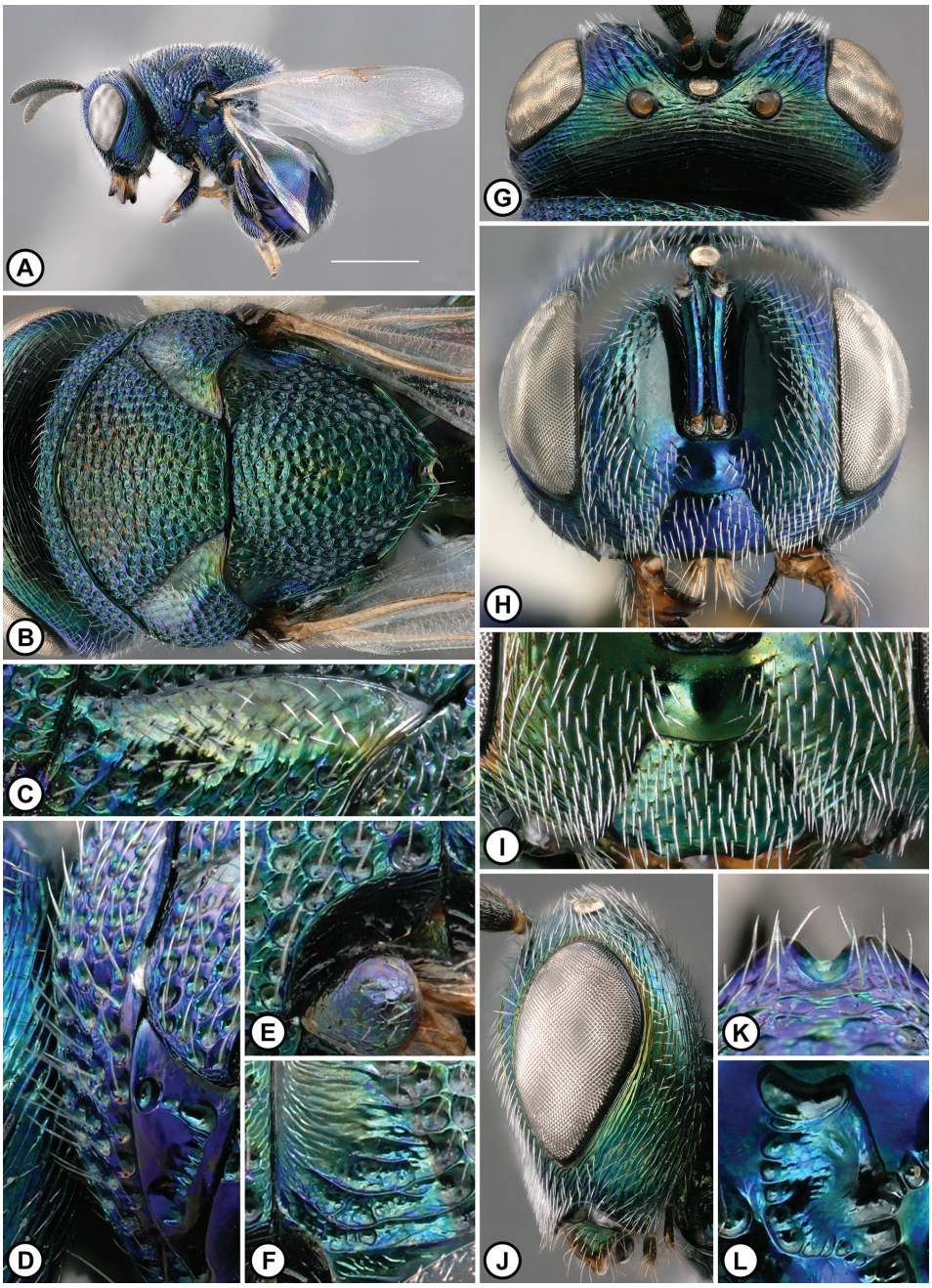

Figure 14. *Perilampus pilosus* Female **A** habitus, lateral view **B** habitus, dorsal view **C** lateral lobe of mesoscutum along notaulus **D** lateral panel of pronotum, posterior oblique view **E** parascutal carina **F** axilla **G** head, dorsal view **H** head, anterior view **I** lower face **J** head, lateral view **K** mesoscutellum apex **L** mesofemoral depression. [**A, H** Holotype, ROME182765; **B, C, E–G, L** Paratype, ROME182819; **I, J** Paratype, ROME189067; **K** ROME189129; **L** Paratype, ROME152679]. Scale bar: 1 mm (**A**).

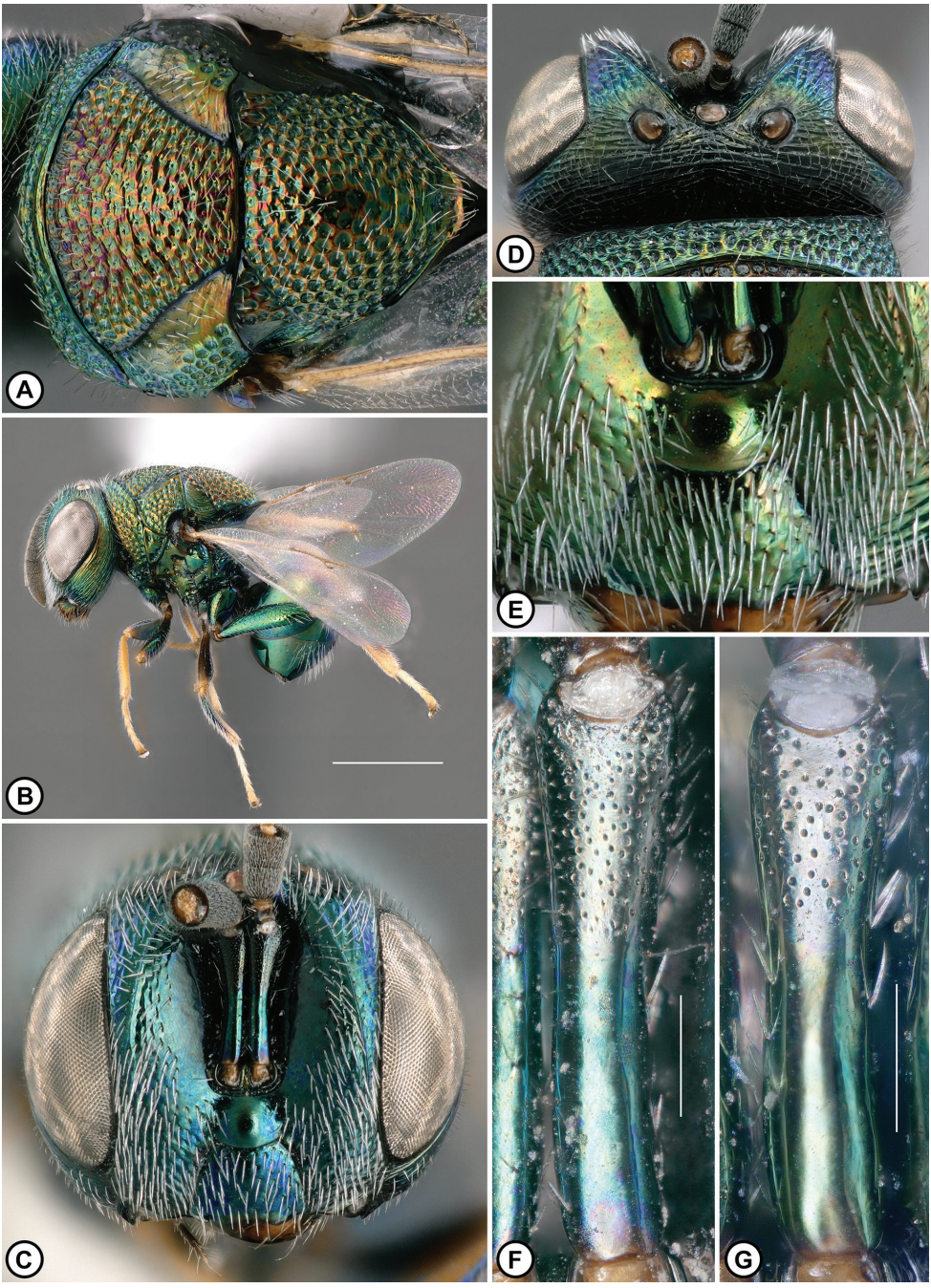

Figure 15. *Perilampus pilosus* Female **A** habitus, dorsal view. Male **B** habitus, lateral view **C** head, anterior view **D** head, dorsal view **E** lower face **F, G** scape. [**A** Paratype, ROME189067; **B** Paratype, ROME152727; **C, D, F** Paratype, ROME182757; **E** ROME152714; **G** ROME152725]. Scale bars: 1 mm (**B**); 100 μm (**F, G**).

Material examined. Mexico: 5 females. USA: 19 females, 29 males. (Suppl. materials).

Additional material examined. Mexico: 1 female. Sonora: 1 female. (1 female: ROME189096-UCDC).

Etymology. The specific epithet is the Latin adjective *pilosus* (hairy), in reference to the densely setose face.

Description. Female (Figs 14, 15A). Length: 3.0–4.4 mm. Color: head, mesosoma, and metasoma iridescent greenish blue or violet with or without weak cupreous mesonotum (Fig. 14B), or iridescent green with strong cupreous mesonotum (Fig. 15A); clypeus ventral margin black (Fig. 14I); antenna with scape and pedicel weakly iridescent greenish blue or violet, flagellum brown or black, lighter ventrad and distad.

Head (Fig. 14G–J): in dorsal view transverse, width slightly greater than twice length, HW/HL 2.1–2.2. Frontal carina: in anterior view straight to weakly sinuate below midlevel of eye; in dorsal view gradually narrowed V shape around median ocellus, FC/MOD 1.5–1.9; distance from lateral ocellus short to long FCLO/LOD 0.6–1.0. Scrobal cavity (Fig. 14H): in anterior view wide, SW/HW about 0.5. Ocelli (Fig. 14G): a line between anterior margin of lateral ocelli nearly bisecting median ocellus or reaching posterior margin of median ocellus. POL/OOL 1.8–2.0. Ocellar ratios LOD: POL: OOL: LOL 1, 2.9–3.5, 1.6–1.8, 1.1–1.4. Vertex: with strong to weak transverse striations, without large piliferous punctures. Parascrobal area: in lateral view gradually narrowed towards lower eye margin; width narrow, PSW/EL 0.2–0.3; sculpture strongly to weakly striate, without large piliferous punctures. Gena (Fig. 14J): entirely striate along outer eye margin, striate posterad. Malar space: MSL/EH about 0.2. Lower face (Fig. 14H, I): with setae dense and widely distributed laterad torulus, and dense below. Clypeus (Fig. 14I): CW/CH 1.4–1.5; ventral margin concave; setae evenly distributed, or with small bare area without setae medially.

Mesosoma (Fig. 14B–F, K, L): Lateral panel of pronotum: about as wide as prepectus, LPP/PPT 0.8–0.9; without flange below level of mesothoracic spiracle in posterior oblique view (Fig. 14D). Mesofemoral depression: smooth or weakly imbricate (Fig. 14L). Mesoscutum: punctures angulate, with narrow or slightly wide and weakly coriarious interspaces (Fig. 14B); lateral lobe smooth or weakly coriarious along notaulus (Fig. 14C); parascutal carina broadly curved, acuminate (Fig. 14E). Mesoscutellum: apex with inner margins gradually diverging (Fig. 14K); punctures angulate, with narrow or slightly wide and weakly coriarious interspaces. Axilla (Fig. 14F): in lateral view imbricate dorsad and rugose-areolate or carinate ventrad. Axillula: smooth dorsad. Fore wing: stigma small, 2.0–2.5 × as wide as postmarginal vein.

Male (Fig. 15B–G). Length: usually smaller, 2.3–3.1 mm. As in female, except: Color: mesonotum with strong or weak cupreous iridescence. Frontal carina: distance from lateral ocellus as wide or shorter, FCLO/LOD 0.5–0.6. Scape: pits sparse, covering 0.3–0.4 × scape length.

Diagnosis. *Perilampus pilosus* can be distinguished by the combination of an advanced median ocellus (Figs 14G, 15D cf. Figs 8G, 9D), dense and widely distributed setae on the face (Figs 14H, 15C cf. Figs 8H, 9C), lateral panel of the pronotum with-

out a flange (Fig. 14D cf. Fig. 16D), and the sparsely pitted male scape (Fig. 15F, G cf. Fig. 17G, H). *Perilampus pilosus* specimens with cupreous mesonota are superficially similar to *P. sonora* (Fig. 15A cf. Fig. 22B) but differ in having dense setae laterad of the torulus (Figs 14I, 15E cf. Figs 22I, 23E).

Distribution (Fig. 25F). Southwestern and central USA, and western and southern Mexico: USA (California, New Mexico, Texas), Mexico (Baja California Sur, Morelos, Sonora).

Host association. *Perilampus pilosus* is a hyperparasitoid, parasitizing dipteran parasitoids of Lepidoptera. Hosts: Tachinidae (Diptera). *Chaetogena* sp. from *Hemileuca juno* Packard (Saturniidae).

Variation. A female from Sonora, Mexico (ROME189096) has the frontal carina close to the lateral ocellus (FCLO/OD about 0.5) and iridescent olivaceous head.

Remarks. This species is supported by both genes (Fig. 1, Suppl. material 5), and there are five BINed specimens on BOLD (AEF0151) from the western and central USA. All specimens except (ROME189067) are grouped as a monophyletic clade in COI (Suppl. material 2). The low COI sequence quality in ROME189067 likely caused its exclusion from the monophyletic clade as evidenced by poor peak shapes in a chromatogram. All specimens including ROME189067 are grouped as monophyletic with both ITS2 and concatenated datasets (Fig. 1, Suppl. material 2).

Perilampus seneca Yoo & Darling, sp. nov.

https://zoobank.org/B7D5FBA5-DA48-498D-A32A-C393A3B62404
Figs 16, 17

Type locality. Canada, Ontario, Chaffey's Locks.

Type material. ***Holotype.*** "CANADA, ONT: Frontenac Co., Chaffey's Locks Oct. 6, 1987 DC Darling. Ex: birch", "LAB REARED Ex: tachinid parasite of Hyphantria cunea". The holotype is point-mounted (Female ROME183977, ROME). BOLD:ACF3436. ROM Online Collection.

Paratypes. Canada: 1 male. Ontario: 1 male. Essex Co., Windsor: (1 male: ROME162263-ROME; BOLD:ACF3436; ITS2). USA: 5 females. Indiana: 1 female. Posey Co., Harmonie State Park: (1 female: ROME182769-TAMU; BOLD:ACF3436; ITS2). Kentucky: 1 female. Jessamine Co., S. of Nicholasville, 37°47'4"N, 84°34'11"W: (1 female: ROME158541-ROME; BOLD:ACF3436; ITS2). Missouri: 1 female. St. Louis Co., St. Louis: (1 female: ROME185906-ROME; BOLD:ACF3436; ITS2). Texas: 1 female. Walker Co., Huntsville: (1 female: ROME185911-TAMU; BOLD:ACF3436; ITS2). West Virginia: 1 female. Hardy Co., 3 mi NE Mathias, 38.9098, -78.8881: (1 female: ROME198142-USNM; BOLD:ACF3436; ITS2).

Material examined. Canada: 13 females, 17 males. USA: 38 females, 29 males. (Suppl. materials).

Additional material examined. USA: 2 females, 3 males. Florida: 2 females, 3 males. Alachua Co., Gainesville: (1 male: ROME204136-SEMC). (2 males:

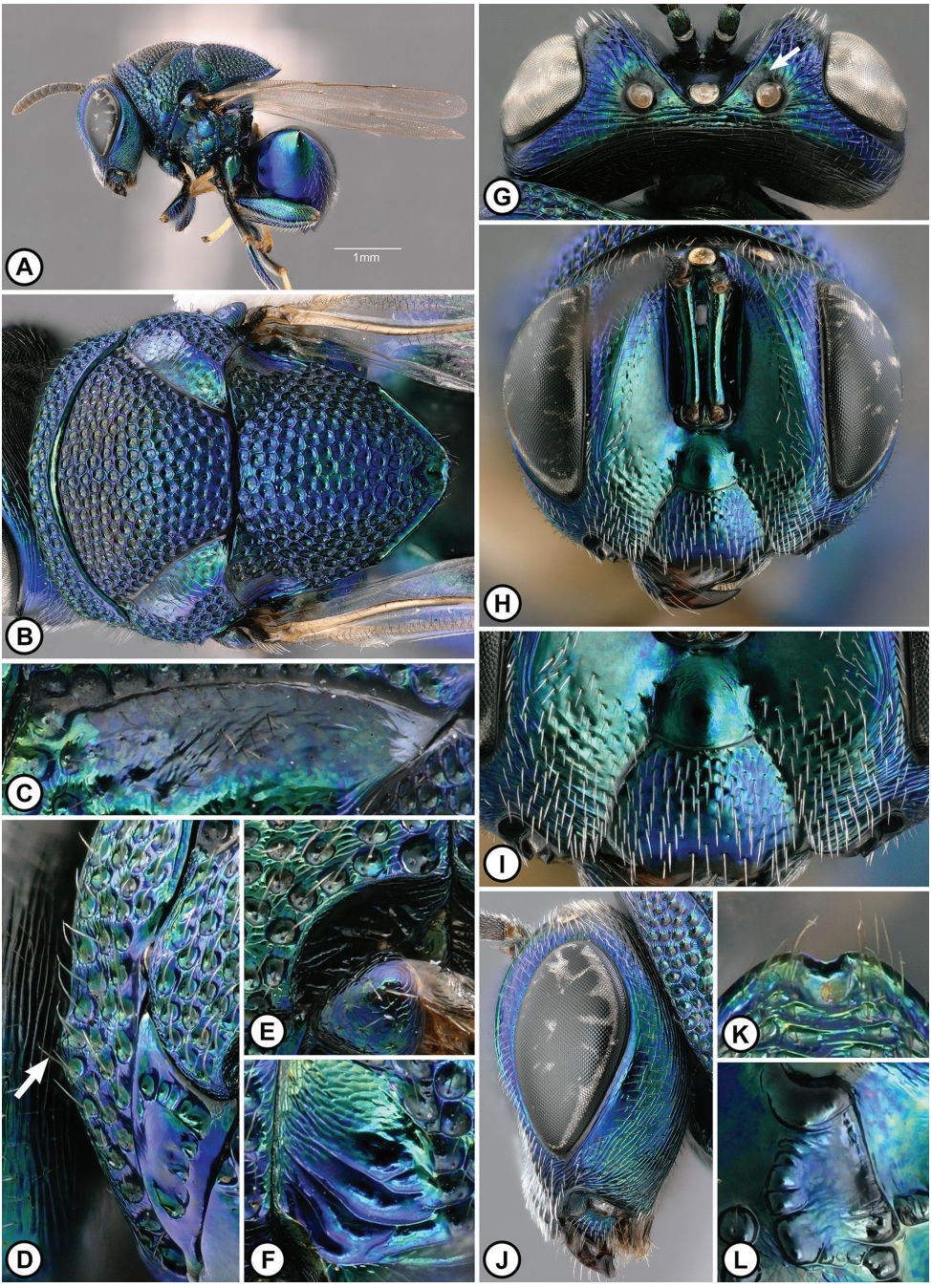

Figure 16. *Perilampus seneca* Female **A** habitus, lateral view **B** habitus, dorsal view **C** lateral lobe of mesoscutum along notaulus **D** lateral panel of pronotum, posterior oblique view **E** parascutal carina **F** axilla **G** head, dorsal view **H** head, anterior view **I** lower face **J** head, lateral view **K** mesoscutellum apex **L** mesofemoral depression. [**A, H, I, J, L** ROME199563; **B, F, G** Paratype, ROME182769; **C** Paratype, ROME158541; **D** ROME199544; **E** Holotype, ROME183977; **K** Paratype, ROME198142]. Scale bar: 1 mm (**A**).

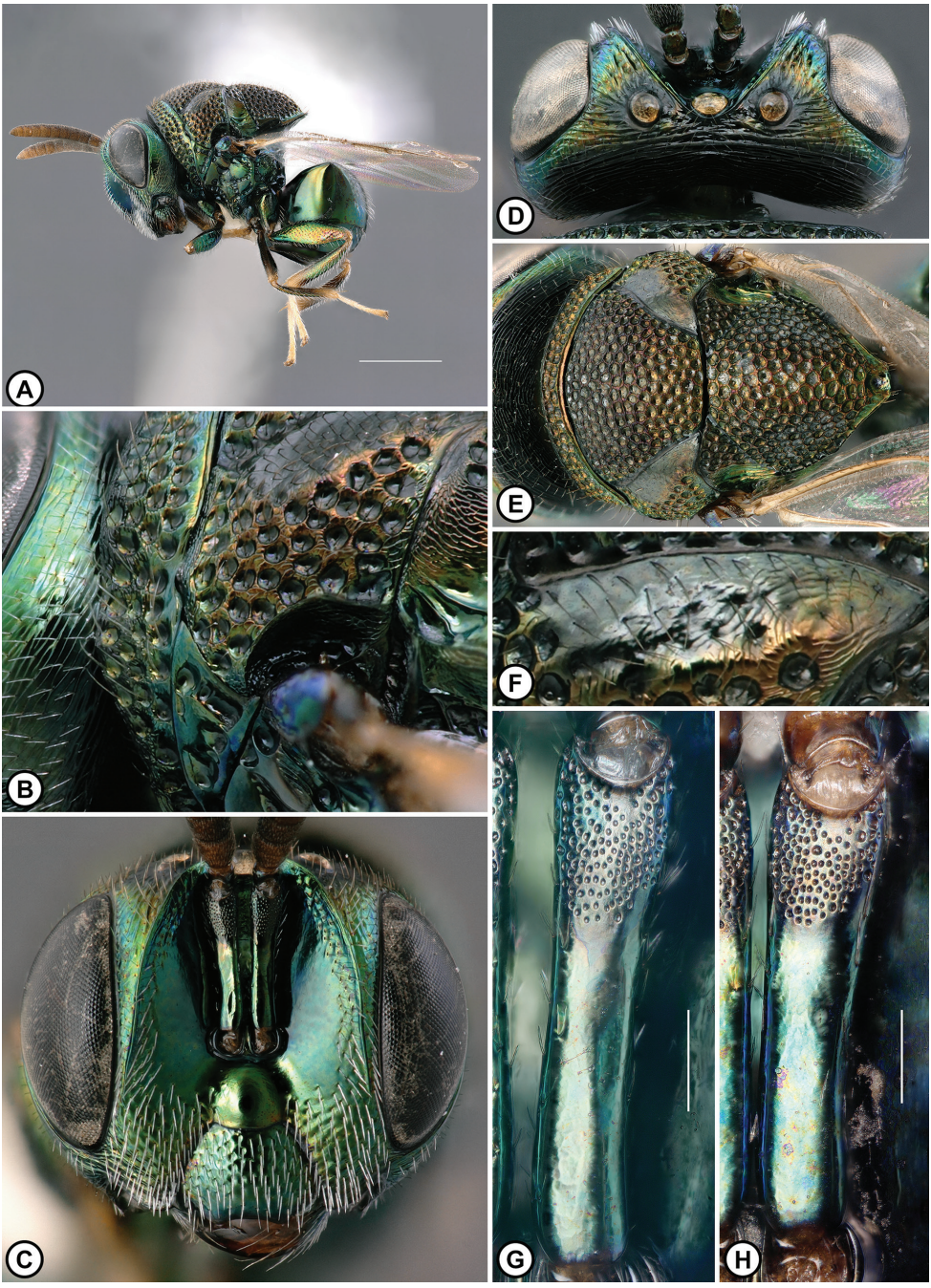

Figure 17. *Perilampus seneca* Male **A** habitus, lateral view **B** lateral panel of pronotum, parascutal carina, and axilla, posterior oblique view **C** head, anterior view **D** head, dorsal view **E** habitus, dorsal view **F** lateral lobe of mesoscutum along notaulus **G, H** scape. [**A–C, F, G** ROME183976; **D** ROME199551; **E** ROME162263; **H** ROME199552]. Scale bars: 1 mm (**A**); 100 μm (**G, H**).

ROME207380-FSCA; ROME207381-FSCA). Orange Co., Orlando, UCF Campus: (1 female: ROME152729-UCFC; BOLD:ACF3436; ITS2). Walt Disney World, Sec 16 T24S R27E: (1 female: ROME152728-UCFC; BOLD:ACF3436; ITS2).

Etymology. The specific epithet is a noun in apposition—a reference to both the Seneca people who are the original inhabitants of the core range of the species and to the county in New York State where most of the specimens were reared.

Description. Female (Fig. 16). Length: 2.9–4.4 mm. Color: head iridescent greenish blue or violet with black coloration between lateral ocellus and frontal carina (Fig. 16G, arrow); mesosoma, and metasoma iridescent greenish blue or violet; clypeus ventral margin black (Fig. 16I); antenna with scape and pedicel weakly iridescent greenish blue or violet, flagellum brown or black, lighter ventrad and distad.

Head (Fig. 16G–J): in dorsal view transverse, width slightly greater than twice length, HW/HL 2.1–2.2. Frontal carina: in anterior view straight to weakly sinuate below midlevel of eye; in dorsal view gradually narrowed V shape around median ocellus, FC/MOD 1.5–1.7; distance from lateral ocellus short, FCLO/LOD 0.5–0.6. Scrobal cavity (Fig. 16H): in anterior view wide, SW/HW about 0.5. Ocelli (Fig. 16G): a line between anterior margin of lateral ocelli touching anterior margin of median ocellus. POL/OOL 1.9–2.1. Ocellar ratios LOD: POL: OOL: LOL 1, 2.9–3.2, 1.5–1.8, 1.0–1.2. Vertex: with strong to weak transverse striations, without large piliferous punctures. Parascrobal area: in lateral view gradually narrowed towards lower eye margin; width narrow, PSW/EL 0.2–0.3; sculpture strongly to weakly striate, without large piliferous punctures. Gena (Fig. 16J): mostly striate along outer eye margin with narrow and short smooth area, striate behind. Malar space: MSL/EH about 0.2. Lower face (Fig. 16H, I): with setae sparse or dense and narrowly distributed laterad torulus, and sparse or dense below. Clypeus (Fig. 16I): CW/CH 1.3–1.4; ventral margin concave; setae evenly distributed, or with small bare area without setae medially.

Mesosoma (Fig. 16B–F, K, L): Lateral panel of pronotum: slightly narrower than or about as wide as prepectus, LPP/PPT 0.7–0.9; usually with small triangular flange below level of mesothoracic spiracle in posterior oblique view (Fig. 16D, arrow). Mesofemoral depression: usually smooth (Fig. 16L), rarely weakly rugulose or weakly imbricate ventrad. Mesoscutum: punctures angulate, with narrow and weakly coriarious interspaces (Fig. 16B); lateral lobe smooth or weakly coriarious along notaulus (Fig. 16C); parascutal carina broadly curved, acuminate (Fig. 16E). Mesoscutellum: apex with inner margins gradually diverging (Fig. 16K); punctures angulate, with narrow and weakly coriarious interspaces. Axilla (Fig. 16F): in lateral view imbricate dorsad and carinate ventrad. Axillula: smooth dorsad. Fore wing: stigma small, 2.0–2.5 × as wide as postmarginal vein.

Male (Fig. 17). Length: usually smaller, 1.6–3.3 mm. As in female, except: Color: mesonotum with strong or weak cupreous iridescence, and mesoscutellum cupreous laterad (Fig. 17E). Frontal carina: distance from lateral ocellus as wide or shorter, FCLO/LOD 0.3–0.5. Scape (Fig. 17G, H): pits dense, covering 0.3–0.4 × scape length. Lateral panel of pronotum: shape below level of mesothoracic spiracle as in female or with large triangular flange.

Diagnosis. *Perilampus seneca* is most similar to *P. ute*, but females can be distinguished by the lateral panel of pronotum which has a small triangular flange (Fig. 16D, arrow cf. Fig. 18D, arrow), and black coloration between the frontal carina and lateral ocelli (Fig. 14G, arrow cf. Fig. 18G). Males of this species can often be differentiated from those of *P. ute* by a smaller flange on the pronotum (Fig. 17B cf. Fig. 19B, C). Males of *P. seneca* with a large triangular flange on the pronotum are similar to those of *P. ute*, but differ in having cupreous iridescence on a mesonotum (Fig. 17E cf. Fig. 19F). Males of *P. seneca* with a small or no flange on lateral panel of pronotum can be confused with *P. sonora*, which also has the strongly cupreous mesonotum (Fig. 17A, E cf. Fig. 23A), but can be distinguished by a densely pitted scape (Fig. 17G, H cf. Fig. 23G, H). In addition, the distribution of *P. seneca* extends to southeastern Canada and eastern USA, while *P. ute* is restricted to the southwestern and central USA.

Distribution (Fig. 25D). Southeastern Canada, and central and eastern USA: Canada (Ontario), USA (Arkansas, Arizona, Georgia, Indiana, Kentucky, Maryland, Massachusetts, Missouri, New York, Texas, Virginia, West Virginia, Wisconsin). Possibly southeastern USA and Mexico: USA (Florida), Mexico (Veracruz).

Host association. *Perilampus seneca* is a hyperparasitoid, primarily parasitizing dipteran and hymenopteran parasitoids of Lepidoptera (Fig. 26F), rarely parasitizing dipteran parasitoids of Orthoptera and Coleoptera. Tachinidae (Diptera). *Lespesia melalophae* (Allen) from Lepidoptera. *Ormia* sp. from *Amblycorypha oblongifolia* (Tettigoniidae) (ROME162263). Tachinids from *H. cunea* and Chrysomelidae (ROME174210). Braconidae (Hymenoptera). *Cotesia hyphantriae* (Riley) from *Hyphantria cunea* (Drury) (Erebidae). Unidentified parasitoids from *Euchaetes egle* (Drury) (Erebidae).

Variation. An unsequenced male from Florida (ROME204136), has a violet mesonotum and two sequenced females from Florida (ROME152728, ROME152729) lack black coloration between the frontal carina and median ocellus. And two unsequenced males from Florida (ROME207380, ROME207381) reared from *Anisomorpha buprestoides* (Pseudophasmatidae, Phasmida) have a violet mesonotum and the lateral lobe of mesoscutum is weakly punctate along notaulus.

Remarks. There are uncertainties about the species limit of *P. seneca*. Although *P. seneca* is differentiated from the other Nearctic species in COI (10 BINed specimens on BOLD, ACF3436), there are Neotropical clades (from Argentina, Costa Rica, and Venezuela) with BIN ACF3436 that cannot be delimited from *P. seneca* and each other. Specimens either morphologically indistinguishable from *P. seneca* ("*P. hyalinus* 1" from Costa Rica and Venezuela) or differ only in the body coloration or subtle male scape morphology ("*P. hyalinus* 2, 3, and 16, from Argentina, Costa Rica, and Venezuela, respectively). *Perilampus seneca* and these Neotropical groups are placed together as a single clade in COI (Suppl. material 2). Interestingly, *P. seneca* is rendered paraphyletic by *P. hyalinus* 2 from Argentina which itself is polyphyletic—the first clade of *P. seneca* is the population from Florida, and the second is the northern population. ITS2 does not support the species delimitation and relationships suggested by COI (Suppl. material 2)—each Neotropical group is delimited as reciprocally monophyletic species and show different or unresolved species relationships, and *P. seneca* is an unresolved

polytomy. And *P. seneca* cannot be morphologically distinguished from the types of *P. americanus* Girault and *P. nigriviridis* Girault, both from Paraguay, based on the images provided by ZMHB (Fig. 24D–F).

Despite these uncertainties we hypothesize that *P. seneca* is a recently diverged Nearctic species distinct from the Neotropical groups with similar COI sequences—the populations north of Florida are monophyletic for COI albeit with poor support in BI (Suppl. materials 2, 3: BS = 71, PP = 0.53). And *P. seneca* is differentiated from the aforementioned Neotropical groups by ITS2 (Suppl. material 2). The polytomy in the ITS2 trees could be a "soft polytomy" caused by insufficient information from a single gene that can only be resolved with additional genetic data (Maddison 1989). There are ten BINed specimens on BOLD (ACF3436) from the Nearctic region.

The relationships between *P. seneca* and the Neotropical specimens shown in COI unsupported by ITS2 may be due to retention of ancestral polymorphism via incomplete lineage sorting (ILS), introgression events between the Neotropical lineages, and/or insufficient phylogenetic information in ITS2 for this group. The paraphyly of *P. seneca* may be explained by ILS instead of hybridization due to the geographical distance between the two groups. However, two females from Florida (ROME152729, ROME152728) without black coloration between the frontal carina and lateral ocellus, and unsequenced males from Florida (ROME204136, ROME207380, ROME207381) with entirely violet body color in contrast to cupreous body color of northern *P. seneca* suggest there could be two independently evolving lineages in the Nearctic region.

A single *Perilampus* was reared as a parasitoid of Tachinidae in Kentucky, USA (ROME174210) from a series of 1,139 tachinid primary parasitoids of *Acalymma vittatum* and *Diabrotica undecimpunctata howardi* (Chrysomelidae) (Skidmore 2018). This is the only Nearctic *P. hyalinus* species complex specimen associated with Coleoptera and is most likely the result of the accidental entry of a planidium into a novel but suitable host, and does not contradict the host preference of *P. seneca* for the parasitoids of Lepidoptera.

Perilampus ute **Yoo & Darling, sp. nov.**

https://zoobank.org/0FDCB57F-2A0C-423C-B06C-34F1CA9C0714

Figs 18, 19

Type locality. USA, Colorado, Idledale.

Type material. ***Holotype.*** "USA, Colorado, Jefferson Co., Idledale, Sawmill Gulch, 1981 m, 39°40'N, 105°14'W, 20–27.viii.2001, Malaise, Irwin, Lambkin, Metz & Hauser". The holotype is point-mounted (Female ROME182768, TAMU). BOLD:AEE9091/ITS2. ROM Online Collection.

Paratypes. USA: 3 females, 1 male. Arizona: 1 female. Cochise Co., Coronado National Forest, Huachuca Mts., Copper Canyon, 31°21'44"N, 110°18'02"W: (1 female: ROME182763-TAMU; BOLD:AEE9091; ITS2). California: 1 male. San Bernardi-

no Co., Kellers Peak, 34°12'22"N, 117°02'36"W: (1 male: ROME182781-UCRC; BOLD:AEO1509; ITS2). Colorado: 1 female. Jefferson Co., Idledale, Sawmill Gulch, 39°40'N, 105°14'W: (1 female: ROME182768-TAMU; BOLD:AEE9091; ITS2). New Mexico: 1 female. Grant Co., 14 mi N Silver City, Cherry Creek Campground, 32°54.8'N, 108°13.6'W: (1 female: ROME152676-CNC; BOLD:AEE9091; ITS2).

Material examined. USA: 9 females, 5 males. (Suppl. materials).

Additional material examined. Mexico: 1 male. Jalisco: 1 male. (1 male: ROME200745-HNHM). USA: 1 male. California: 1 male. Mono Co., Golden Gate Mine, 4.6 mi NW Walker: (1 male: ROME201998-CAS).

Etymology. The specific epithet is a noun in apposition—a reference to the Ute, indigenous people of the Great Basin regions of present-day Utah and Colorado where the holotype was collected.

Description. Female (Fig. 18). Length: 3.0–3.5 mm. Color: head iridescent greenish blue or violet; mesosoma and metasoma iridescent greenish blue or violet; clypeus ventral margin black (Fig. 18I); antenna with scape and pedicel weakly iridescent greenish blue or violet, flagellum brown or black, lighter ventrad and distad.

Head (Fig. 18G–J): in dorsal view transverse, width slightly greater than twice length, HW/HL 2.1–2.2. Frontal carina: in anterior view straight to weakly sinuate below midlevel of eye; in dorsal view gradually narrowed V shape around median ocellus, FC/MOD about 1.5; distance from lateral ocellus short, FCLO/LOD 0.5–0.6. Scrobal cavity (Fig. 18H): in anterior view wide, SW/HW about 0.5. Ocelli (Fig. 18G): a line between anterior margin of lateral ocelli reaching anterior margin of median ocellus. POL/OOL 1.7–1.9. Ocellar ratios LOD: POL: OOL: LOL 1, 2.7–3.1, 1.5–1.8, 1.1–1.2. Vertex: with strong to weak transverse striations, without large piliferous punctures. Parascrobal area: in lateral view gradually narrowed towards lower eye margin; width narrow, PSW/EL 0.2–0.3; sculpture strongly to weakly striate, without large piliferous punctures. Gena: mostly striate along outer eye margin with narrow and short smooth area, striate behind. Malar space: MSL/EH about 0.2. Lower face (Fig. 18H, I): with setae sparse or dense and narrowly distributed laterad torulus, and sparse or dense below. Clypeus (Fig. 18I): CW/CH about 1.4; ventral margin concave; setae evenly distributed, or with small bare area without setae medially.

Mesosoma (Fig. 18B–F, K, L): Lateral panel of pronotum: about as wide or wider than prepectus, LPP/PPT 0.8–1.1; usually with large triangular flange below level of mesothoracic spiracle in posterior oblique view (Fig. 18D, arrow). Mesofemoral depression: usually smooth, rarely weakly rugulose or weakly imbricate ventrad (Fig. 18E). Mesoscutum: punctures angulate, with narrow and weakly coriarious interspaces (Fig. 18B); lateral lobe smooth along notaulus (Fig. 18C), rarely coriarious; parascutal carina broadly curved, acuminate. Mesoscutellum: apex with inner margins gradually diverging (Fig. 18K); punctures angulate, with narrow and weakly coriarious interspaces. Axilla: in lateral view imbricate dorsad and carinate ventrad. Axillula: smooth dorsad. Fore wing: stigma small, 2.0–2.5 × as wide as postmarginal vein.

Male (Fig. 19). Length: usually smaller, 2.6–2.9 mm. As in female, except: Color: black coloration often present between frontal carina and lateral ocellus, and mesonotum almost

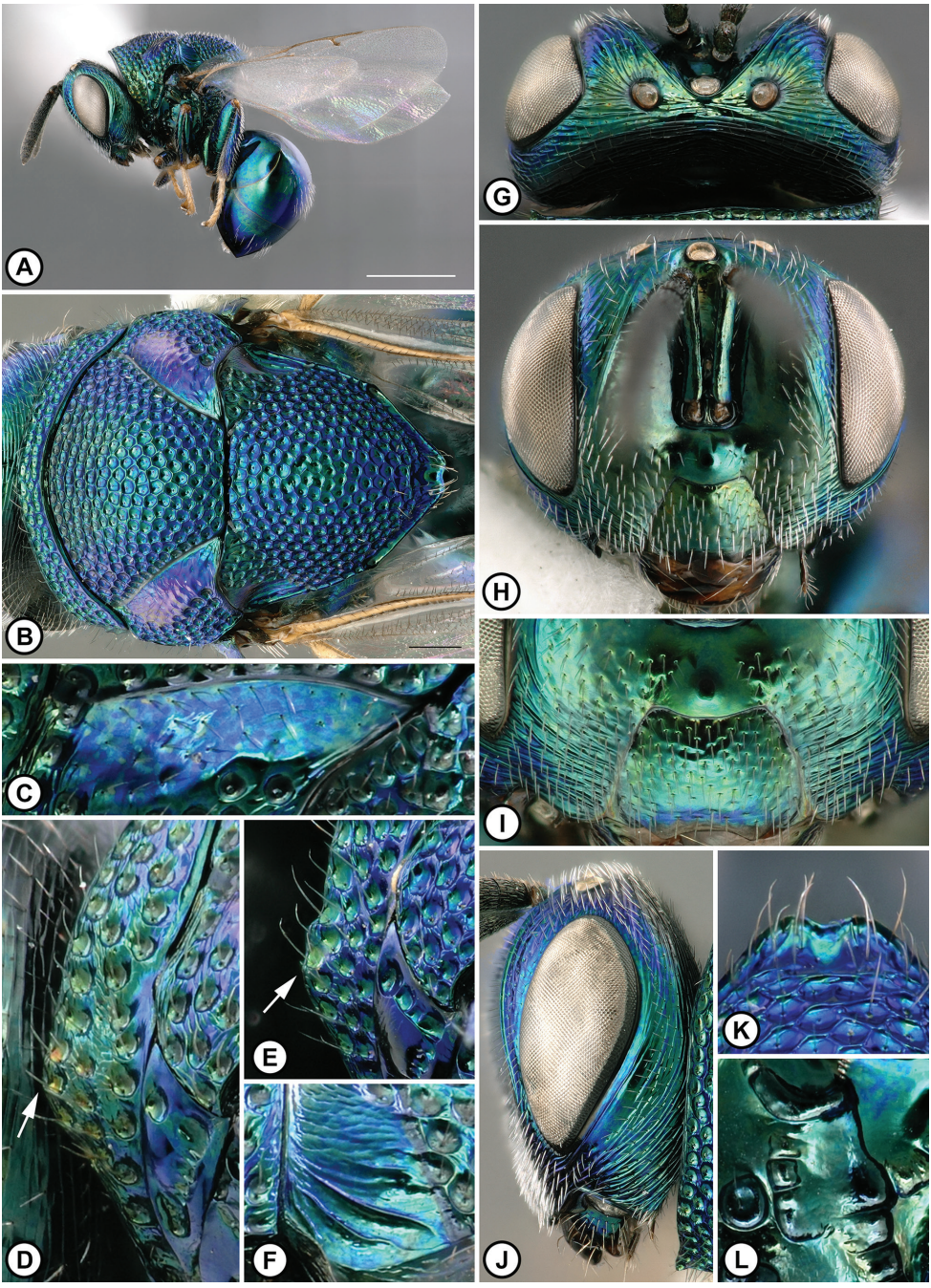

Figure 18. *Perilampus ute* Female **A** habitus, lateral view **B** habitus, dorsal view **C** lateral lobe of mesoscutum along notaulus **D, E** lateral panel of pronotum, posterior oblique view **F** axilla **G** head, dorsal view **H** head, anterior view **I** lower face **J** head, lateral view **K** mesoscutellum apex **L** mesofemoral depression. [**A, C, D, F, G, H** Holotype, ROME182768; **B, E, I–L** Paratype, ROME182763]. Scale bar: 1 mm (**A**).

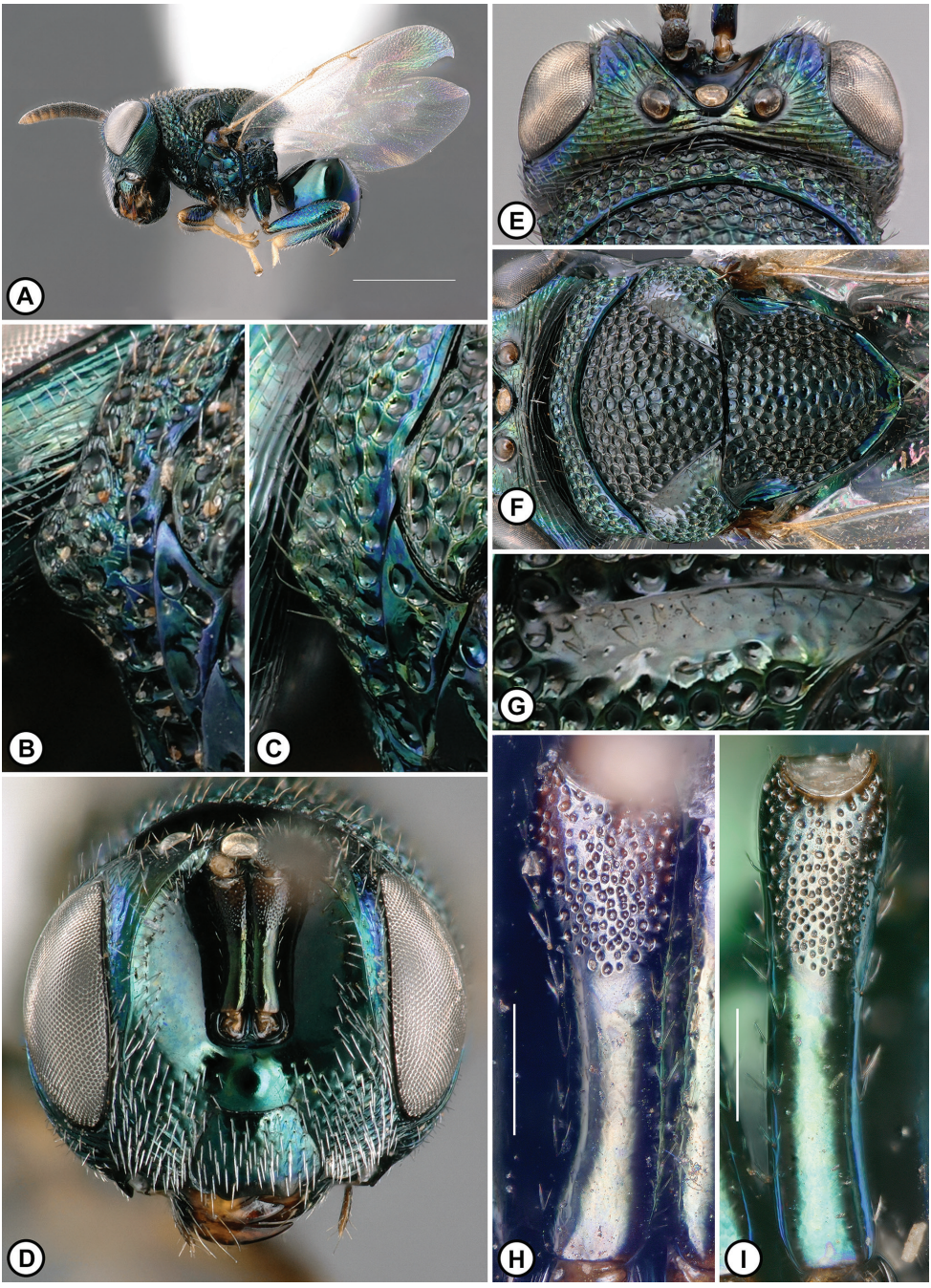

Figure 19. *Perilampus ute* Male **A** habitus, lateral view **B, C** lateral panel of pronotum, posterior oblique view **D** head, anterior view **E** head, dorsal view **F** habitus, dorsal view **G** lateral lobe of mesoscutum along notaulus **H, I** Scape. [**A, B, D–F, H** Paratype, ROME182781; **C, G, I** ROME198139]. Scale bars: 1 mm (**A**); 100 μm (**H, I**).

entirely black with weak bluish iridescence mesad (Fig. 19F) or rarely green with weak cupreous iridescence laterad. Frontal carina: distance from lateral ocellus shorter, FCLO/LOD 0.3–0.4. Scape (Fig. 19H, I): pits dense, covering about 0.3–0.4 × scape length.

Diagnosis. *Perilampus ute* can usually be distinguished by the lateral panel of pronotum with an expanded triangular flange in posterior oblique view (Figs 18D, 19B, C cf. Figs 16D, 17B) and densely pitted male scape (Fig. 19H, I cf. Fig. 15F, G). Females rarely have a small flange on a pronotum as in *P. seneca* (Fig. 18E, arrow), but can be reliably differentiated from the latter by the lack of black coloration between the frontal carina and lateral ocellus (Fig. 18G cf. Fig. 16G, arrow). Males can be confused with *P. seneca* with an expanded triangular flange on the pronotum in posterior oblique view but can be distinguished by the lack of cupreous iridescence on the mesonotum (Fig. 19F cf. Fig. 17E). *Perilampus ute* is restricted to the southwestern and central USA and the range of *P. seneca* extends to southeastern Canada and eastern USA.

Distribution (Fig. 25F). Southwestern and southcentral USA, and possibly western Mexico: USA (Arizona, California, Colorado, New Mexico, Utah), Mexico (Jalisco).

Host association. *Perilampus ute* is a hyperparasitoid, parasitizing dipteran parasitoids of Lepidoptera. Hosts: Tachinidae (Diptera), *Lespesia aletiae* (Riley) from *Apatelodes pudefacta* Dyar (Apatelodidae).

Variation. An unsequenced male from California (ROME201998) has a greenish iridescence along the midline of a mesonotum with a weak cupreous iridescence laterad.

Remarks. *Perilampus ute* is recovered as monophyletic (Fig. 1), but the molecular species delimitation methods identify the specimen from California (ROME182781) as a unique molecular taxonomic unit in COI while merging it with the eastern specimens in ITS2 (Suppl. materials 2, 5). This is likely due to the relatively large genetic divergence in COI between ROME182781 and the eastern specimens (1.7–2.0%), possibly a result of reduced gene flow between disjoint coastal and eastern inland glacial refugia in California (Roberts and Hamann 2015) prior to range re-expansion of the parasitoid populations. There are currently two unique BINs on BOLD assigned for five specimens of this species: AEO1509 for the specimen from California (ROME182781) and AEE9091 for the four specimens from the more eastern regions. The color of the mesonotum is used to differentiate the males of *P. ute* from those of *P. seneca.* However, more thorough genetic sampling is required because only a single male from California has been sequenced and there are no sequenced *P. seneca* specimens from the southwestern USA.

Perilampus arcus Yoo & Darling, sp. nov.

https://zoobank.org/92B1492B-F849-4212-9096-5311ADD6415C
Figs 20, 21

Type locality. USA, West Virginia, Hardy County, 3 mi NE Mathias.

Type material. *Holotype*. "WEST VIRGINIA: Hardy Co. 3 mi NE Mathias 38.9098, -78.8881, 14–31.VII.2007, Malaise David R. Smith". The holotype is point-mounted (Female ROME189051, USNM). BOLD:AEE7608/ITS2. ROM Online Collection.

Paratypes. Canada: 1 male. Ontario: 1 male. Norfolk Co., Normandale Fish Hatchery, 42°43'08"N, 80°20'23"W: (1 male: ROME198214-CNC; BOLD:AEE7608; ITS2). USA: 5 females. Kentucky: 1 female. Jessamine Co., S. of Nicholasville, 37°47'04"N, 84°34'11"W: (1 female: ROME158551-ROME; BOLD:AEE7608). West Virginia: 4 females. Hardy Co., 3 mi NE Mathias, 38.9098, -78.8881: (4 females: ROME185944-USNM; BOLD:AEE7608; ITS2; ROME189050-USNM; ITS2; ROME189052-USNM; BOLD:AEE7608; ITS2; ROME189131-USNM; ITS2).

Material examined. Canada: 2 females, 1 male. USA: 6 females, 1 male. (Suppl. materials).

Etymology. The specific epithet is the Latin noun *arcus* (arch), in reference to the steeply curved parascutal carina.

Description. Female (Fig. 20). Length: 2.7–4.0 mm. Color: head iridescent greenish blue or violet; mesosoma and metasoma iridescent greenish blue or violet; clypeus ventral margin black (Fig. 20I); antenna with scape and pedicel weakly iridescent greenish blue or violet, flagellum brown or black, lighter ventrad and distad.

Head (Fig. 20G–J): in dorsal view transverse, width slightly greater than twice length, HW/HL 2.1–2.2. Frontal carina: in anterior view straight to weakly sinuate below midlevel of eye; in dorsal view gradually narrowed V shape around median ocellus, FC/MOD 1.5–1.6; distance from lateral ocellus short, FCLO/LOD 0.5–0.6. Scrobal cavity (Fig. 20H): in anterior view wide, SW/HW about 0.5. Ocelli (Fig. 20G): a line between anterior margin of lateral ocelli reaching anterior margin of median ocellus. POL/OOL 1.6–1.9. Ocellar ratios LOD: POL: OOL: LOL 1, 2.5–2.9, 1.6–1.8, 0.8–1.0. Vertex: with strong to weak transverse striations, without large piliferous punctures. Parascrobal area: in lateral view gradually narrowed towards lower eye margin; width narrow, PSW/EL 0.2–0.3; sculpture strongly to weakly striate, without large piliferous punctures. Gena (Fig. 20J): mostly striate along outer eye margin with narrow and short smooth area, striate behind. Malar space: MSL/EH about 0.2. Lower face (Fig. 20H, I): with setae sparse or dense and narrowly distributed laterad torulus, and usually sparse below. Clypeus (Fig. 20I): CW/CH 1.3–1.4; ventral margin concave; setae evenly distributed, or with small bare area without setae medially.

Mesosoma (Fig. 20B–F, K, L): Lateral panel of pronotum: slightly narrower than prepectus, LPP/PPT 0.7–0.8; usually with small triangular flange below level of mesothoracic spracle in posterior oblique view (Fig. 20D, arrow). Mesofemoral depression: usually smooth, rarely weakly rugulose or weakly imbricate ventrad (Fig. 20L). Mesoscutum: punctures angulate, with narrow and weakly coriarious interspaces (Fig. 20B); lateral lobe smooth or weakly punctate along notaulus (Fig. 20C); parascutal carina steeply curved, often weakly flanged (Fig. 20E, arrow). Mesoscutellum: apex with inner margins gradually (Fig. 20K) or abruptly diverging; punctures angulate, with narrow and weakly coriarious interspaces. Axilla (Fig. 20F): in lateral view imbricate dorsad and carinate ventrad. Axillula: smooth dorsad. Fore wing: stigma small, 2.0–2.5 × as wide as postmarginal vein.

Male (Fig. 21). Length: usually smaller, 3.1–3.5 mm. As in female, except: Color: mesonotum sometimes with weak cupreous iridescence. Frontal carina: distance from

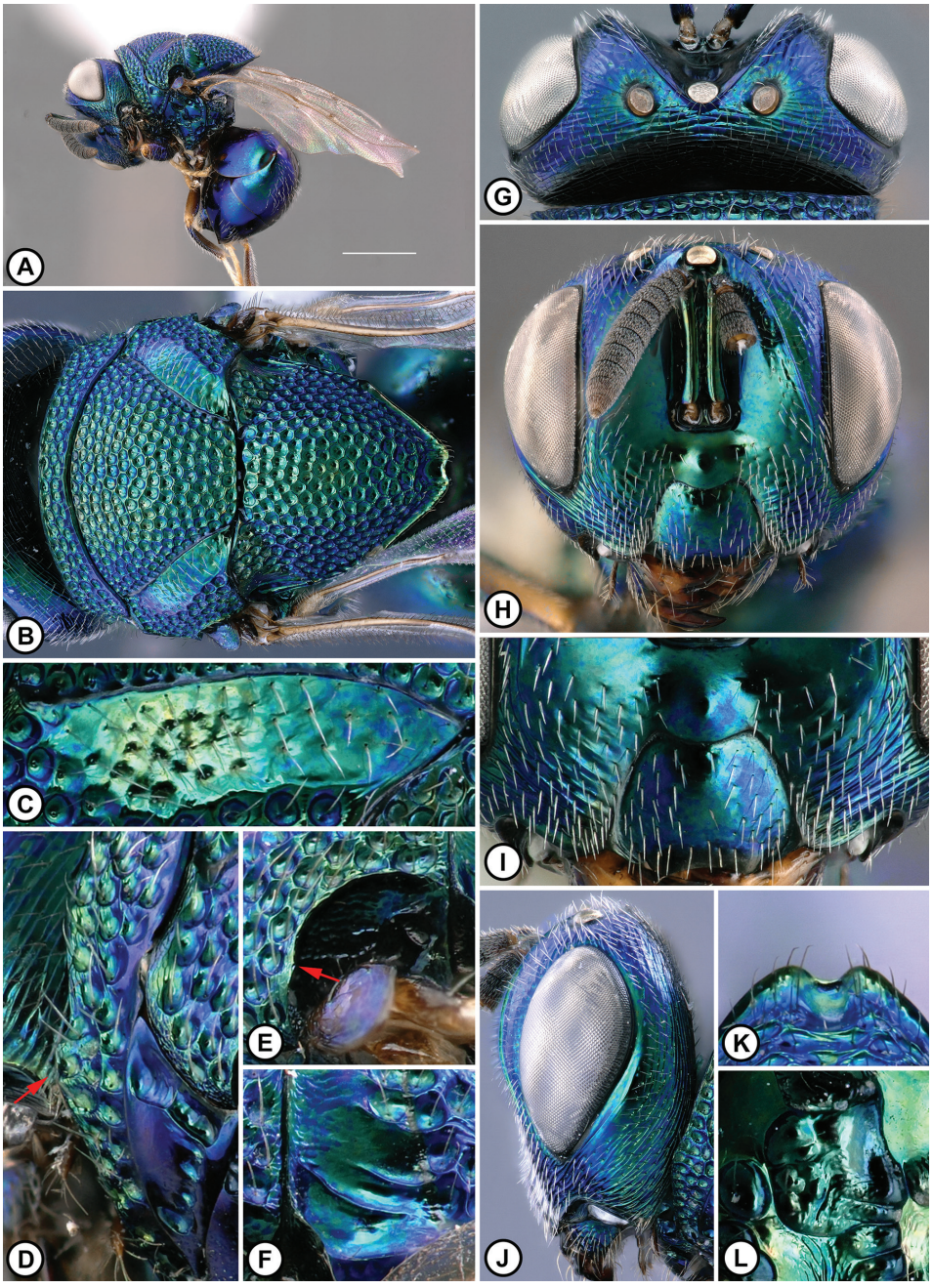

Figure 20. *Perilampus arcus* Female **A** habitus, lateral view **B** habitus, dorsal view **C** lateral lobe of mesoscutum along notaulus **D** lateral panel of pronotum, posterior oblique view **E** parascutal carina **F** axilla **G** head, dorsal view **H** head, anterior view **I** lower face **J** head, lateral view **K** mesoscutellum apex **L** mesofemoral depression. [**A, D, E** Holotype, ROME189051; **B, C, H, J, L** Paratype, ROME185944; **F** Paratype, ROME189050; **G** Paratype, ROME158551; **I, K** Paratype, ROME189131]. Scale bar: 1 mm (**A**).

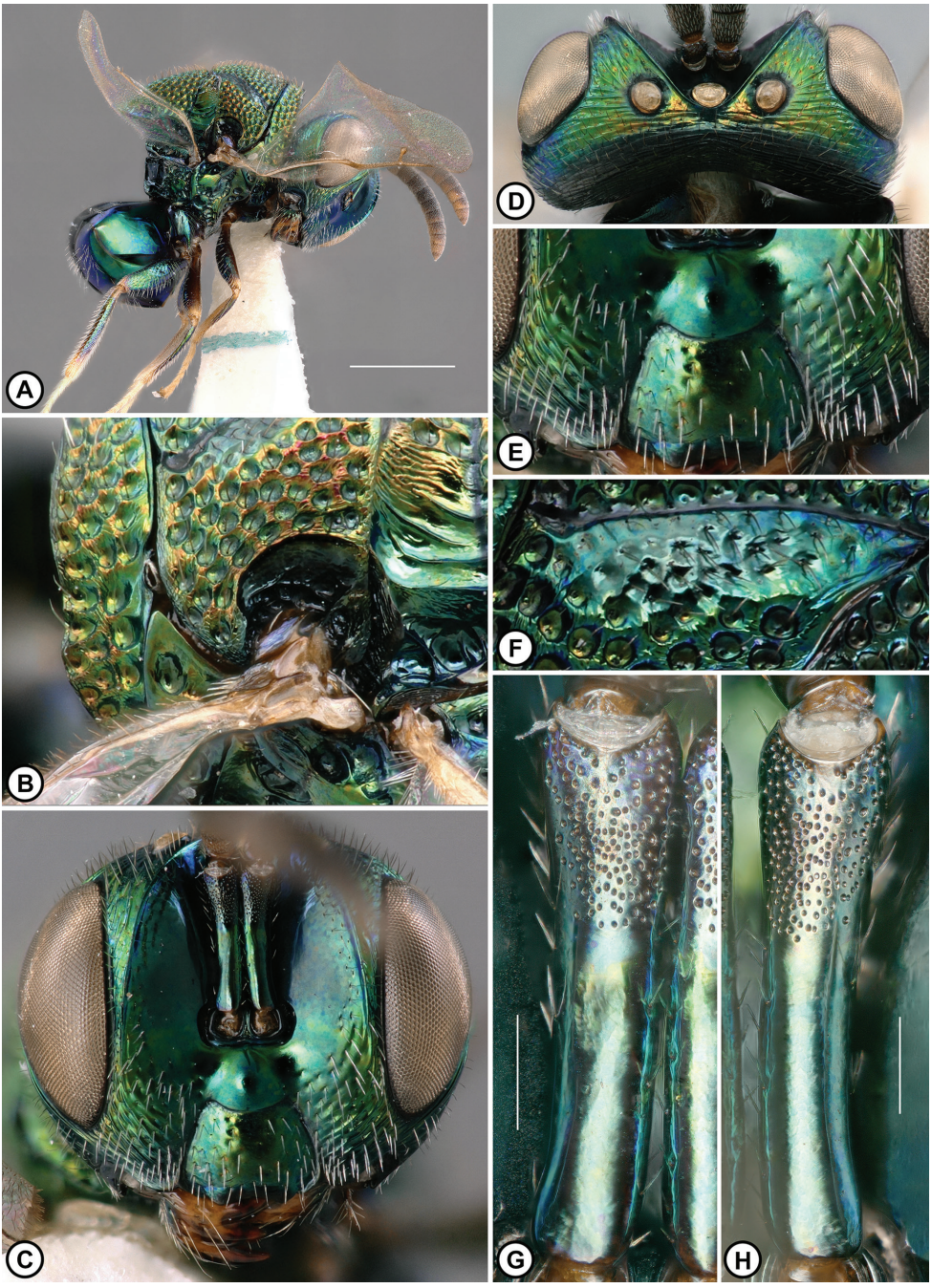

Figure 21. *Perilampus arcus* Male **A** habitus, lateral view **B** lateral panel of pronotum, parascutal carina, and axilla **C** head, anterior view **D** head, dorsal view **E** lower face **F** lateral lobe of mesoscutum along notaulus **G, H** scape. [**A–E, G** ROME185954; **F, H** Paratype, ROME198214]. Scale bars: 1 mm (**A**); 100 μm (**G, H**).

lateral ocellus shorter, FCLO/LOD 0.3–0.4. Scape (Fig. 21G, H): pits dense, covering about 0.4 × scape length.

Diagnosis. The steeply curved parascutal carina often with a flange distinguishes *P. arcus* from the majority of the species of the *P. hyalinus* species complex (Figs 20E, 21B cf. Figs 16E, 17B). *Perilampus sirsiris* also has a similar parascutal carina (Figs 6F, 7B), but it is always steeply curved in *P. arcus* and usually angulate in *P. sirsiris* (Fig. 20E cf. Fig. 6F). *Perilampus arcus* also differs from *P. sirsiris* by having the lateral panel of pronotum with a small triangular flange in posterior oblique view (Fig. 20D, arrow cf. Fig. 6D, E) and a male scape with a densely pitted surface (Fig. 21G, H cf. Fig. 7F, G). In addition to the shape of the parascutal carina, sparser setae on the lower face usually distinguish *P. arcus* from *P. seneca* (Figs 20I, 21C cf. Figs 16I, 17C), which also has a small triangular flange on the pronotum (Figs 16D, 17B) and a densely pitted male scape (Fig. 17G, H).

Distribution (Fig. 25E). Southeastern Canada and eastern USA, possibly south-central USA: Canada (Ontario), USA (Arkansas, Kentucky, Ohio, West Virginia, Wisconsin).

Host association. Unknown.

Remarks. This species is supported by both genes (Fig. 1, Suppl. material 5), and there are five BINed specimens on BOLD (AEE7608) from eastern Canada and USA. A single female was collected in Arkansas, indicating that the range of *P. arcus* may include the southern USA.

Perilampus sonora Yoo & Darling, sp. nov.

https://zoobank.org/D3A8E02F-F4C3-4F8E-A133-63BC6E72C27F
Figs 22, 23

Type locality. USA, Arizona, Santa Cruz County, Sonoita.

Type material. ***Holotype.*** "ARIZONA: Santa Cruz Co. Sonoita, 2 mi S of town center 31°38'N, 110°39'W, 16–22. VI.2008 Malaise trap in juniper/oak grasslands, EE Grissell". The holotype is point-mounted (Female ROME152670, USNM). BOLD:AEO0861/ITS2. ROM Online Collection.

Paratypes. Mexico: 1 male. Oaxaca: 1 male. 19 mi S San Miguel Suchixtepec at Puente Jalatengo: (1 male: ROME182754-TAMU; BOLD:AEO0861; ITS2). USA: 1 female, 1 male. Arizona: 1 female, 1 male. Cochise Co., Coronado National Forest, Chiricahua Mts., 1 mi N Rustler Park, 31°54'53"N, 109°16'07"W: (1 female: ROME186060-TAMU; BOLD:AEO0861; ITS2). Santa Cruz Co., (1 male: ROME198215-USNM; ITS2).

Material examined. Mexico: 15 females, 3 males. USA: 3 females. (Suppl. materials).

Additional material examined. USA: 1 female. Arizona: 1 female. Cochise Co., Bisbee, 1429 Franklin St., 31°24'23.8"N, 109°55'57.6"W: (1 female: ROME152671-USNM; BOLD:AEO0861; ITS2).

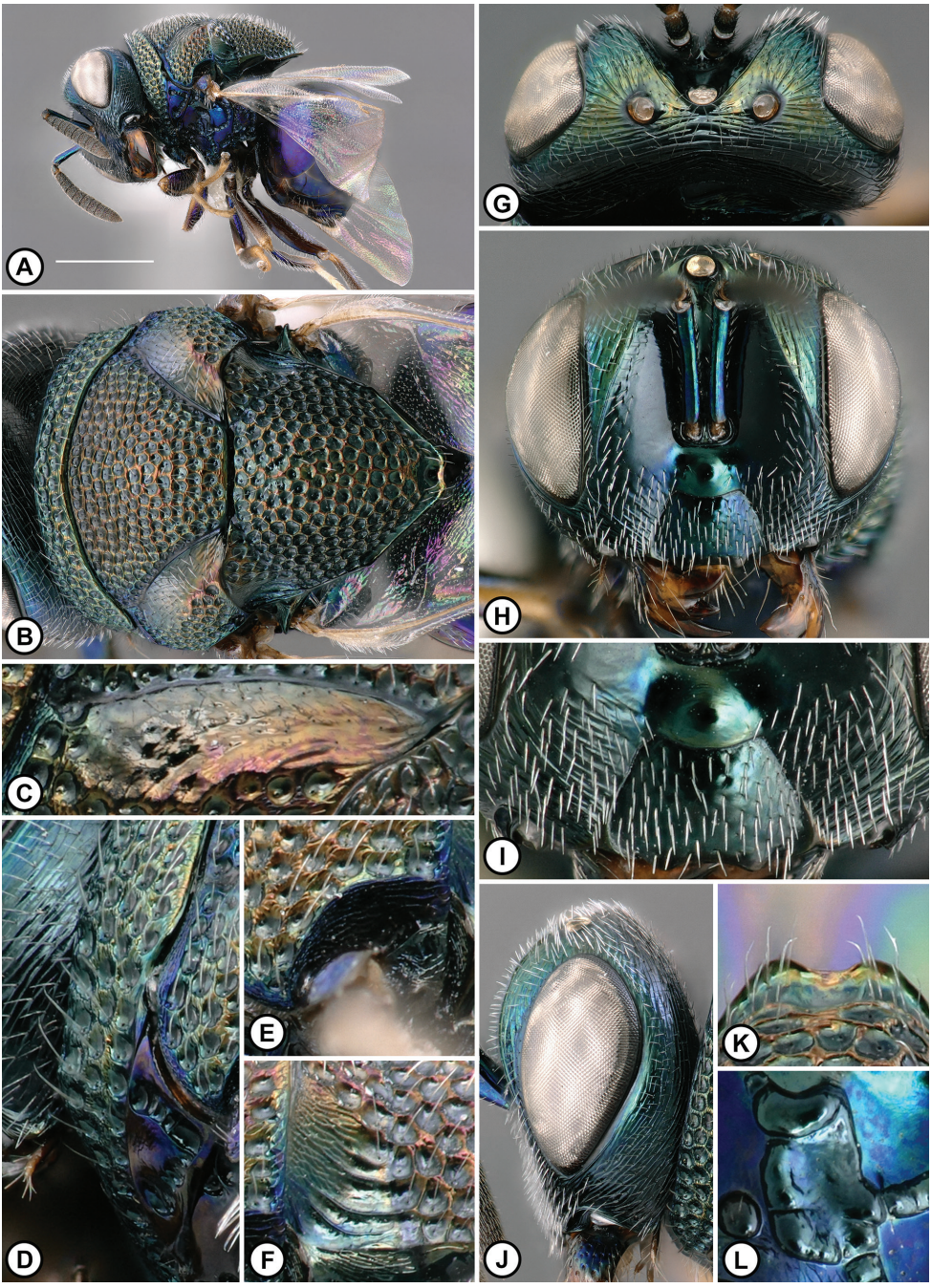

Figure 22. *Perilampus sonora* Female **A** habitus, lateral view **B** habitus, dorsal view **C** lateral lobe of mesoscutum along notaulus **D** lateral panel of pronotum, posterior oblique view **E** parascutal carina **F** axilla **G** head, dorsal view **H** head, anterior view **I** lower face **J** head, lateral view **K** mesoscutellum apex **L** mesofemoral depression. [**A, B, D, G, H, J, K** Holotype, ROME152670; **C, E, I** Paratype, ROME186060; **L** ROME189110]. Scale bar: 1 mm (**A**).

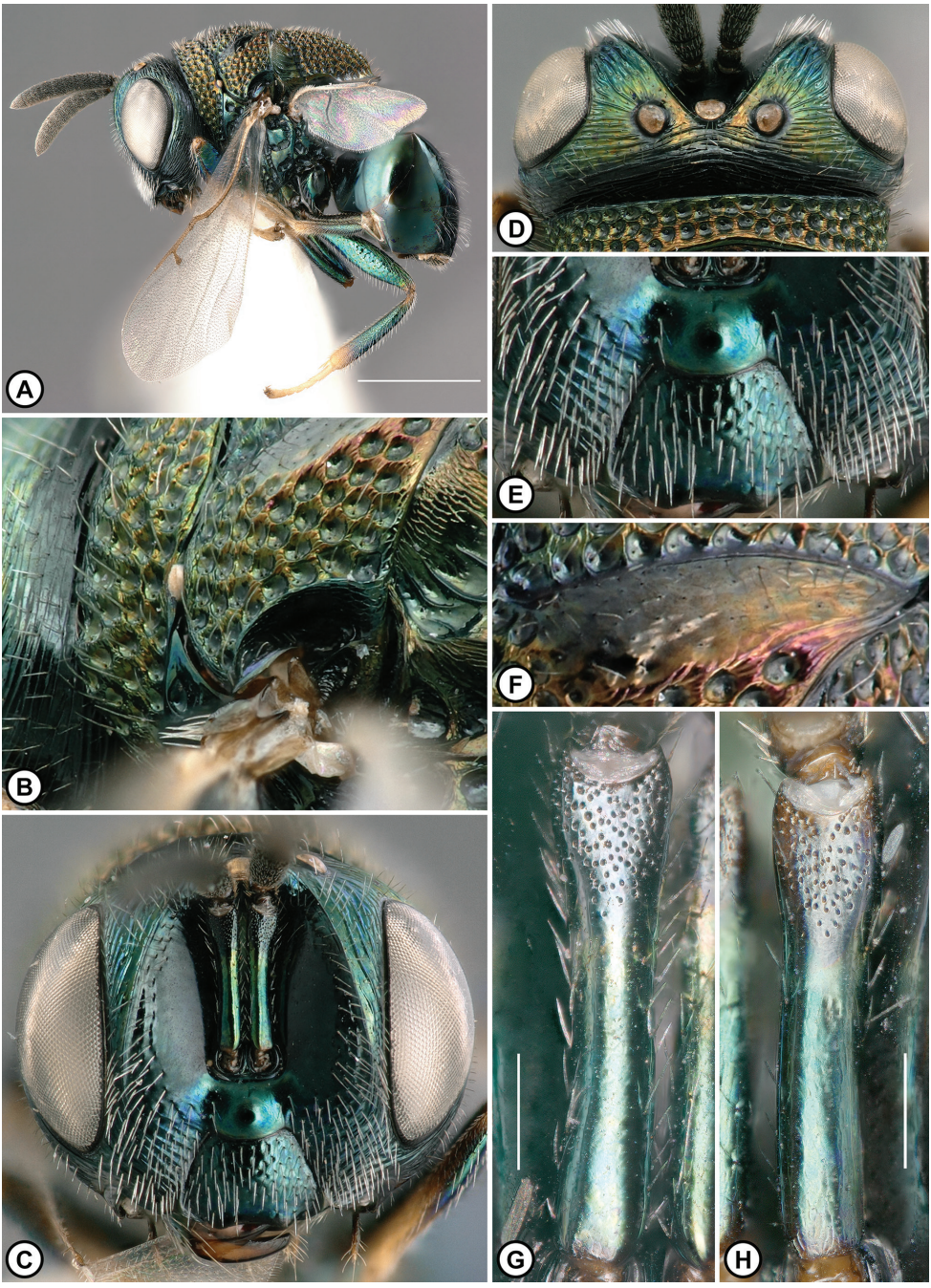

Figure 23. *Perilampus sonora* Male **A** habitus, lateral view **B** lateral panel of pronotum, parascutal carina, and axilla, posterior oblique view **C** head, anterior view **D** head, dorsal view **E** lower face **F** lateral lobe of mesoscutum along notaulus **G, H** scape. [**A–F, G** Paratype, ROME182754; **H** Paratype, ROME198215]. Scale bars: 1 mm (**A**); 100 μm (**G, H**).

Etymology. The specific epithet is a noun in apposition—a reference to both the Sonoran Desert and to the state of Mexico where most of the specimens were collected.

Description. Female (Fig. 22). Length: 2.1–3.2 mm. Color: head iridescent olive with cupreous tinge, with or without black coloration between lateral ocellus and frontal carina; pronotum and mesonotum cupreous, prepectus, meso- and metapleuron, and metasoma iridescent bluish violet; clypeus ventral margin black (Fig. 22I); antenna with scape and pedicel weakly iridescent greenish blue or violet, flagellum brown or black, lighter ventrad and distad.

Head (Fig. 22G–J): in dorsal view transverse, width slightly greater than twice length, HW/HL 2.1–2.2. Frontal carina: in anterior view straight to weakly sinuate below midlevel of eye; in dorsal view gradually narrowed V shape around median ocellus, FC/MOD 1.5–1.7; distance from lateral ocellus short to long FCLO/LOD 0.6–1.0. Scrobal cavity (Fig. 22H): in anterior view wide, SW/HW about 0.5. Ocelli (Fig. 22G): a line between anterior margin of lateral ocelli reaching anterior margin of median ocellus or nearly bisecting median ocellus. POL/OOL 1.8–2.1. Ocellar ratios LOD: POL: OOL: LOL 1, 2.9–3.3, 1.5–1.8, 1.1–1.3. Vertex: with strong to weak transverse striations, without large piliferous punctures. Parascrobal area: in lateral view gradually narrowed towards lower eye margin; width narrow, PSW/EL 0.2–0.3; sculpture strongly to weakly striate, without large piliferous punctures. Gena: entirely striate along outer eye margin, striate posterad. Malar space: MSL/EH about 0.2. Lower face (Fig. 22H, I): with setae sparse or dense and narrowly distributed laterad torulus, and sparse or dense below. Clypeus (Fig. 22I): CW/CH 1.4–1.5; ventral margin concave; setae evenly distributed, or with small bare area without setae medially.

Mesosoma (Fig. 22B–F): Lateral panel of pronotum: about as wide as prepectus, LPP/PPT about 0.9; without flange (Fig. 20D) or with small rounded flange below level of mesothoracic spiracle in posterior oblique view. Mesofemoral depression: usually smooth (Fig. 22L), rarely weakly rugulose or weakly imbricate ventrad. Mesoscutum: punctures angulate, with narrow and weakly coriarious interspaces (Fig. 22B); lateral lobe smooth or weakly coriarious along notaulus (Fig. 22C); parascutal carina broadly curved, acuminate. Mesoscutellum: apex with inner margins gradually diverging; Axilla: in lateral view imbricate dorsad and usually carinate (Fig. 22F), rarely rugose-areolate ventrad. Axillula: smooth dorsad. Fore wing: stigma small, 2.0–2.5 × as wide as postmarginal vein.

Male (Fig. 23). Length: usually smaller, 2.5–2.8 mm. As in female, except: Frontal carina: distance from lateral ocellus as wide or shorter, FCLO/LOD 0.5–0.6. Scape (Fig. 23G, H): pits sparse, covering about 0.3 × scape length.

Diagnosis. This species is distinguished by the strong cupreous iridescence on the mesonotum of both females and males (Figs 22B, 23A cf. Figs 4B, 5A), in combination with the lateral panel of pronotum without a flange or with a small and rounded flange below the level of mesothoracic spiracle (Figs 22D, 23B cf. Figs 16D, 17B). *Perilampus pilosus* can also have a strong cupreous iridescence on the mesonotum (Fig. 15A), but *P. sonora* has sparser setae laterad of the torulus (Figs 22I, 23E cf. Figs 14I, 15E). Also,

the female metasoma of *P. sonora* is always violaceous but usually mostly greenish in the strongly cupreous *P. pilosus* specimens (Fig. 22A cf. Fig. 15B). *Perilampus seneca* males also often have a strongly iridescent mesonotum (Fig. 17E), but *P. sonora* males differ in having sparser pits on scapes (Fig. 23G, H cf. Fig. 17G, H). And the Nearctic distribution of *P. sonora* is limited to southwestern USA and western Mexico, and the range of *P. seneca* extends to southeastern Canada and eastern USA,

Distribution (Fig. 25). Southwestern USA, and western and southern Mexico: USA (Arizona), Mexico (Chiapas, Guerrero, Morelos, Oaxaca, Sonora).

Host association. *Perilampus sonora* is a hyperparasitoid, parasitizing dipteran and hymenopteran parasitoids of Lepidoptera. Hosts: Probably Tachinidae (Diptera) and/or Ichneumonoidea (Hymenoptera) from *Utetheisa ornatrix* (Linnaeus) (Erebidae). The potential hosts are: *Gymnosoma* sp. (Tachinidae), *Lespesia* sp. (Tachinidae), and *Cotesia* sp. (Braconidae) (G. R. Buckingham, personal communication).

Variation. A female from Arizona (ROME152671) has an iridescent green head and weakly iridescent green midlobe of mesoscutum and scutellum. COI and ITS2 suggest that this specimen is a morphological variant of *P. sonora*. A female from Sonora, Mexico (ROME189103), has a strongly transverse clypeus with CW/CH about 1.7.

Remarks. The distribution ranges of *P. sonora* and its undescribed Neotropical sister species, *P. hyalinus* 17 (Fig. 1), appear to be divided by the Central Mexican Plateau. *Perilampus sonora* occurs along the western side of the plateau from Chiapas to Arizona (Fig. 25) and the Central American population of *P. hyalinus* 17 is distributed along the eastern side of the plateau from Panama to Tamaulipas, which may indicate allopatric or parapatric speciation. *Perilampus sonora* is supported by both genes (Fig. 1, Suppl. material 5), and there are four BINed specimens on BOLD (AEO0861) from Arizona and Oaxaca, Mexico.

Discussion

There is considerable complexity in the host associations of the *P. hyalinus* species complex and the host associations and modes of parasitism are congruent with the newly delimited species. *Perilampus hyalinus* Say is a hyperparasitoid that parasitizes Tachinidae and Sarcophagidae (Diptera) parasitoids of Orthoptera or a parasitoid of dipteran kleptoparasites of Crabronidae and Sphecidae (Hymenoptera) that provision their nests with Orthoptera. Two new species are associated with pine sawflies or cedar sawflies, (Diprionidae) and are able to develop as both primary parasitoids or as hyperparasitoids that parasitize the tachinid and ichneumonid parasitoids of diprionid sawflies. And four new species are described for hyperparasitoids, associated with Lepidoptera, parasitizing Tachinidae or Ichneumonoidea.

The molecular analyses and outgroup comparison with the *P. platigaster* species group suggests that hyperparasitoids are basal in the *P. hyalinus* species group and development as a primary parasitoid is derived. These and other host shifts may have been facilitated by parasitism involving the mobile planidial first-instar larva. Planidia

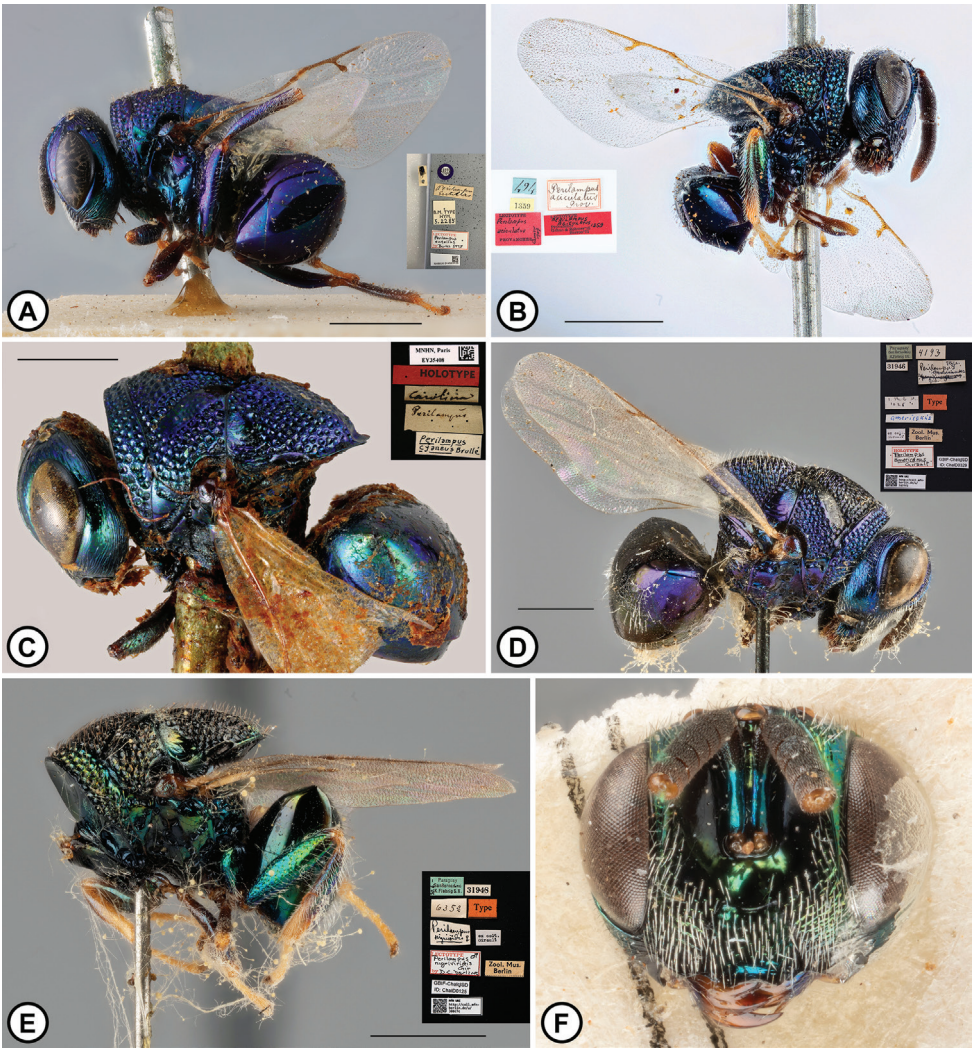

Figure 24. Type specimens of the previously described species of the *Perilampus hyalinus* species complex **A** *P. entellus* Walker (synonym of *P. hyalinus* Say), lectotype, female **B** *P. aciculatus* Provancher (synonym of *P. hyalinus* Say), lectotype, male **C** *P. sirsiris* (Argaman), holotype, female **D** *P. americanus* Girault, holotype, female **E, F** *P. nigriviridis* Girault, lectotype, male. Photo credits: **A** ©The Trustees of the Natural History Museum, London (Licensed under CC BY 4.0) **B** Joseph Moisan-De Serres (Ministry of Agriculture, Fisheries and Food in Québec) **C** National Museum of Natural History, Paris **D, E, F** Museum of Natural History, Berlin.

that successfully make contact and burrow into a novel but suitable host (e.g. sawfly larva) could successfully develop which may ultimately have resulted in the evolution of the species capable of developing as primary parasitoids, e.g., *P. neodiprioni* and *P. monocteni*. Planidia that make contact with a novel but unsuitable host (e.g. Orthoptera) may be "rescued" by subsequent parasitism by primary parasitoids (e.g. Diptera or Hymenoptera) on which the planidia can develop (Perlman 1995), which may have

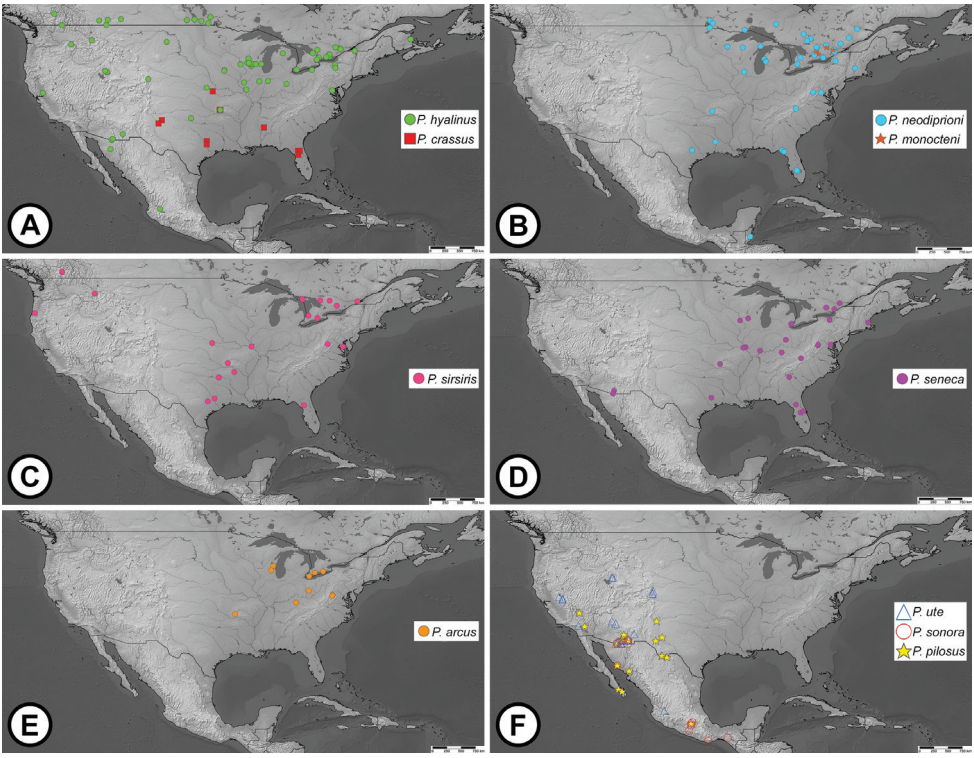

Figure 25. Distribution of the Nearctic species of the *Perilampus hyalinus* species complex **A** *P. hyalinus* (green circles) and *P. crassus* (red squares) **B** *P. neodiprioni* (cyan circles) *P. monocteni* (red stars) **C** *P. sirsiris* **D** *P. seneca* **E** *P. arcus* **F** *P. pilosus* (yellow stars) *P. ute* (blue triangles) *P. sonora* (red circles).

led to the evolution of parasitoids associated with novel hosts. A well-documented example of host shifts involves *P. hyalinus* Say. This is the only known species to strictly develop as parasitoids which parasitize dipteran parasitoids (Sarcophagidae and Tachinidae) of Orthoptera and dipteran kleptoparasites of Crabronidae and Sphecidae (Hymenoptera) that provision their nests with Orthoptera prey containing planidia (Medler 1965; Spofford and Kurczewski 1984). The planidial larva and indirect parasitism could also explain the overlap in associated caterpillar species by sympatric species of *Perilampus* (e.g., *P. seneca* and *P. sirsiris* associated with *Hyphantria cunea*).

The morphological characters used to distinguish the species in the *P. hyalinus* species complex are often subtle (e.g. widely vs deeply curved parascutal carina) and can show interspecific variation (e.g. the sculpture of axillula in *P. neodiprioni* varies between punctate and smooth). Despite the fine distinctions, these morphological characters should allow the identification of most specimens in the absence of host information or molecular data, particularly series of specimens with males and females. It is noteworthy that eight of ten Nearctic species were successfully delimitated by COI and ITS and that each species has a unique BIN number and is monophyletic on the maximum likelihood and Bayesian trees of the *P. hyalinus* species group (Fig. 1, Suppl. material 1).

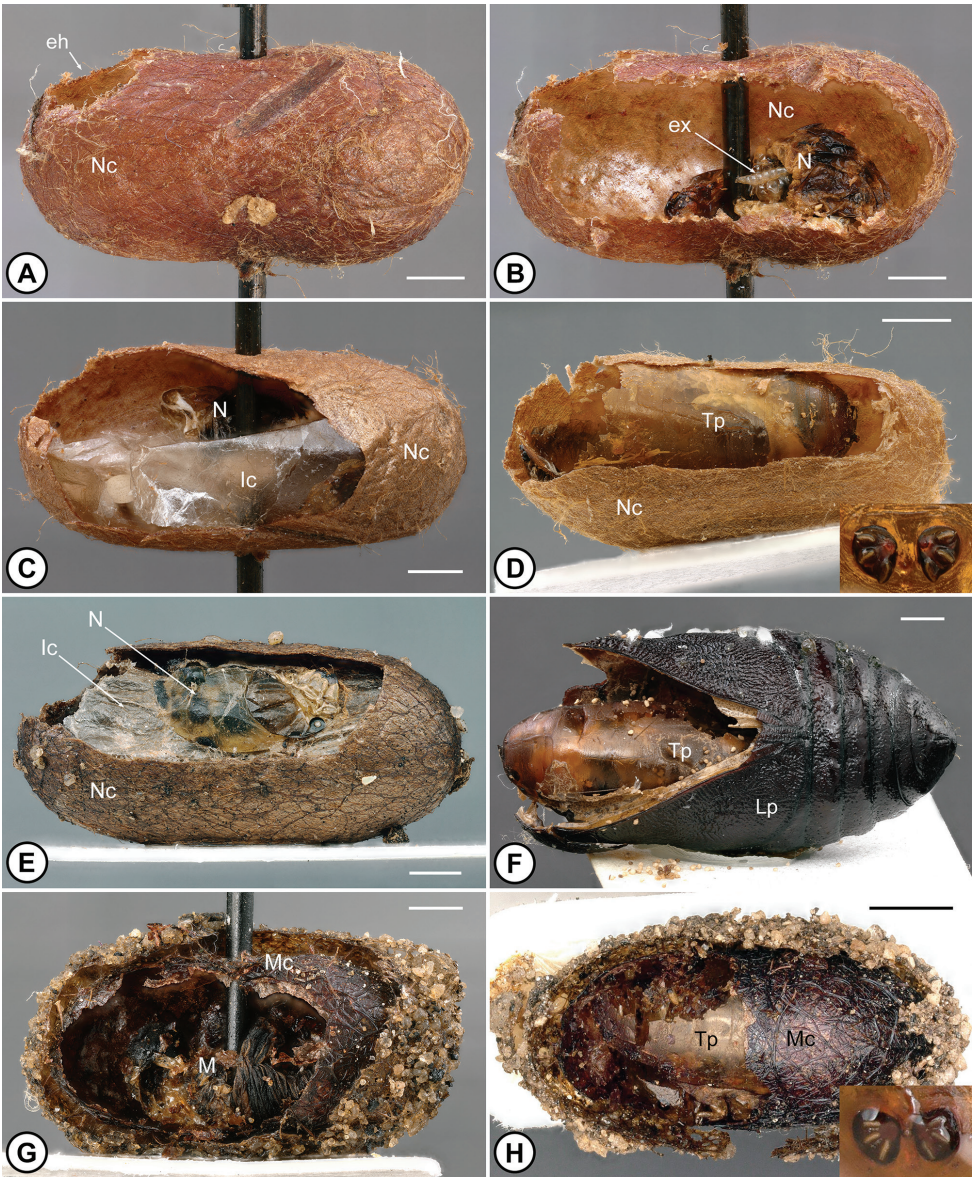

Figure 26. Cocoons, pupa, and host remains associated with reared specimens of *Perilampus*. **A–C, E** *Neodiprion lecontei* cocoons **A, B** *P. neodiprioni* as primary parasitoid **C, E** *P. neodiprioni* as hyperparasitoid, parasitoid of Ichneumonidae **D** *Neodiprion virginianus* cocoon, *P. neodiprioni* as hyperparasitoid, parasitoid of Tachinidae [insert: tachinid puparium spiracles] **F** Lepidoptera pupa, *P. seneca* as hyperparasitoid, parasitoid of Tachinidae **G, H** *Monoctenus suffusus* cocoons **G** *P. monocteni* as primary parasitoid **H** *P. monocteni* as hyperparasitoid, parasitoid of Tachinidae [insert: tachinid puparium spiracles]. Abbreviations: eh, emergence hole; ex, *Perilampus* pupa exuvia; Ic, ichneumonid cocoon; Lp, lepidopteran pupa; M, *Monoctenus* remains; Mc, *Monoctenus* cocoon; N, *Neodiprion* remains; Nc, *Neodiprion* cocoon; Tp, tachinid puparium. [associated *Perilampus*: **A, B** ROME207376 **C** ROME207377 **D** ROME198223 **E** ROME162273 **F** ROME202000 **G** ROME207330 **H** ROME207328]. Scale bars: 1 mm.

The phylogenetic analyses of COI and ITS2 suggest a Neotropical origin of the *P. hyalinus* species complex (Fig. 1, Suppl. material 1). The 9 Nearctic species are distributed across the three separate clades of New World gene trees and the majority of the Nearctic species (5 of 9) belong to the *P. hyalinus* clade 2 (IIIb), whose southernmost species are from Costa Rica (Suppl. material 2). The phylogenetic placements of the Nearctic species suggest independent dispersals of multiple ancestors into the Nearctic region. Intraspecific mitochondrial genetic differentiation suggests that at least two Nearctic species, *P. neodiprioni* and *P. ute*, underwent fragmentation of once widespread populations during the last glacial maximum, approximately 20,000 to 18,000 years ago (Bagely et al. 2016). Small to zero intraspecific divergences in nuclear DNA suggest that these populations experienced subsequent demographic expansion and secondary contact during the post-glacial period.

This revision provides resolution to 100 years of the confusion surrounding *P. hyalinus* in the Nearctic region. However, the phylogenetic relationships and species diversity of the *P. hyalinus* species complex in the Mexican transition zone and Neotropical region needs further study (Yoo 2023). Several Nearctic species range into Mexico and/or near to the Isthmus of Tehuantepec. But the scarcity of specimens available for study from Mexico (28) compared to Canada and USA (754) underscores the need for more comprehensive sampling in Mexico for clearer understanding of the distribution of the Nearctic species. And the northern Neotropical range of *P. neodiprioni* needs to be confirmed with molecular sequencing of the populations in Belize. Further investigation with additional genes and sampling in the Neotropical region and Florida is needed to clarify the species status and distribution limit of *P. seneca* and its relationships with the Neotropical groups similar in morphology and COI, especially from Argentina. Finally, the molecular sampling of the parasitoids reared from *Monoctenus* spp. is needed to test the species hypothesis of *P. monocteni* and its phylogenetic relationships with the other species of the *P. hyalinus* species complex.

Acknowledgements

We would like to thank Andrew Bennett and James O'Hara from CNC for providing their extensive collections and expertise on the hymenopteran and dipteran hosts of the *Perilampus hyalinus* species complex. We are also grateful to Kevin Barber from GLFC for providing specimens and useful insights and feedback. We also extend our gratitude to the staff of the Royal Ontario Museum: Brad Hubley and Brenna Wells for their invaluable technical support and database management, and Kristen Choffe for her expertise in molecular work. Finally, thanks to Emily Darling for her R-code wizardry which greatly facilitated our workflow. This paper was derived in part from a thesis submitted by the first author in partial fulfillment for a M.Sc. degree from the University of Toronto and the members of the supervisory committee are gratefully acknowledged: Douglas C. Currie and Sebastian Kvist.

References

Alfaro RI, Fuentealba A (2016) Insects affecting regenerating conifers in Canada: natural history and management. Canadian Entomologist 148: S111–S137. https://doi.org/10.4039/tce.2015.50

Argaman Q (1990) A synopsis of *Perilampus* Latreille with descriptions of new genera and species (Hymenoptera, Perilampidae), II. Acta Zoologica Hungarica 37: 1–19.

Barrass R (1960) The courtship behaviour of *Mormoniella vitripennis* Walk. (Hymenoptera Pteromalidae). Behaviour 15: 185–209. https://doi.org/10.1163/156853960X00223

Brullé MA (1846) [In Lepeletier de Saint-Fargeau.]. Histoire Naturelle des Insectes: Hyménoptères IV., [viii+]650 pp. [48 plates.]

Burks BD (1963) The Provancher species of Chalcidoidea (Hymenoptera). Canadian Entomologist 95: 1254–1263. https://doi.org/10.4039/Ent951254-12

Burks BD (1975) The species of Chalcidoidea described from North America north of Mexico by Francis Walker (Hymenoptera). Bulletin of the British Museum (Natural History) (Entomology) 32: 139–170.

Burks BD (1979) Family Pteromalidae. In: Krombein KV, Hurd Jr PD, Smith DRBD (Eds) Catalogue of Hymenoptera in America North of Mexico, Vol. 1, Smithsonian Institute Press, Washington, DC, 768–835.

Clausen CP (1940) Entomophagous Insects. McGraw-Hill Book Co., New York and London, 688 pp.

Dalla Torre KW von (1898) Catalogus Hymenopterorum Hucusque Descriptorum Systematicus et Synonymicus, Vol. V. Chalcididae et Proctotrupidae. G. Engelmann, Leipzig, Germany, 598 pp.

Darriba D, Taboada GL, Doallo R, Posada D (2012) jModelTest 2: more models, new heuristics and parallel computing. Nature Methods 9: 772. https://doi.org/10.1038/nmeth.2109

Dahms E (1984) An interpretation of the structure and function of the antennal sense organs of *Melittobia australica* (Hymenoptera: Eulophidae) with the discovery of a large dermal gland in the male scape. Memoirs of the Queensland Museum 21: 361–377.

Darling DC (1983) A review of the New World species of *Euperilampus* (Hymenoptera; Chalcidoidea), with notes about host associations and phylogenetic relationships. Quaestiones Entomologicae 19: 1–40.

Darling DC (1996) Generic concepts in the Perilampidae (Hymenoptera: Chalcidoidea): an assessment of recently proposed genera. Journal of Hymenoptera Research 5: 100–130.

Darling DC, Yoo J (2021) The Perilampidae of the United Arab Emirates and Yemen (Hymenoptera: Chalcidoidea). Zootaxa 5020: 101–129. https://doi.org/10.11646/zootaxa.5020.1.5

Edgar RC (2004) MUSCLE: multiple sequence alignment with high accuracy and high-throughput. Nucleic Acids Research 32: 1792–1797. https://doi.org/10.1093/nar/gkh340

Folmer O, Black M, Hoeh W, Lutz R, Vrijenhoek R (1994) DNA primers for amplification of mitochondrial cytochrome c oxidase subunit I from diverse metazoan invertebrates. Molecular Marine Biology and Biotechnology 3: 294–299.

Ford N (1922) An undescribed planidium of *Perilampus* from *Conocephalus* (Hym.). Canadian Entomologist 54: 199–204. https://doi.org/10.4039/Ent54199-9

Gahan AB, Rohwer SA (1918) Lectotypes of the species of Hymenoptera (except Apoidea) described by Abbé Provancher. Canadian Entomologist 50: 166–171. https://doi.org/10.4039/Ent49391-11

Gibson GAP (1997) Chapter 2. Morphology and terminology. In: Gibson GAP, Huber JT, Woolley JB (Eds) Annotated Keys to the Genera of Nearctic Chalcidoidea (Hymenoptera). National Research Council of Canada Research Press, Ottawa, 16–41.

Girault AA, Sanders GE (1910) The chalcidoid parasites of the common house or typhoid fly (*Musca domestica* Linn.) and its allies. Psyche (London) 17: 9–28. https://doi.org/10.1155/1910/17925

Goodpasture C (1975) Comparative courtship behaviour and karyology in *Monodontomerus* (Hymenoptera: Torymidae). Annals of the Entomological Society of America 68: 391–397. https://doi.org/10.1093/aesa/68.3.391

Graenicher S (1909) Wisconsin flowers and their pollination: Compositae, Part I, Bulletin of the Wisconsin Natural History Society 7: 19–77.

Haack RA, Mattson WJ (1993) Life history patterns of North American tree-feeding sawflies. In Wagner M, Raffa KF (Eds.) Sawfly life history adaptations to woody plants (pp. 503–545). San Diego, CA: Academic Press Inc.

Hajibabaei M, deWaard JR, Ivanova NV, Ratnasingham S, Dooh RT, Kirk SL, Mackie, PM, Hebert PDN (2005) Critical factors for assembling a high volume of DNA barcodes. Philosophical Transactions of the Royal Society: Biological Sciences 360: 1959–1967. https://doi.org/10.1098/rstb.2005.1727

Hinks, C.F. 1971. Observations on larval behaviour and avoidance of encapsulation of *Perilampus hyalinus* (Hymenoptera: Perilampidae) parasitic in *Neodiprion lecontei* (Hymenoptera: Diprionidae). Canadian Entomologist 103: 182–187. https://doi.org/10.4039/Ent103182-2

Hoang DT, Chernomor O, Von Haeseler A, Minh BQ, Vinh LS (2018) UFBoot2: Improving the ultrafast bootstrap approximation. Molecular Biology and Evolution 35: 518–522. https://doi.org/10.1093/molbev/msx281

Huelsenbeck JP, Ronquist F, Nielson R, Bollback JP, (2001) Bayesian inference of phylogeny and its impacts on evolutionary biology. Science 294: 2310–2314. https://doi.org/10.1126/science.1065889

International Commission on Zoological Nomenclature (1999) International Code of Zoological Nomenclature, 4th edn., International Trust for Zoological Nomenclature, The Natural History Museum, London. https://www.iczn.org

Isidoro N, Bin F (1995) Male antennal gland of *Amitus spiniferus* (Brethes) (Hymenoptera: Platygastridae), likely involved in courtship behavior. International Journal of Insect Morphology and Embryology 24: 365–373. https://doi.org/10.1016/0020-7322(95)00014-U

Janzen DH, Hallwachs W (2009) Dynamic database for an inventory of the macrocaterpillar fauna, and its food plants and parasitoids, of Area de Conservacion Guanacaste (ACG), northwestern Costa Rica (nn-SRNP-nnnnn voucher codes) http://janzen.sas.upenn.edu

Johns RC, Flaherty L, Carleton D, Edwards S, Morrison A, Owens E (2016) Population studies of tree-defoliating insects in Canada: a century in review. Canadian Entomologist 148: S58–S81. https://doi.org/10.4039/tce.2015.69

Katoh S (2013) MAFFT: multiple sequence alignment software version 7: improvements in performance and usability. Molecular Biology and Evolution 30: 772–780. https://doi.org/10.1093/molbev/mst010

Kelly EOG (1914) A new sarcophagid parasite of grasshoppers. Journal of Agricultural Research 2: 435–445.

Kumar S, Stecher G, Li M, Knyaz C, Tamura K (2018) MEGA X: Molecular evolutionary genetics analysis across computing platforms. Molecular Biology and Evolution 35: 1547–1549. https://doi.org/10.1093/molbev/msy096

Kvist S (2016) Does a global DNA barcoding gap exist in Annelida? Mitochondrial DNA, Part A, DNA mapping, sequencing, analysis. 27: 2241–2252. https://doi.org/10.3109/19401736.2014.984166

Maddison W (1989) Reconstructing character revolution on polytomous cladograms. Cladistics 5: 365–377. https://doi.org/10.1111/j.1096-0031.1989.tb00569.x

Mawdsley JR (1993) The entomological collection of Thomas Say. Psyche 100: 163–171. https://doi.org/10.1155/1993/59616

Medler JT (1965) Biology of *Isodontia* (*Murrayella*) *mexicana* in trap nests in Wisconsin (Hymenoptera: Sphecidae). Annals of the Entomological Society of America 58: 137–142. https://doi.org/10.1093/aesa/58.2.137

Nguyen LT, Schmidt HA, von Haeseler A, Minh BQ (2015) IQ-TREE: A fast and effective stochastic algorithm for estimating maximum likelihood phylogenies. Molecular Biology and Evolution 32: 268–274. https://doi.org/10.1093/molbev/msu300

Özdikmen H (2011) New names for some preoccupied specific epithets in Chalcidoidea II: families Eupelmidae, Eurytomidae, Mymaridae, Perilampidae, Pteromalidae, Torymidae (Hymenoptera: Parasitica). Munis Entomology & Zoology 6: 832–855.

Peck O (1963) A catalogue of the Nearctic Chalcidoidea (Insecta: Hymenoptera). The Canadian Entomologist (Supplement) 30: 1–1092. https://doi.org/10.4039/entm9530fv

Perlman SJ (1995) The evolution of indirect hyperparasitism, with special reference to the family Perilampidae (Hymenoptera: Chalcidoidea) [Unpublished master's thesis]. University of Toronto.

Pitts JP, Tilgner EH, Dalusky MJ (2002) New host records for *Perilampus hyalinus* (Hymenoptera: Perilampidae) and Phasmophaga antennalis (Diptera: Tachinidae). Journal of Entomological Science 37: 128–129. https://doi.org/10.18474/0749-8004-37.1.128

Provancher L (1887) Faune entomologique de Canada, 2. Additions et corrections à la faune Hyménoptèrologique de la province de Québec., 165–272. https://doi.org/10.5962/bhl.title.38326

Puillandre N, Lambert A, Brouillet S, Achaz G (2011) ABGD, Automatic Barcode Gap Discovery for primary species delimitation. Molecular Ecology 21: 1864–1877. https://doi.org/10.1111/j.1365-294X.2011.05239.x

Rambaut A (2018) FigTree v1.4.4. https://github.com/rambaut/figtree/releases

Rambaut A, Drummond AJ, Xie D, Baele G, Suchard MA (2018) Posterior Summarization in Bayesian Phylogeny Using Tracer 1.7. Systematic Biology 67: 901–904. https://doi.org/10.1093/sysbio/syy032

Ratnasingham S, Hebert PDN (2007) BOLD: the barcode of life data system (http://www.barcodinglife.org). Molecular Ecology Notes 7: 355–364. https://doi.org/10.1111/j.1471-8286.2007.01678.x

Ratnasingham S, Hebert PDN (2013) A DNA-based registry for all animal species: the barcode index number (BIN) system. PLoS ONE 8: e66213. https://doi.org/10.1371/journal.pone.0066213

Ronquist F, Teslenko M, van der Mark P, Ayres, DL, Darling A, H¨ohna S, Larget B, Liu L, Suchard MA, Huelsenbeck JP (2012) MrBayes 3.2: efficient Bayesian phylogenetic inference and model choice across a large model space. Systematic Biology 61: 539–542. https://doi.org/10.1093/sysbio/sys029

Rose AH, Lindquist OH, Nystrom KL (2000) Insects of eastern larch, cedar, and juniper. Natural Resources Canada — Canadian Forest Service Forestry Technical Report 28.

Say T (1829) Descriptions of a new species of Hymenoptera of the United States. Contributions of the Maclurian Lyceum to the Arts and Sciences, Philadelphia 1: 67–83.

Schooler SS, De Barro P, Ives AR (2011) The potential for hyperparasitism to compromise biological control: Why don't hyperparasitoids drive their primary parasitoid hosts extinct? Biological control 58: 167–173. https://doi.org/10.1016/j.biocontrol.2011.05.018

Shirley XA, Woolley JB, Hopper KR, Isidoro N, Roman R (2019) Evolution of glandular structures on the scape of males in the genus *Aphelinus* Dalman (Hymenoptera, Aphelinidae). Journal of Hymenoptera Research 72: 27–43. http://doi.org/10.3897/jhr.72.36356

Shorthouse DP (2010) SimpleMappr, an online tool to produce publication-quality point maps. https://www.simplemappr.net

Skidmore A (2018) Impact of selected integrated pest management techniques on arthropods in cucurbit production systems. Theses and Dissertations-Entomology. 44. https://uknowledge.uky.edu/entomology_etds/44

Smith HS (1912) Technical results from the gypsy moth parasite laboratory. V. The chalcidoid genus *Perilampus* and its relations to the problem of parasite introduction. Technical Series, Bureau of Entomology, United States Department of Agriculture 19: 33–69.

Smith RW (1958) Parasites of nymphal and adult grasshoppers (Orthoptera: Acrididae) in western Canada. Canadian Journal of Zoology 36: 217–262. https://doi.org/10.1139/z58-022

Smulyan MT (1936) A revision of the chalcid flies of the genus *Perilampus* Latreille occurring in America north of Mexico. Proceedings of the United States National Museum 83: 369–412. https://doi.org/10.5479/si.00963801.2990.369

Spofford MG, Kurczewski FE (1984) A new host for *Perilampus hyalinus* (Hymenoptera: Perilampidae). Proceedings of the Entomological Society of Washington 86: 663.

Swofford DL (2003) PAUP*. Phylogenetic analysis using parsimony (*and Other Methods). Version 4. Sunderland, MA, USA: Sinauer Associates.

Tripp HA (1962) The biology of *Perilampus hyalinus* Say (Hymenoptera: Perilampidae), a primary parasite of *Neodiprion swainei* Midd. (Hymenoptera: Diprionidae) in Quebec, with descriptions of the egg and larval stages. Canadian Entomologist 94: 1250–1270. https://doi.org/10.4039/Ent941250-12

Viereck HL (1910) Chalcidoidea. In: Smith EA (Ed.) Report of the insects of New Jersey 1909: 637–650.

Walker F (1843) Descriptions of some new species of Chalcidites. Annals and Magazine of Natural History 12: 103–104. https://doi.org/10.1080/03745484309442495

Wiemers M, Fiedler K (2007) Does the DNA barcoding gap exist? - A case study in blue butterflies (Lepidoptera: Lycaenidae). Frontiers in Zoology 4: 8. https://doi.org/10.1186/1742-9994-4-8

Wilkinson RC, Becker GC, Benjamin DM (1966) The biology of *Neodiprion rugifrons* (Hymenoptera: Diprionidae), a sawfly infesting jack pine in Wisconsin. Annals of the Entomological Society of America 59: 786–792. https://doi.org/10.1093/aesa/59.4.786

Yoo JJ (2023) Species delimitation and phylogenetic relationships of the *Perilampus hyalinus s*pecies group and the description of six new species (Order No. 30245611). Available from Dissertations & Theses @ University of Toronto; ProQuest Dissertations & Theses Global; ProQuest Dissertations & Theses Global Closed Collection. (2832649826). https://www.proquest.com/docview/2832649826

Zhang J, Kapli P, Pavlidis P, Stamatakis A (2013) A general species delimitation method with applications to phylogenetic placements. Bioinformatics 29: 2869–2876. https://doi.org/10.1093/bioinformatics/btt499

Supplementary material 1

Bayesian inference 50% majority consensus tree for *Perilampus hyalinus* species group based on concatenated dataset of COI and ITS2 (Yoo 2023)

Authors: Jeong Jae Yoo, D. Christopher Darling

Data type: tif

Explanation note: Bayesian inference 50% majority consensus tree for *Perilampus hyalinus* species group based on concatenated dataset of COI and ITS2 (Yoo 2023). Posterior probabilities above 0.50 are shown on the left side of the nodes.

Link: https://doi.org/10.3897/jhr.97.133255.suppl1

Supplementary material 2

Maximum likelihood trees of *Perilampus hyalinus* species group retrieved from the separate analyses of COI and ITS2, and the results of morphological analyses (M) and molecular species delimitation (ABGD, BIN, and PTP) (modified from Yoo 2023)

Authors: Jeong Jae Yoo, D. Christopher Darling

Data type: zip

Explanation note: Maximum likelihood trees of *Perilampus hyalinus* species group retrieved from the separate analyses of COI and ITS2, and the results of morphological analyses (M) and molecular species delimitation (ABGD, BIN, and PTP) (modified from Yoo 2023). Bootstrap support values are shown on the left sides of the nodes. The grey bars indicate the result of species delimitations, and the letters within represents identical delimited species. Colored bars under M indicate the morphological partitions that can only be accomplished by the subtle differences in body coloration and male scape morphology. The roman numerals and black dots adjacent to the nodes indicate the major morphological clades recovered as monophyletic (I = *P. hyalinus* species group; II = *P. carolinensis* species complex; IIa = "pseudocarolinensis" clade; IIb = *P. carolinensis* clade; III = *P. hyalinus* species complex; IIIa = *P. hyalinus* clade 1; IIIb = *P. hyalinus* clade 2; IIIc = *P. hyalinus* clade 3; IIId = “regalishyalinus” clade. The morphospecies designation for the sequences is marked by names and vertical bars, which were colored according to their placements within their respective morphological subgroups. The names of the species described herein are indicated in white boxes.

Link: https://doi.org/10.3897/jhr.97.133255.suppl2

Supplementary material 3

Bayesian inference 50% majority consensus tree for *Perilampus hyalinus* species group based on COI (Yoo 2023)

Authors: Jeong Jae Yoo, D. Christopher Darling

Data type: tiff

Explanation note: Bayesian inference 50% majority consensus tree for *Perilampus hyalinus* species group based on COI (Yoo 2023). Posterior probabilities above 0.50 are shown on the left side of the nodes.

Link: https://doi.org/10.3897/jhr.97.133255.suppl3

Supplementary material 4

Bayesian inference 50% majority consensus tree for *Perilampus hyalinus* species group based on ITS2 (Yoo 2023)

Authors: Jeong Jae Yoo, D. Christopher Darling

Data type: tiff

Explanation note: Bayesian inference 50% majority consensus tree for *Perilampus hyalinus* species group based on ITS2 (Yoo 2023). Posterior probabilities above 0.50 are shown on the left side of the nodes.

Link: https://doi.org/10.3897/jhr.97.133255.suppl4

Supplementary material 5

The summary of congruence between *Perilampus hyalinus* species group morphospecies, phylogenetic analyses, the molecular species delimitation methods (ABGD, BIN, PTP) (modified from Yoo 2023)

Authors: Jeong Jae Yoo, D. Christopher Darling

Data type: xlsx

Explanation note: The summary of congruence between *Perilampus hyalinus* species group morphospecies, phylogenetic analyses, the molecular species delimitation methods (ABGD, BIN, PTP) (modified from Yoo 2023). The colored bars indicate support for each criterion of candidate species: unambiguous morphological character states; monophyly in both optimality criteria; and molecular delimitation congruent with morphology. The bolded names under Morphology represent the confirmed candidate species. (S) = singleton morphospecies S = DNA singleton Sp = morphospecies divided into multiple groups L = morphospecies lumped with the other sequences + = morphospecies successfully delimited.

Link: https://doi.org/10.3897/jhr.97.133255.suppl5

Supplementary material 6

The type specimens of species previously described in the *Perilampus hyalinus* species group

Authors: Jeong Jae Yoo, D. Christopher Darling

Data type: xlsx

Explanation note: The type specimens of species previously described in the *Perilampus hyalinus* species group. AMNH = American Museum of Natural History; HNHM = Hungarian National Museum, Budapest; MNHB = Natural History Museum, Berlin; MNHM = National Museum of Natural History, Paris; NMHUK = Natural History Museum, London; USNM = Smithsonian National Museum of Natural History, Washington D. C.

Link: https://doi.org/10.3897/jhr.97.133255.suppl6

Supplementary material 7

Material examined

Authors: Jeong Jae Yoo, D. Christopher Darling

Data type: docx

Explanation note: Material examined for each species other than the types and additional material.

Link: https://doi.org/10.3897/jhr.97.133255.suppl7